REMOVAL OF MERCURY FROM WASTEWATER BY NANOPARTICLE PYRITE (FES2) AND ULTRAFILTRATION (UF) MEMBRANE SYSTEM

A Thesis

by

MD SOLAYMAN KAWSHER

Submitted to the Office of Graduate and Professional Studies of
Texas A&M University
in partial fulfillment of the requirements for the degree of

MASTER OF SCIENCE

Chair of Committee,	Ahmed Abdel-Wahab
Committee Members,	Mohamed Nounou
	Ibrahim Galal Hassan
Head of Department,	Muhammad Nazmul Karim

August 2015

Major Subject: Chemical Engineering

ABSTRACT

This research investigated the removal of mercury by Reactive Adsorbent Membrane (RAM) hybrid filtration process to attain high quality water from wastewater or water resources contaminated with Hg(II), while producing stable final residuals. Pyrite (FeS_2) nanoparticles were employed as the reactive adsorbent and the FeS_2-contacted mercury residuals were separated by either Dead End Ultrafiltration (DE-UF) or Cross Flow Ultrafiltration (CF-UF) system.

The first task of this research was to synthesize pyrite nanoparticles with high purity in short reaction time. Microwave irradiation process was used to synthesize pyrite as microwave digestion method has the advantage of producing fine particles of highly pure pyrite with minimal reaction time. Scanning electron microscopy (SEM) and Energy dispersive X-ray spectroscopy (EDS/EDX) were used to characterize pyrite. Synthesized pyrite were used in all experiments. Reaction mechanism for Hg(II) removal by pyrite and behavior of the treatment system were characterized by observing flux decline, pH change, and Hg and Fe concentration in permeate water with time. Effects of the presence of anions (Cl^-, SO_4^{2-}, NO_3^-) and natural organic matter (HA) on Hg(II) removal were investigated. Also, stability of final residuals was evaluated by using thiosulfate solution ($Na_2S_2O_3$) as desorbing reagent. This study also examined the possibility of continuous removal of mercury by reusing Hg/pyrite laden membrane to remove additional Hg(II) contaminated water.

Analytical techniques used in this study included cold vapor atomic absorption spectrometry (CV-AAS) for mercury measurement, inductively coupled plasma optical emission spectrometry (ICP-OES) for Fe measurement and thermo triode pH meter calibrated with 4, 7 and 10 pH buffers for pH measurement. The surface of Hg/pyrite-deposited membranes were characterized using surface analysis techniques, including scanning electron microscopy (SEM) for sample's surface topography and X-ray photoelectron spectroscopy (XPS) to analyze the surface chemistry (oxidation state) of solids.

Results of this research indicated that the Hg(II)-contacted FeS_2 was completely rejected by both dead-end and cross-flow ultrafiltration membrane system regardless of the presence of anions and humic acid. However, Hg(II) removal was accompanied by considerable flux decline and pH change. Desorption tests were conducted using thiosulfate and almost no release of Hg(II) or iron was observed in permeate water indicating that the formed residuals are very stable. Recycle test showed that this system successfully achieved the goal of continuous and complete removal of mercury from water.

DEDICATION

This thesis is dedicated to my family and many friends, especially to my parents for their unconditional love, support and encouragement throughout my life.

ACKNOWLEDGEMENTS

First and foremost, I would like to offer my sincerest gratitude to almighty Allah for every infinitesimal to large work I have done so fur in my life. Then at first chance, I would like to express my respectful gratitude to my committee chair, Professor Dr. Ahmed Abdel-Wahab, who has supported me throughout my research work with his patience and vast knowledge. I attribute the level of my Master's degree or success to his encouragement and persistent help and without him this thesis would not have been possible.

I am also grateful to my other committee members: Professor Dr. Mohamed Nounou and Professor Dr. Ibrahim Galal Hassan for their encouragement, insightful comments and guidance. Despite their extremely busy schedule they spent a lot of time on my thesis and provided useful suggestions. I hope their academic achievements will continue to increase in future.

I am deeply thankful and indebted to Dr. Han Dong Suk for enlightening me the first glance of research. He spent a lot of time instructing me how to search literature, how to do experiments, how to collect data and how to write a good thesis. I am also thankful to him for his assistance with the SEM and XPS analysis. I must offer my thanks to Dr. Ahmed Khodary, Dr. Bahngmi Jung and Sherine Ahmed for their assistances in many aspects that I cannot list because of limited space.

I would like to thank all of my lab mates in TAMUQ, for the stimulating discussion, for their assistances and for all the fun we have had in the last two years.

Special thanks are given to Qatar National Research Fund. This research was made possible by a grant from the Qatar National Research Fund under its National Priorities Research Program award number NPRP 4-279-2-094. The thesis contents are solely the responsibility of the authors and do not necessarily represent the official views of the Qatar National Research Fund.

I wish to express my sincere thanks to the Department of Chemical Engineering of Texas A&M University at Qatar (TAMUQ) for providing a good work environment and necessary facilities throughout the successful completion of the research. I would also like to thank Mr. Kashim of central material facilities for his assistance with the SEM analysis.

Finally, I wish to express my deepest gratitude to my parents for supporting me throughout my studies and career.

NOMENCLATURE

DE/UF	Dead End/Ultrafiltration
CF/UF	Cross Flow/Ultrafiltration
UF	Ultrafiltration
HA	Humic Acid
PES	Polyethersulfone
RC	Regenerative Cellulose
SEM	Scanning Electron Microscopy
XPS	X-ray Photoelectron Spectroscopy
DDW	Deoxygenated, Deionized Water
MWCO	Molecular weight cut-off

TABLE OF CONTENTS

Page

LIST OF FIGURES

Page

LIST OF TABLES

Page

1. INTRODUCTION

1.1 Problem statement and motivation

Mercury is a global contaminant and of significant concern for centuries due to its high toxicity and bioaccumulation via the aquatic food chain, which seriously affects natural ecosystems and human health. Mercury can exist in various forms in the environment, exhibiting toxicological properties that are harmful to human health.

Various treatment processes for mercury(II) removal from water such as adsorption [1], filtration [2], precipitation/co-precipitation [3], ion exchange [4] and bioremediation [5] have been used. Each removal technology has its inherent advantages and disadvantages. Chemical precipitation of mercury was found to be slow and incomplete [3]. Both precipitation and adsorption techniques produce Hg(II)-contaminated sludge which can release Hg(II) back to the environment after their disposal in landfills [3, 6]. The reported disadvantages of ion exchange technique include variable effluent quality, metallic fouling on the ion exchange media and fairly high operating cost [3, 7]. For separation technology using membrane, it is costly due to membrane fouling [8] if there is no appropriate pretreatment process. Also the membrane technology cannot remove dissolved mercury effectively because the molecular size of dissolved mercury is usually smaller than the size of the membrane applied. Moreover, the presence of natural organic matter and coexisting ions affect mercury removal by aforementioned treatment methods. Therefore, new technologies are

required to remove mercury efficiently from water while producing stable solid residuals that can be effectively separated from water and then safely disposed off.

A new process called Reactive Adsorbent/Membrane (RAM) hybrid filtration process to attain high quality water from wastewater or water resources contaminated with Hg(II) is proposed herein. Mercury is a Lewis acid which has strong affinity to soft Lewis bases. Since thiol functional group is a soft base, sulfur containing chemicals have been widely used to remove mercury from water [1, 8-11]. Accordingly, mercury forms very insoluble solids with sulfide [12]. However, stoichiometric ratio of Hg to S is very important for the formation of stable solids. Excess of sulfur at high pH may lead to formation of soluble mercury disulfide (HgS_2^{2-}) that can still pose risk to the environment [13, 14].

The most common sulfide minerals are pyrite (FeS_2), mackinawite (FeS) and pyrrhotite ($Fe_{1-x}S$, x= 0 to 0.2). The abundance of pyrite on the earth surface and its low cost led many environmental engineers and researchers to use them as possible scavengers of many toxic elements including mercury [1, 10, 15, 16]. Therefore, an attractive alternative for effective mercury removal is to adopt pyrite as reactive adsorbent, possibly producing stable residuals after contact with Hg(II) which can overcome the disadvantage of precipitation using aqueous sulfide. In most previous studies, adsorption species and adsorption mechanism for mercury removal has not been fully understood. However, three potential mechanisms may occur for removal of Hg by pyrite: formation of hydrolyzed Hg species (Eq 1.1), adsorption of hydrolyzed Hg onto the pyrite surface [9] and new solid-phase formation through ion exchange.

$$Hg^{+2} + H_2O = Hg(OH)_m^{(2-m)+} + mH^+ \quad (1.1)$$

$$\equiv Py + Hg(OH)_m^{(2-m)+} = \equiv Py\text{-}Hg(OH)_m^{(2-m)+} \quad (1.2)$$

$$FeS_2(s) + 4Hg^{+2} + 4H_2O = 3Hg^0 + HgS(s) + Fe^{+2} + SO_4^{2-} + 8H^+ \quad (1.3)$$

Even though mercury is strongly adsorbed onto pyrite surface, desorption of Hg from Hg- contacted pyrite is possible when some strong ligands that has high affinity to Hg(II) specie are present in the solution. NO_3^- and NH_3 are considered as weak ligands for desorption of Hg(II), SO_3^{2-} and Cl^- as middle ligands and I^-, $S_2O_3^{2-}$ and CN^- as strong ligands [1, 17]. Also the presence of dissolved organic matter (DOM) and some complexing anions may negatively affect Hg sorption onto pyrite. Anions such as Cl^- and SO_4^{2-} may decrease the sorption of mercury [18, 19] by forming strong nonsorbing aqueous complexes, thus reducing free Hg^{2+} ions available to sorb onto the surface of sorbent. In addition, complexation between mercury and DOM [20-24], adsorption of humic acid on the surface of pyrite [25], and the competition between organic S of DOM and inorganic S of pyrite for complexation with Hg [26] may influence the adsorption of Hg onto pyrite.

Pyrite is very prone to oxidation either by aqueous media especially with dissolved oxygen or redox reaction between Hg(II) and structural Fe of pyrite. Because of the oxidation, the solution pH in the system cannot be so stable that it tends to decrease to the acidic range as reactions proceed [1, 27]. Under such oxidizing condition, the speciation of structural S and Fe of pyrite usually change with pH by oxidative dissolution of pyrite. Moreover, at high pH, the oxidized surface of pyrite can

be covered by Fe(III) oxyhydroxides as monolayer [1, 27]. This surface heterogeneity may strongly influence the sorption behavior of Hg onto pyrite.

On the other hand, the separation of Hg-contacted solid is a technological challenge. Ultrafiltration-supported technique can be used to remove mercury [2, 28-30] from water as well as other heavy metals [31, 32] in the presence of natural organic matters [33, 34]. Herein, the rejection of contaminants will depend on membrane properties (pore size, hydrophobicity and surface charge of membrane), solution properties (concentration, charge, hydrophobicity) and operating conditions (pressure, mode of operation) [2, 33-36]. All of microfiltration, ultrafiltration, nanofiltration and reverse osmosis are capable of reducing mercury concentration below 2 ng/L [2] after appropriate pretreatment. However, microfiltration and ultrafiltration processes are preferred because they can achieve the goal at lower operating pressure which reduces the capital and operating costs [2]. Most contaminant solutions are potential foulants of membrane and the fouling mechanism will depend on membrane properties, species in the feed solution (presence of anions and NOM) and size, ionic strength, pH and mode of operation [33-35, 37, 38]. Appropriate pretreatment and choice of membrane and operation conditions are needed to reach highest removal efficiency of contaminants.

However, previous experimental results reported in the literature using FeS reactive adsorbent [11], support the hypothesis that RAM technology using FeS_2 as a reactive adsorbent has the potential to remove mercury from wastewater while making stable solid residuals. The main advantages of the RAM process over standard precipitation process are that final residuals can be easily separated from the water and

that additional removal of Hg would occur by forming a solid-solution of nanoscale reactive adsorbents on the surface of the membrane, eventually leading to cost-effective performance. On the other hand, the major challenge of the RAM process is to develop a method to effectively make the reactive layers of nRA on the support that can highly remove contaminant while effectively retaining contaminant-contacted nRA in the system until final disposal. Wastewater itself that contains competing anions and NOM could be another challenge due to possible complexation of Hg with these compounds before its contact with pyrite.

1.2 Objectives

The objective of this study is to develop pyrite-supported UF treatment process for removal of mercury from wastewater by forming stable solid residuals on pyrite that are deposited on the UF membrane. Herein, nano-scale pyrite (FeS_2) is used as reactive sorbent combined with ultrafiltration membranes (with cross-flow or dead-end flow ultrafiltration mode) to separate the Hg-loaded residuals from treated wastewater. This study will also examine the ability of Hg/FeS_2-laden membrane for continuous removal of mercury. Moreover, this study will investigate the possible reaction mechanism and characterize final solid residual by surface analysis techniques including SEM and XPS.

1.3 Research tasks

To achieve the objectives of this research, the following tasks were pursued,

- Synthesize FeS_2 nanoparticles using microwave irradiation process
- Evaluate rejection of Hg-contacted pyrite in a continuous contact system using both cross-flow (CF) and dead-end (DE) flow ultrafiltration (UF) system

- Evaluate physical and chemical stability of the final residuals deposited on UF membrane using thiosulfate solution
- Evaluate additional removal capacity of pyrite-deposited UF membrane for Hg(II)
- Study the effect of anions and natural organic matter on mercury removal in continuous contact system

1.4 Thesis organization

Section 2 of this thesis presents a literature review that includes background information on species and sources of mercury, chemistry of mercury in water, health effects of mercury, and the properties of pyrite as well as available technologies to remove mercury from water. Section 3 presents the methodologies for synthesis of pyrite, experimental procedures, analytical methods for analysis of mercury and iron, surface characterization. These analyses were performed using analytical tools including Atomic Absorption Spectroscopy (AAS), Inductively Coupled Plasma (ICP), Scanning Electron Microscope (SEM) and X-ray Photoelectron Spectroscopy (XPS). Section 4 present results and discussions of experiments on separation of Hg(II)-contacted pyrite from water using UF membrane system, the physical and chemical stability of Hg(II)-contacted pyrite solids deposited on the UF membrane, and the additional ability of the Hg(II)-contacted pyrite solids deposited on the UF membrane for continuous removal of Hg(II). The last Section (section 5) includes conclusion of this study and recommendations.

2. BACKGROUND

2.1 Mercury

Mercury is one of the basic natural elements which make up the Earth's composition and it is the only metallic element that is liquid at standard temperature and pressure. Mercury is known as "heavy metal" because of its high density (13.534 $g \cdot cm^{-3}$ at 0 °C and 101.325 kPa). Forms of mercury include elemental mercury (Hg^0), inorganic mercurous (Hg^+) and mercuric (Hg^{2+}) salts, or organic compounds (e.g. methyl-, ethyl and phenyl-mercury).

Mercury is emitted to the environment by natural phenomena (e.g. volcanic eruption, geothermal activity and erosion of mineral deposits) as well as several anthropogenic activities. Re-emission is the third category of mercury sources. Some recent models of the flow of mercury through environment estimates that at present around 5500-8900 tons of mercury are being emitted or re-emitted to the environment from all of sources [39]. The percentile contributions of three major categories are: i) natural sources (10%), ii) anthropogenic sources (60%), iii) re-emission and re-mobilization (30%). Figure 1 shows the relative contribution of mercury emissions from anthropogenic sources measured by United Nations Environment Program. A recent study predicted that in 2020, the present status of mercury emission will cause an increase in mercury levels 2-25% in industrial area and 1.5-5% in remote area while applying current emissions controls worldwide will cause an decrease of 25-35% in industrial area and 15-20% in remote area [39].

Until now, mercury has been extensively used in thermometers, dental amalgam, and fluorescent light tubes. It is also present in coal production, coal-fired power plants, gold mining, chlor-alkali plants, metal smelting, pulp/paper production, chemical synthesis/use (mercuric chloride), vehicle, appliances and some devices (gauge, electric switch, barometer, batteries, cement production and oil exploration/production/transportation).

Mercury has adverse health effects on humans. Different forms of mercury can affect central and peripheral nervous system, digestive and immune systems, lungs and kidneys, and if the level of exposure is high, it may be fatal [40, 41]. Fetal brain is more sensitive than adult brain and more susceptible to mercury induced damage [42].

Methylmercury (MeHg) is the most dangerous form of mercury to human health. Several large outbreaks were caused by consumption of MeHg. Minamata disease is representative of the MeHg poisoning which attacked the people of Minamata bay in Kyushu, Japan in the 1950's. The number of victims by Minamata disease was over 2,200 [40]. Another outbreak of MeHg poisoning was recorded in Niigata prefecture in 1965 and more than 700 victims were recorded [40].

The Maximum Contaminant Level (MCL) for mercury in drinking water has been set as 2 μg/L by the US Environmental Protection Agency (USEPA). A land disposal restriction (LDR) standard has also been set by USEPA as 0.15 mg/L [43] for treatment of wastewater.

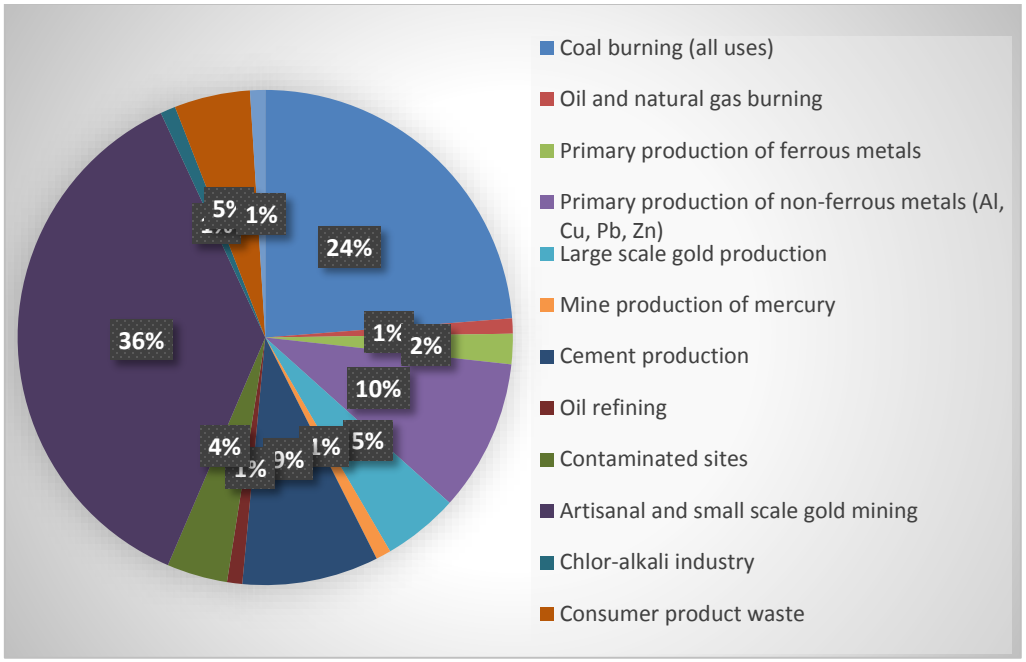

Figure 1. Relative contribution of anthropogenic sources of mercury in 2010 [39].

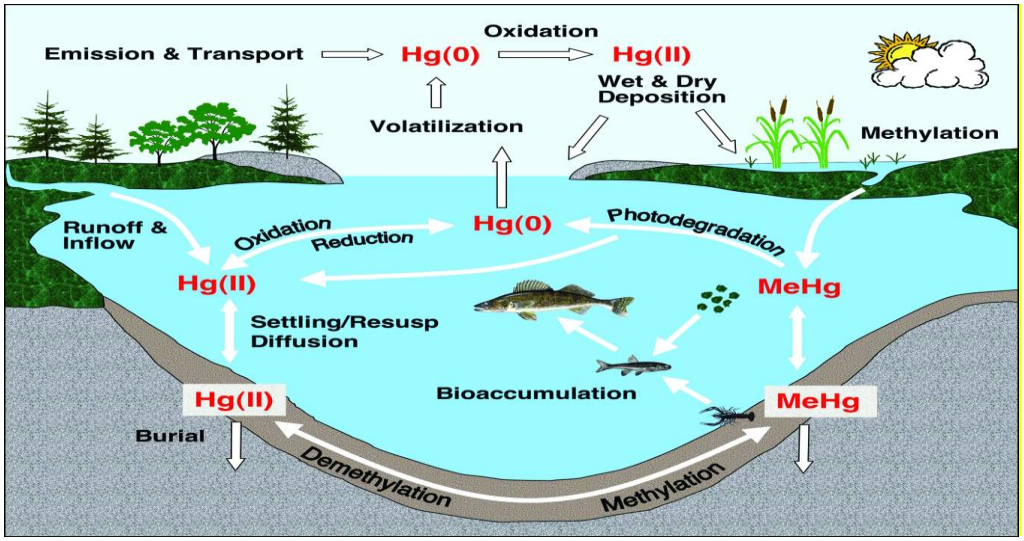

Figure 2. Mercury cycling in watershed [44].

2.2 Aquatic chemistry of mercury

The occurrence and migration of different forms of mercury in water depend on reduction and oxidation conditions, pH, presence of ions and the content of dissolved organic carbon (DOC). Figure 2 shows mercury cycling in a watershed.

Hg(0) in surface waters occurs as a result of Hg(II) compounds reduction by aquatic microorganisms [45, 46], abiotic reduction by humic substances [47], photoreduction [48] and from anthropogenic discharges [45]. In mild oxidizing or reducing conditions, Hg(0) is unreactive and stable, but oxidation to Hg(II) can be stimulated in the presence of chloride ions by ligand-stimulated oxidation mechanism [45, 49, 50] .

Both Hg^{2+} and CH_3Hg^+ have strong tendency to form complexes, particularly in presence of soft ligands like sulfide and chloride. Dominance diagrams of different hydroxo and chloro complexes of Hg as a function of ligand concentration and pH are available in the literature [45, 51, 52]. In freshwaters in the absence of sulfide, the dominant inorganic mercury complexes are three uncharged complexes: $Hg(OH)_2$, HgOHCl and $HgCl_2$ (Figure 3). With increasing chloride concentrations, Hg^{2+} forms HgCl, $HgCl_2$, $HgCl_3^-$ and $HgCl_4^{2-}$ complexes and in full strength seawater containing around 0.6 M of Cl^- (3.5% salinity), Hg^{2+} exists primarily as $HgCl_3^-$ and $HgCl_4^{2-}$ [45]. In freshwater, methylmercuric hydroxide (CH_3HgOH), is the most stable whereas in seawater MeHg is present mainly as the chloride, CH_3HgCl [45]. In natural water, rather than chloride and hydroxide complexes, organic mercury complexes dominates the mercury speciation where mercury is strongly bound to thiol groups of humic matter

[51]. In seawater, the percentage of Hg-humic complexes is low because of chloride ion competition [53]. The association of Hg with humic substances also depends on pH, redox potential and sulfide concentration [45].

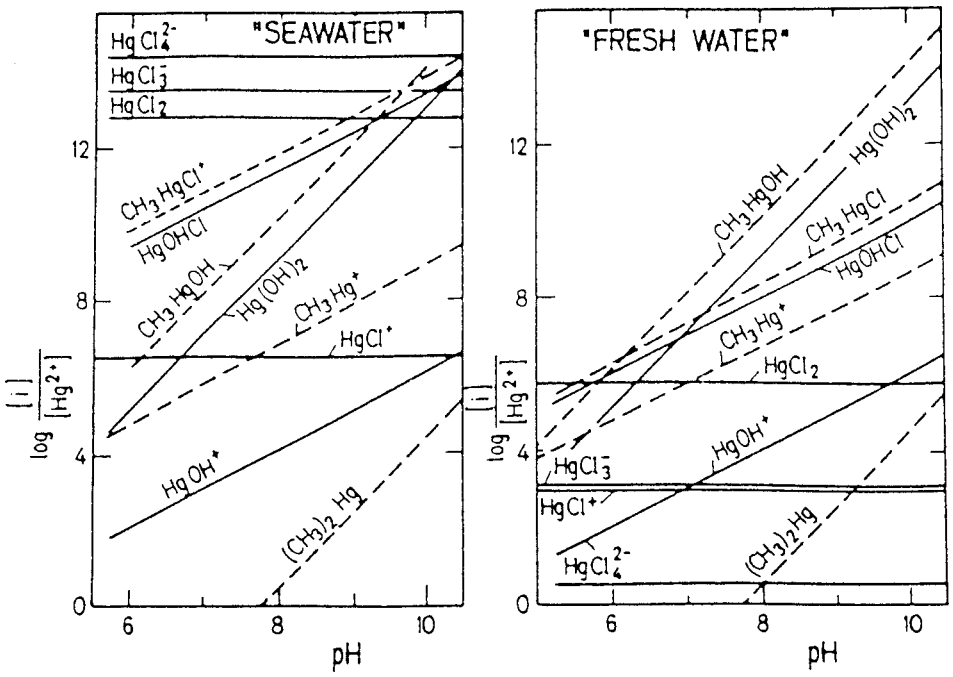

Figure 3. Concentration ratio diagrams illustrating the relative thermodynamic stability of mercury species in fresh water and sea water. Conditions: sea water [Cl] = 0.6 M, [CH_4(aq)] = 10^{-4} M. fresh water [Cl] = 2×10^{-4} M, [CH_4(aq)] = 10^{-4} M [45, 54]

Though organic complexes dominate at oxic conditions, at anoxic conditions sulfide controls the mercury speciation. Mercuric sulfide (HgS) is the main insoluble inorganic Hg compound, commonly found in aquatic systems along with some sparingly soluble HgO. HgS is the most dominant natural sink for Hg even in the oxic conditions,

where strong Hg-S interaction may outcompete O for bonding [8]. HgS formation is favored by low pH and low sulfide concentration, but at high pH and high sulfide concentration, HgS can be converted to soluble HgS_2^{2-} [45, 52]. However, other researchers found that HgS are generally formed at alkaline condition [13]. HgS solubility can increase in the presence of organic matter [55]. At high sulfide concentration, Hg forms soluble $HgSH^+$, $Hg(SH)_2$, $Hg(SH)S^-$, HgS_2^{2-}, and $Hg(S_x)OH$ depending on the pH, redox potential and S^0/S^{2-} concentrations [45, 52, 56-58].

Only methylmercury and dimethylmercury occur naturally in waters from divalent inorganic Hg by a process called methylation which is facilitated by some sulfate and iron reducing bacteria, and organic carbon. Factors affecting the methylation and demethylation processes include bioavailability of mercury to bacteria, activity of bacteria, pH, temperature, dissolved oxygen, redox potential, presence of organic and inorganic ligands, salinity etc. [44, 45, 59]. Methylmercury and dimethylmercury are the dominated methylated species in freshwater and deep ocean water, respectively [45]. Methylmercury that is bioconcentrated in living organisms can be accumulated through the food chain, but usually Hg(0) and $(CH_3)_2Hg$ are not bioaccumulated because they are not retained by phyto- or bacterio-pico-plankton.

2.3 Pyrite

Pyrite (FeS_2) is the most common sulfide mineral in earth surface environments and many ancient sedimentary rocks. The formation and occurrence of pyrite are important in determining the global redox balance and the global cycles of iron and sulfur. The crystal structure of pyrite is very similar to NaCl structure as shown in Figure

4. The S_2^{2-} groups are situated at the cubic center and the midpoints of cube edges, while the low-spin Fe are located at the corners and face centers. The distance between the two S atoms is 2.1 0 A°, much less than twice that of the S atom radius, suggesting covalence in the S_2 group[60].

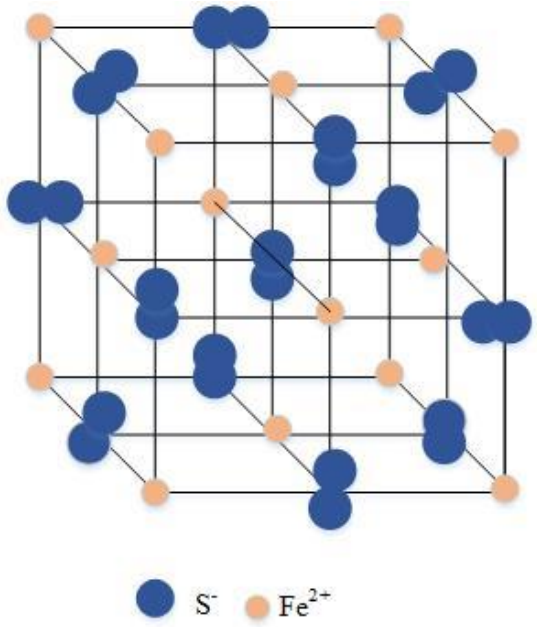

Figure 4. Schematic representation of the structure of pyrite, based on a cubic array of ferrous iron cations (Fe^{2+}) and sulfur anions (S^-).

The abundance of pyrite on the earth surface and its low cost led it to being an attractive solid for use as possible scavenger of many toxic elements. Pyrite has been used as an adsorbent for removing toxic heavy metals such as arsenic [61, 62], mercury [1, 8, 9], zinc, cadmium [9] etc. In order to understand the pyrite formation mechanism,

several laboratory experiments have been carried out and the results showed that pyrite might form by different mechanisms using various sources of iron and sulfur. Various iron sources such as FeOOH, $FeSO_4$, $FeCl_2$, $FeCl_3$, $FeCO_3$, Fe_3S_4, and sulfur sources such as H_2S, NaHS, Na_2S, Na_2S_n have been used to synthesize pyrite [60, 63-65]. In laboratory experiments, the time period for pyrite synthesis ranges from few minutes to 1 year depending on the experiment conditions such as pH, temperature and source of Fe and S [63, 64, 66]. Optimum conditions of pH, temperature, aging time and iron to sulfide ratio were previously investigated. The optimum pH for pyrite synthesis ranges from 3-6.8 for different sources of iron and sulfur [63-66]. It was reported that pyrite formation is not thermodynamically feasible above pH 7 [62, 63]. Temperature affects the rate of pyrite formation. At low temperature, the rate of reaction is slow, while high temperature increases the rate of pyrite formation [62, 66]. Recently microwave energy has been used for pyrite synthesis. Microwave synthesis has been reported to have the advantage of producing small particle with high purity as well as a short time of nuclei formation and crystal growth comparing to conventional heating process [62, 66]. A lower iron to sulfide ratio is favorable for pyrite formation [63]. The reagent concentrations can also affect the particle size. With increasing reagent concentration particle size decreases [66]. In contrast, other researcher found the particle size to be small when reactant concentration was decreased [63]. The difference in relation between reactant concentration and particle size may be related to the different synthesis process and different reaction time. Pyrite formation involves two distinct physical processes: a first nucleation of pyrite followed by a slow growth of the particles [64].

Results reported in the literature suggest that supersaturation of pyrite forming precursors will cause pyrite to nucleate spontaneously and at supersaturation level pyrite nucleation is fast [65]. Both elemental sulfur and iron monosulfide are essential precursors for pyrite formation [63-66]. The overall reaction of pyrite formation using Fe^{3+} and HS^- in aqueous solution is as follows [60, 62-64, 66]:

$$2Fe^{3+} + HS^- = 2\ Fe^{2+} + S^0 + H^+ \quad (2.1)$$

$$Fe^{2+} + HS^- = FeS + H^+ \quad (2.2)$$

$$FeS + S^0 = FeS_2 \quad (2.3)$$

$$FeS + S_n^{2-} = FeS_2 + S_{n-1}^{2-} \quad (2.4)$$

2.4 Mercury removal technologies

Removal of Hg from water is not an easy task because of its different oxidation states (0, +1 and +2) and their interaction with different inorganic and organic components in aquatic systems. Moreover, Hg forms nonsorbing complexes with different anions in solutions which reduces free Hg to be sorbed on an adsorbent. Several technologies have been evaluated for mercury removal from wastewater or water contaminated with mercury. The following subsections provide an overview of common Hg removal technologies:

2.4.1 Adsorption

Adsorption process is the most prominently used technology for the removal of mercury because of its high efficiency with low cost and/or low effluent mercury

concentration [6, 7]. Adsorption process offers flexibility in design and operation because of its reversibility and regeneration by suitable desorption process. Adsorption processes utilize a sorbent material that can remove mercury from water or wastewater by various chemical forces such as hydrogen bonds, dipole-dipole interactions and van der walls forces that hold mercury onto the sorbent. The adsorption process removes both particulate and dissolved mercury. This process can reduce mercury concentration below 2 μg/L [43]. Types of sorbents that were used to remove mercury include granular activated carbon [67], sulfur-impregnated activated carbon [68], coal fly ash [69], hardwickia binata bark [70], exhausted coffee ground [71], waste rubber [72], carbonaceous sorbents derived from flax sieve [73], rice husk [74], walnut shell [75] etc. Among different sorbents activated carbon has been widely used to remove mercury because pretreatment or modification of activated carbon by carbon disulfide (CS_2) has been reported to improve the sorption capacity [3, 7]. A number of sulfur-based adsorbents have been used because of their affinity for mercury [1, 11, 12, 15]. Besides conventional adsorption processes, several organic materials are used as biosorbents to remove mercury from water [76, 77].

The effectiveness of adsorption technologies depends on the water pH, flow rate through adsorption media, contact time, spent sorbent media requiring treatment or disposal, concentrations of mercury and other compounds that may compete with mercury for adsorption, and the presence of suspended solids and organic compounds that can foul the adsorption media [43, 78]. Adjustment of pH to the range where adsorption is most effective is also a common pretreatment step [3].

2.4.2 Membrane filtration

Membrane filtration technologies are used for heavy metal removal because of their high efficiency, easy operation, space savings and adaptability to wide fluctuations of feed quality [6, 79]. Filtration process involves passing the wastewater under pressure through an appropriate porous membrane (cellulose acetate, polyamide, polysulfone, etc.) to separate mercury (both dissolved and particulate) and withdraw the permeate product water. A pressure differences between both sides of membrane serves as a driving force to separate pure water from contaminated water. Filtration processes can be run either in batch or continuous mode. Filtration technologies include microfiltration, ultrafiltration nanofiltration, and reverse osmosis. In case of reverse osmosis the applied pressure must be considerably greater than the osmotic pressure of the rejected solute to obtain good water flux. The primary differences among various membrane systems are in their pore sizes and the required pressure to operate these membranes.

Table 1 lists typical pore sizes and applied pressure of various membrane technologies. All types of filtration system are capable of reducing mercury concentration below 2 ng/L with the proper pretreatment [2]. However, microfiltration and ultrafiltration processes are preferred because they can achieve the goal at lower operating pressure which reduces the capital and operating costs [2]. The percentage removal of contaminants depend on pore size, MWCO, membrane charge, hydrophobicity of membrane and contaminants [80].

Table 1. Various pressure driven membranes [81].

Process	Typical pore size	Typical pressure	Molecular mass
Microfiltration	> 0.1 μm	< 2 bar	> 5000 kDa
Ultrafiltration	2-100 nm	1-10 bar	5-5000 kDa
Nanofiltration	2-1 nm	3-20 bar	0.1-5 kDa
Reverse osmosis	< 1nm	10-80 bar	< 100 Da

The type of membrane is selected based on the size and molecular weight of target contaminants, fouling propensity and the pressure required to move water through the membrane [2, 82]. Ultrafiltration technology is usually used to remove high molecular weight (MW>1000) contaminants and solids [3]. There are two types of ultrafiltration: cross-flow and dead-end flow ultrafiltration. In cross flow membrane, feed solution is forced tangentially to the surface of the membrane while in the dead end flow feed is directed perpendicular to the surface of the membrane. Two filtration modes can be applied: constant flux and constant pressure mode. In a constant pressure mode, the driving force for filtration is kept constant, so that the permeate flux is proportional to pressure and inversely proportional to resistance. In a constant flux mode, the pressure is increased over time to compensate for an increase in membrane resistance. Sorptive ultrafiltration(UF) membrane (polyethersulphone, poly vinyl alcohol and poly vinyl pyridine) provides the advantages of high permeate flux, high retaining efficiency for metal ions because of its reactive functional groups, eventually leading to consumption of low energy comparing to the conventional UF membrane [29, 31]. For effective

removal of mercury by filtration operation, a pretreatment step such as precipitation/co-precipitation, prefiltration and adsorption can be applied before filtration because dissolved mercury ions are too small to be effectively removed by low pressure filtration [43]. The main drawback of membrane separation technology is high operating cost due to membrane fouling [31]. Fouling mechanisms include pore constriction, partial/complete pore blocking, cake/gel layer formation, concentration polarization, organic adsorption and biological fouling [83]. Membrane fouling depends on many parameters such as particle size of solution, hydrophobicity and the mode of filtration (constant pressure, constant flux) [35, 80]. Constant pressure filtration system has shown improved permeate flux comparing with constant flux mode [35].

2.4.3 Chemical processes

Chemical processes involve chemical reactions through the addition of compounds that react with mercury and immobilize it or change its chemical form. Chemical processes to remove mercury include precipitation/co-precipitation, chemical separation, chemical reduction processes and chemical oxidation processes. By far chemical precipitation is the most widely used process in industry to remove heavy metals from industrial wastewater [3]. Precipitation/co-precipitation processes have been widely used to remove mercury from wastewater both in dissolved and particulate forms due to its simplicity, availability and low operating cost [84]. Chemical precipitants used in precipitation processes are ferric salts (e.g., ferric chloride, ferric sulfate), alum, lime softening, limestone, calcium hydroxide and sulfide [3]. The most widely used precipitation technique is hydroxide precipitation due to its simplicity, low cost and ease

of pH control [3, 6]. Sulfide precipitation has been reported to be an effective alternative than hydroxide precipitation. One of the primary advantages of using sulfide instead of hydroxide is that sulfide precipitate is usually less soluble in water than hydroxide precipitate. However, the limitation of this process involve the potential for H_2S gas evolution, sulfide toxicity [3, 6], and soluble sulfide complexes due to excess dosage of sulfide [7]. Though precipitation is useful to remove other heavy metals, chemical precipitation of mercury may be slow and incomplete. Another disadvantage of precipitation technique is large amount of sludge produced and difficult dewatering of sludge due to its amorphous particle structure [3, 6]. However, sulfide precipitation technique can remove 99.9% mercury [7].

Co-precipitation technique is less effective comparing to other removal technologies, but is inexpensive. The most common coagulants that have been employed are aluminum sulfate (alum), iron salts and lime [7]. The other chemical process involves chemical reduction in which metal or metal complexes that are higher in the electromotive series are used to reduce mercury. Most commonly used reductants are zinc, iron, aluminum, sodium borohydrate [7], and stannous chloride [85]. The effectiveness of chemical processes depends on pH of solutions, concentration of mercury, presence of other compounds, chemical dosages, treatment goal and the amount of sludge that needs to be disposed [43].

2.4.4 Ion exchange

Ion exchange is an effective means of removing mercury from wastewater because of its many advantages such as high treatment capacity, high removal efficiency

and fast kinetics [86]. Ion exchange is a reversible chemical reaction that removes unwanted ions (cations or anions) from water by the exchange of ions on the charged resin. Ion exchange is typically operated as columns in which the resin is contacted with contaminated water. Ion exchanger resin consists of detachable ion (typically either H^+/Na^+ or OH^-/Cl^-) depending on the type of resin (cationic or anionic). Anionic resins are mainly employed for cationic mercury but the thiol resin, Duolite GT-73 has been reported to be selective for mercury in any of its three oxidation state [4, 7]. When the resin is saturated, they can be regenerated using high concentration of acid or alkaline medium to remove metal ions from the resin bed. Ion exchanger can be compromised of synthetic organic or inorganic gel, weak base chelating resins [7], weak base anion resin [87], strong base anion resin [7], weak acid cation thiol [4], natural zeolites, clay and soil humus [84]. The ion exchange process usually involves pH adjustment due to the effect of pH on the oxidation state of ions to be removed and their interaction with ions of resin beds. Most anion resins perform better at low pH values whereas cation exchanger work well at high pH values due to less proton competition for adsorption site [84]. An ion exchange resin can consistently remove mercury to below $1\mu g/L$, following prefiltration [4]. Ion exchange resin treatment technology has the advantage of almost zero level of effluent concentration and there is a large variety of exchange resins [3, 7]. The reported disadvantages include variable effluent quality, metallic fouling on the ion exchange media, fairly high operating cost and the presence of free acid reduce the efficiency of operation [3, 7].

2.4.5 Bioremediation

Bioremediation is the use of microorganisms to remove Hg from water. This process is relatively cheap and effective to remove mercury from waste streams. In bioremediation process, mercury resistant bacteria has been used in a bioreactor to remove mercury from wastewater by enzymatic reduction of Hg(II) to water insoluble Hg(0) [5, 88, 89] and then the elemental mercury can be recovered from the reactor. Various natural organisms have been used to remove mercury from water including Karaya gum (Sterculia urens) [90], mera gene [5], Bacillus sp [88], Pseudomonas aeruginosa and Bacillus thuringiensis [91]. The reactor bed is usually made of silica (SiO_2) and alumina (Al_2O_3) for suitable microbial growth. More than 98% mercury removal has been reported in literature by bioremediation process [89]. Factors which affect the bioremediation processes are pH, contaminant concentration, available nutrients, and temperature [5].

2.4.6 Air stripping

Air stripping is a process where dissolved molecules from wastewater are transferred from water into a flowing gas, usually air. Air stripping is applicable for the removal of undesirable volatile compounds from contaminated water. In mercury contaminated water, Hg(II) is usually converted to volatile Hg(0) by a reducing agent and carried away by air. Mercury removal by combined effect of chemical reduction and air stripping has been reported by Looney et al. [85]. They used low levels of stannous chloride to reduce Hg(II) to volatile Hg(0). The removal efficiency depends on the stoichiometric ratio of Sn to Hg. For an initial Hg(II) concentration of 138 ng/L, the

dose-response results indicated that removal efficiency increased with increasing stannous chloride dose and for Sn:Hg ratio of 5 to 25, more than 94% removal was achieved. As stannous chloride react with other dissolved molecules such as oxygen, nitrate and dissolve organic matter, the stoichiometric ratio may vary for complete removal depending on the relative ratio of mercury concentration to other dissolved materials [85]. The ratio of air to water through the air stripper controls the strippability by air. With increasing air to water ratio, the removal rate increases. An air to water ratio of 20 may provide complete removal of Hg(0) [92]. This treatment technology has the advantages of treating large amount of water with trace amount of mercury at low operating and maintenance cost compared to other conventional removal methods without producing secondary liquid or solid waste and without the necessity of off-gas treatment system [93]. However, reduction by Sn(II) followed by removal by air stripping may not be effective when mercury is in the form of organic mercury (methylmercury), particulate mercury, or strongly bound mercury complexes [92].

2.4.7 Nanotechnology

Nanotechnology is one of the most prominent technologies with precisely tailored physical-chemical properties; thus significantly increasing their potential effectiveness in removing heavy metals from water. Nanotechnology is the art of manipulating matter at nanoscale. Significant improvement in the performance of sorbent materials toward removal of heavy metals has been observed due to the development and enhancement of nanoporous structured sorbent materials. A dispersible sorbent with large surface area would be very advantageous for removal of heavy metals

from water. The nanoparticles are highly dispersible and stable in the solution and have a high surface area [94]. Additionally, nanoparticles have the ability to functionalize with different functional groups to enhance their ability towards removing target metals. Combining nanotechnology with other mercury removal technologies can lead to the optimization of the development of a water purification system, small amounts of raw material and less energy consumption. Recent research work has shown promising results for using nanoparticles to remove heavy metals from water [3, 95].

2.4.7.1 Nanoparticles

Metal-oxide nanoparticles have been widely used for the removal of various contaminants from water. Their larger surface area and high reactivity make them an ideal candidate for removal of mercury from water. Sometimes the metal oxides are mixed with other metal or metal oxide nanoparticles to make the mercury removal more efficient and faster. Recent reports have shown different forms of mercury have been removed by gold nanoparticle-aluminum oxide (Au NP Al_2O_3) [96], iron oxide nanoparticles modified with 2-mercaptobenzothiazole [97], Combined Tween 20-Stabilized Gold Nanoparticles and Reduced Graphite Oxide–Fe_3O_4 Nanoparticle [98], zinc oxide nanoparticles [99], Nanocomposites of graphene oxide, Ag nanoparticles, and magnetic ferrite nanoparticles [100], copper oxide, silicon dioxide, aluminum oxide, titanium oxide and iron oxide[101]. The low-cost, effective, and stable metal oxide nanoparticle adsorbent shows great potential for economical removal of various mercury species.

2.4.7.2 Carbon nanotube

Carbon nanotubes (CNTs) are tubular cylinders of carbon atoms that have extraordinary mechanical, electrical, thermal, optical and chemical properties. CNTs have received special attention in adsorption technology because of their capability to establish ($\boldsymbol{\pi}$-$\boldsymbol{\pi}$) electrostatic interactions with heavy metals as well as their large surface area[102].

Synthesis techniques of CNTs include chemical vapor deposition, catalytic development, arc discharge, laser ablation and plasma torch [103, 104]. There are two types of carbon nanotubes: single walled CNTs (SWCNT) and multi-walled CNTs (MWCNT). Chemical functionalization of CNTs improve their physical and chemical properties by providing more active sites, leading to enhanced performance as a sorbent for contaminants [102, 105]. The sorption capacity is mainly dominated by the functional group attached on the surface. Among many functional groups thiols have an excellent binding capacity with many heavy metals. Many researchers have developed amino [102], thiol [102, 105], silver [106], chitosan [107] functionalized groups on the CNTs in order to improve the sorption capacity, selectivity and overall removal efficiency of heavy metals. Functionalized CNTs have been reported to be better adsorbents in all cases. Synthesis technique of functionalized CNT include condensation reaction [102, 105], cross linking method [107], wet chemistry and thermal reduction [106]. Membranes made from CNTs have been gaining considerable attention because of their easy recyclable and reusable capabilities and because of cost effective compared to conventional membranes [105, 108].

3. RESEARCH DESIGN AND METHODOLOGY

3.1 Materials

All materials and chemicals used in this research were reagent grades. Water was distilled by Barnstead Mega-pure distillation device and then deionized by passing distilled water through a Labconco purifier system. Subsequently, the distilled/deionized water was purged with 99.99% N_2 to produce deoxygenated, deionized water (DDW). All stock solutions and chemical reagents used in this study were prepared by dissolving these high quality chemicals with DDW in anaerobic chamber with atmosphere of 99.99 % nitrogen. Also, all experimental works were conducted in anaerobic atmosphere.

Iron (III) chloride hexahydrate ($FeCl_3.6H_2O$, Sigma-Aldrich, 97%) and sodium sulfide nonahydrate ($Na_2S.9H_2O$, Sigma-Aldrich, 99.9%) were used as iron and sulfur sources, respectively, to synthesize pyrite. Mercury stock solutions were prepared using mercuric chloride ($HgCl_2$) obtained from Mallinckrodt Chemicals, Phillipsburg, NJ. Anhydrous sodium sulfate (Na_2SO_4, BDH), sodium chloride (NaCl, Fisher Scientific) and sodium nitrate ($NaNO_3$, sigma-aldrich) were used as source of anions. Humic acid (HA) was purchased from sigma-aldrich as representative of natural organic matter and anhydrous sodium thiosulfate ($Na_2S_2O_3$) was purchased from AMRESCO for desorption tests of Hg(II). All the solutions used in experiments were adjusted to pH 8.0 ± 0.1 using 0.1M NaOH and 0.1M HCl (J. T. Baker). The pH was monitored with a Thermo Scientific pH meter calibrated with three Orion buffer solutions (4.0, 7.0 and 10).

A dead-end flow ultrafiltration (DE/UF) membrane system was set up with low pressure-driven stirred cell UF system provided by Millipore Company, where 800-mL glass reservoir container is connected to a 300 mL glass cell with the membrane. Pressure was maintained at 14.5 psi by a compressed N_2 cylinder connected to the system. Membrane material used for the DE/UF system was 30 kDa regenerated cellulose (RC) ultrafiltration membrane with 31.7 cm^2 of surface area. The cross flow ultrafiltration (CF/UF) has 1000-mL reservoir container connected a Pellicon® XL cassette containing 1000 kDa polyethersulphone (PES) UF membrane (50 cm^2), in which the PES membrane was placed in layers with spacers to carry feed and permeate water.

3.2 Methodology

A series of filtration experiments for separation of Hg(II)-contacted pyrite from water were conducted with two major sets: 1) Rejection test, 2) Recycle test. In rejection test, extent of rejection of Hg-contacted pyrite by UF membrane and its stability were evaluated. In recycle test, additional removal capacity of Hg-contacted pyrite deposited on the surface of ultrafiltration membrane for Hg(II) was determined. The rejection test involves three steps: Step I) Pre-contact of Hg(II) with pyrite for 30 minutes, Step II) Rejection of Hg(II)-contacted pyrite by ultrafiltration membrane, and Step III) Desorption test of Hg(II)/pyrite-deposited membrane using 0.1M thiosulfate ($S_2O_3^{2-}$) solution.

The recycle test followed the first two steps (Step I and II) that were conducted for the rejection test, followed by evaluating the additional Hg(II) removal capacity of

the same Hg(II)/pyrite-deposited membrane by continuously feeding more Hg(II) solution. In each step except step I, permeate water was collected over time in order to measure flux, pH and concentrations of Hg and Fe to obtain removal efficiency and identify the possible reaction mechanism, fouling propensity of membrane and overall retention capacity of the ultrafiltration system.

3.3 Synthesis of pyrite nanoparticles using microwave digestion method

Pyrite (FeS_2) was synthesized in anaerobic chamber using a modified method of Kim et al. [66], which used $Na_2S.9H_2O$ and $FeCl_3.6H_2O$ as precursors of sulfur and iron. pH was adjusted to 6.5 that is optimum pH to avoid the possible presence of FeS and S^0 formation [64]. The detailed procedure to synthesize FeS_2 is listed as below:

- 1L of de-ionized water was purged with N_2 for 2 hours and then deionized deoxygenated water (DDW) was stored in the anaerobic chamber.
- 0.1M of $Na_2S.9H_2O$ and 0.05M of $FeCl_3.6H_2O$ were prepared in 500 mL bottles using DDW.
- 500 mL of 0.1M $Na_2S.9H_2O$ was added into 500 mL of 0.05M $FeCl_3.6H_2O$ to make 1:2 mole ratio of Fe:S and pH was adjusted to 6.5.
- To facilitate the formation of nuclei, heat was applied by a microwave device with ramp temperature of 100^0C and wavelength-power of 1600W for half an hour. A microwave digestion bomb (45 mL, Parr Instrument Company) was used as a container to endure high pressure and temperature.
- Initial pH of the prepared pyrite suspensions was measured.

- The prepared pyrite suspensions was centrifuged with 40 mL centrifuge tubes for 30 minutes at 10,000 rpm and 15^0C to separate solids from liquid. Centrifugation was done for three times to ensure maximize separation and then the separated pyrite was washed several times with DDW to remove the remaining Fe and S ions on the surface of pyrite. All pyrite solid suspension was transferred into 250 ml polystyrene bottles and then the pH of the washed pyrite solid suspension was immediately measured.
- To determine solid concentration of pyrite suspensions, 1 mL of pyrite solid suspension was transferred to known mass of eight vials and then these vials were dried in the oven overnight. The mass difference of vials with and without pyrite determines the amount of FeS_2 prepared (g/L) and this pyrite suspension was used as stock solution of pyrite in all mercury removal experiments.

The pyrite synthesized in our laboratory was characterized by surface analysis. SEM/EDX analysis showed that the mass percentage of synthesized pyrite was 83% (Figure **5**). Average particle size of synthesized pyrite was around 400 nm.

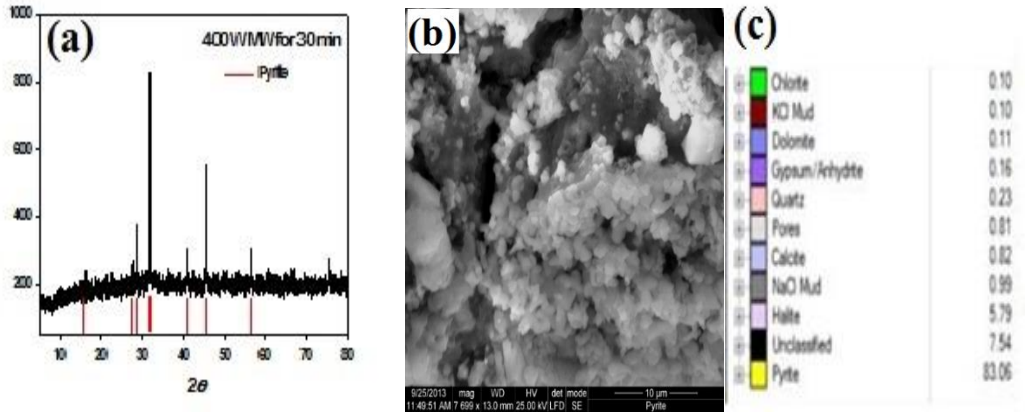

Figure 5. **(a) X-ray diffraction pattern and (b) Scanning electron microscopy image of synthetic Pyrite and (c) mass distribution of synthetic pyrite.**

3.4 Mercury removal experiments

For the rejection test, each of 0.2 g/L of pyrite suspension (6 g/L Pyrite dry weight) and 2 mg/L of Hg(II) were prepared in each 250 mL volumetric flask and they were added into UF reservoir to make a feed solution of 1 mg/L Hg(II) in the presence of 0.1 g/L pyrite. Although mercury concentrations in natural water were reported to be as low as μg/L range [109, 110], higher concentration of Hg(II) was chosen in this experiment to evaluate the efficiencies of our system for mercury removal from wastewater contaminated with mg/L level of mercury. Since the sorption capacity of pyrite for mercury was found to be 7 mg Hg/g [15], 0.1 g/L of pyrite suspension could be appropriate for filtration experiment in this system. In addition, the pH higher than neutral has been reported to be favorable for efficient removal of mercury by pyrite in short time [111]. Moreover, Hg-chloro complexes predominate at pH less than 8 which

might be unfavorable for adsorption of mercury onto pyrite [9, 111]. Therefore, pH of all solutions were adjusted to around 8.0 ± 0.1 by deoxygenated NaOH and HCl.

Each chemical solution of feed water was prepared in anaerobic chamber and they were kept in the chamber until the experiment starts. For the desorption test, 0.1M thiosulfate ($S_2O_3^{2-}$) solution was fed into the UF cell possessing Hg/pyrite-deposited membrane in order to investigate the extent of desorption of Hg(II) that was attached to pyrite on the membrane surface. For the evaluation of additional removal capacity of the Hg(II)-contacted pyrite deposited on the membrane that was made in the previous steps, additional volumes of water containing 1 mg/L Hg(II) were fed into the UF cell. Once the filtration experiment is finished, the Hg/pyrite-deposited membrane was collected and stored in the anaerobic chamber until analysis for surface characterization.

To study the effect of anions (SO_4^{2-}, $NO_3^{2-}$and Cl^-) on the behavior of mercury removal by pyrite (FeS_2), experiments were conducted in the presence of 0.01 M of each of SO_4^{2-}, NO_3^{2-}, and Cl^-. Anions were reported to affect significantly the sorption behavior of Hg and other heavy metals by pyrite [23, 112]. Although the reported values of anions in the environment are very low [112], high concentration of anions was chosen in this study to evaluate the efficiencies of our system for mercury removal from wastewater in the presence of high concentrations of anions. To study the effect of natural organic matter (NOM) on filtration experiments, humic acid (HA) was used as a representative of NOM. Two different concentrations of HA (1 mg/L and 0.2 mg/L) was combined with the 1 mg/L Hg(II) solution to evaluate the effect of HA on Hg removal. Increased concentration of HA can reduce the adsorption of Hg(II) onto pyrite by

competing with Hg(II) for active site of pyrite and subsequently passivating pyrite surface by reversible and irreversible adsorption of HA onto pyrite [25]. At low ratio of HA to Hg, Hg(II) can be reduced to Hg(0) by HA, whereas this reduction decreases with increasing HA concentration by complexation of Hg and HA and at very high HA concentration the reduction is completely outcompeted by complexation [113].

3.5 Removal of Hg(II)-contacted FeS_2 using ultrafiltration membrane system

Both DE/UF and CF/UF membrane systems were used to evaluate the separation (or rejection) of Hg-contacted pyrite. In DE/UF system, an 800 mL glass reservoir container was connected to a 300 mL glass cell. Inside the glass cell, a regenerated cellulose (RC) membrane of 30 kDa MWCO with surface area of 31.7 cm^2 was placed. Pressure was kept constant at 14.5 psi (1 bar) by a compressed N_2 cylinder connected to the system. Ultrafiltration membrane can be initiated under low pressure ranging from less than 1 bar to 10 bar [2, 79]. At high pressure permeate rate increases. The effect of permeate rate on fouling was investigated and increased fouling was reported at high permeation rate [22] because of the rapid accumulation of particles by convective transport onto the surface. With high pressure small contaminants may pass through the membrane pores and deteriorate permeate quality. Also high operating pressure increases the operating cost. That is why low operating pressure was used in both cases.

In CF/UF system, solutions were prepared in a 1000 mL glass reservoir that is connected to CF/UF membrane cassette possessing a polyethersulphone ultrafiltration membrane of 1000 kDa with surface area of 50 cm^2 through flow tube lines. Pressure was kept at 5 psi transmembrane pressure. Prior to initiation of the filtration

experiments, the virgin membrane was washed with 1 L of DDW and then the initial flux of the clean membrane was obtained.

3.5.1 Operation procedures of DE/UF system

To evaluate the continuous removal of Hg(II) adsorbed by pyrite, several experiments were performed using a low pressure-driven dead-end (DE) ultrafiltration (UF) device with non-stirred mode under N_2-purged system. The setup of the DE/UF system is schematically represented in Figure 6, in which a reservoir for feed water and a UF reactor for rejection of solid suspension were connected with lines through an adapter box for control of both gas and water flow. At the beginning of rejection test, two stock solutions of 2-mg/L Hg and 0.2-g/L pyrite were poured into UF reservoir to provide 1 mg/L Hg as initial concentration in the presence of 0.1 g/L pyrite and then the inflow air was immediately evacuated several times by nitrogen gas to ensure anoxic conditions. Afterwards, those stock solutions were mixed by stirrer for 30 minutes allowing reactions to occur and then all solutions was transferred into UF stirred cell as feed water by a pressure of 14.5 psi. This is an initiation of the step II experiment. Herein, permeate water was collected over time until all feed solution was consumed in order to investigate water flux, pH change and particle rejection. Subsequently, 0.1M thiosulfate ($S_2O_3^{2-}$) solution was fed into the UF stirred cell possessing Hg/pyrite-deposited membrane in order to investigate the extent of desorption for Hg(II). This is the step III which is the final step for the rejection test.

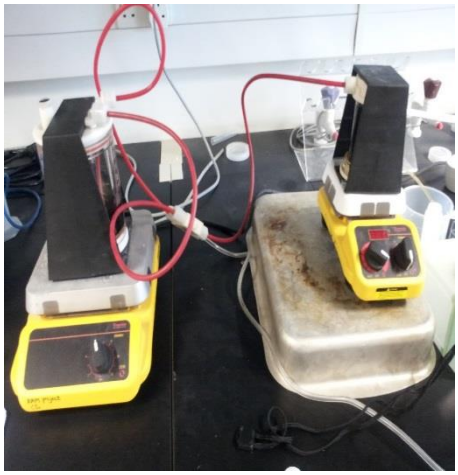

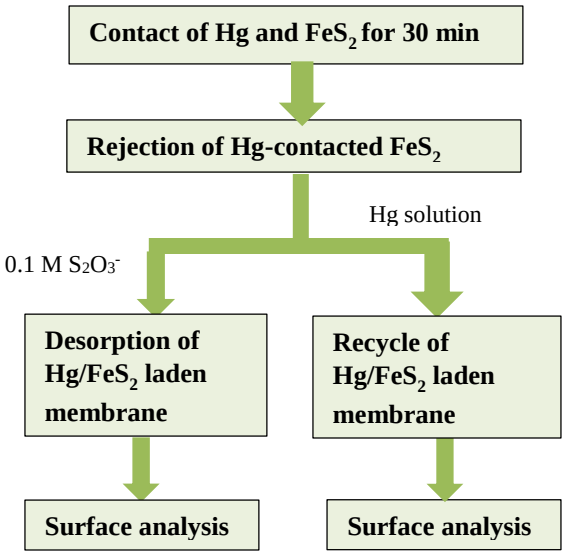

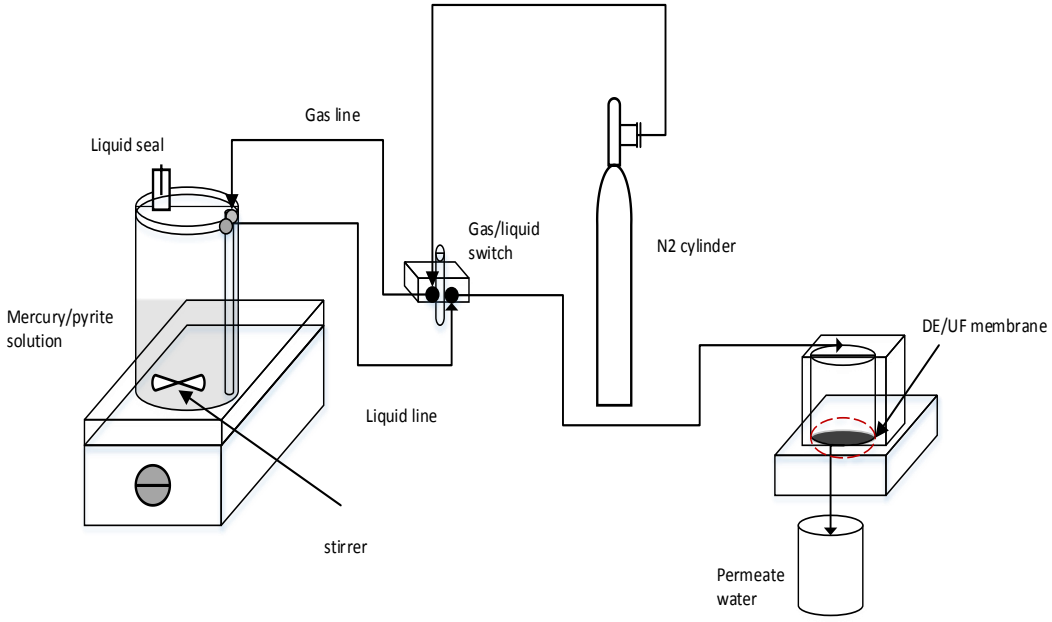

Figure 6. Schematic representation and flow chart of the dead-end ultrafiltration membrane system experiments.

For recycle test, steps I and II and preparation of all solutions followed the same procedure of the rejection test. Subsequently, additional removal capacity of the membrane was evaluated as step III by feeding more Hg(II) solutions (1 mg/L) into the UF cell. To evaluate the effect of anions and HA, each anions and HA were added to Hg(II) solution in the presence of pyrite in step I. Once the filtration experiment is finished, the Hg/pyrite-deposited membrane was collected and stored in the anaerobic chamber until surface analysis.

The flux and percentage of Hg removal were calculated using the following equations:

$$\text{Flux } (L/m^2.min) = \frac{\text{volume of water (L)}}{\text{surface area of membrane } (m^2) \times \text{time to collect permeate water (min)}} \quad 3.1$$

$$\%\ \text{Hg removed} = \frac{(\text{Hg concentration in feed solution} - \text{Hg concentration in permeate solution}) \times 100\%}{\text{Hg concentration in feed solution}} \quad 3.2$$

3.5.2 Operational procedure of CF/UF system

The CF/UF system was also used for rejection of Hg(II)-contacted pyrite. Figure 7 shows the flow diagram of the CF/UF system where feed water flows from water reservoir to CF/UF membrane unit by a peristaltic pump. For step I, 0.1 g/L pyrite was contacted with 1 mg/L Hg(II) at pH 8 for 30 minutes by magnetic stirring allowing reactions to occur. In the step II, these Hg(II)-contacted pyrites were circulated with retentate mode as feed water through Pellicon® XL cassette containing 1000 KDa Polyethersulfone (PES) UF membrane (50 cm^2) where the PES membrane is placed between sieve-like two layers (Figure 8). In step III, 0.1 M thiosulfate solution was continuously passed through the Hg-contacted pyrite deposited on the membrane while retentate line is closed. Similar to DE/UF system, the permeate water during operation of CF/UF system was collected over time. For recycle test, it followed the same procedure of steps I and II for rejection test. Subsequently, additional removal capacity of the membrane was evaluated as step III by feeding more Hg(II) solutions (1 mg/L) into the UF cell. To evaluate the effect of anions and HA, each anions and HA were added to Hg(II) solution in the presence of pyrite in step I. Once the filtration experiment is finished, the Hg/pyrite-deposited membrane was collected and stored in the anaerobic chamber until surface analysis.

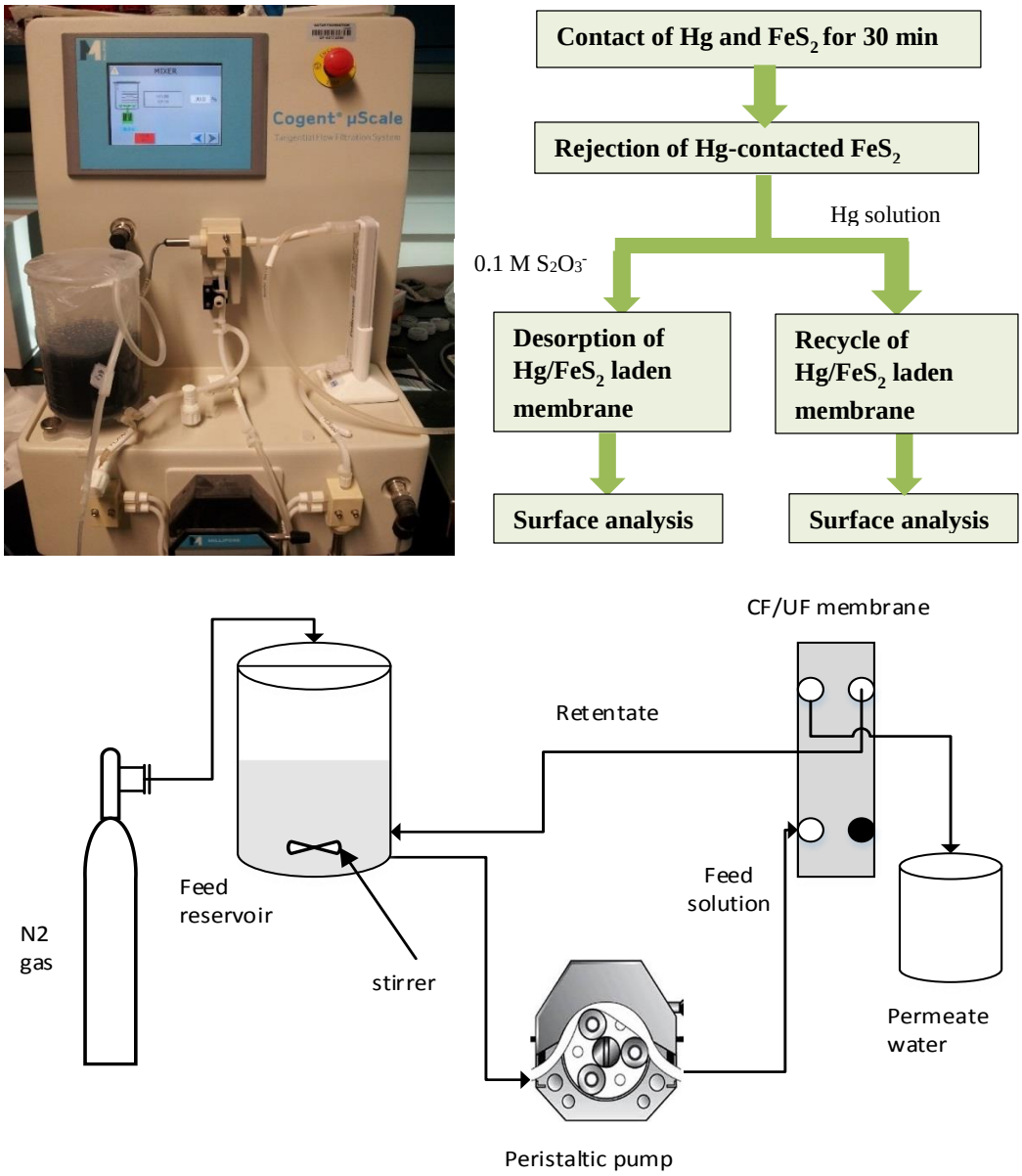

Figure 7. Schematic representation and flow chart of the cross-flow ultrafiltration membrane system experiments.

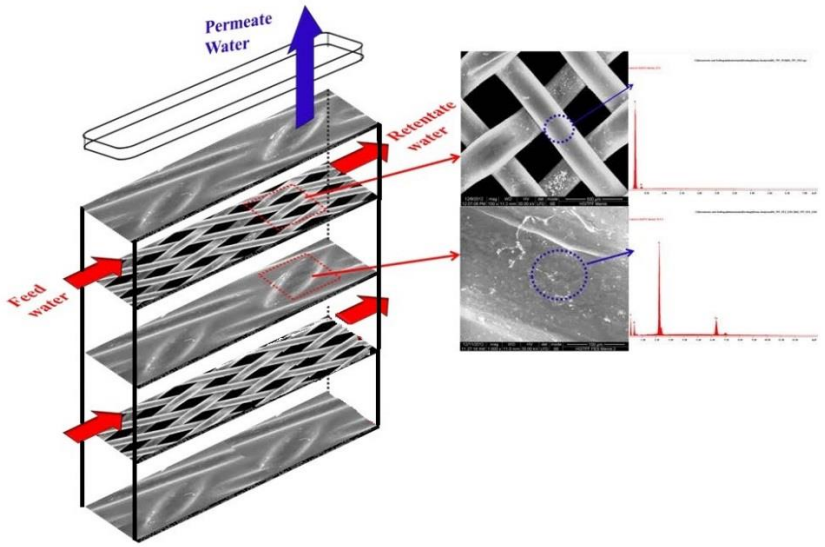

Figure 8. Structure of PES UF membranes and SEM/EDS images of PES membranes after contact with pyrite suspension.

3.6 Analysis of aqueous-phase and solid-phase samples

Permeate water collected from filtration experiments was analyzed for Hg, Fe and pH. The pH was monitored using thermo triode pH meter calibrated with 3 different standard buffers (4, 7 and 10 pH) to minimize the uncertainty of the determined pH value. Even using accurate standard solutions uncertainty cannot be reduced below ±0.02 pH units and can be increased by a factor of 2 while moving from 7 to 2 or 11 [114]. In this study, a standard error of ± 0.1 pH unit was assumed. Mercury concentration in permeate water was measured using cold vapor atomic absorption spectrometry (CV-AAS). The average recovery (accuracy) and the relative standard deviation (precision) of the Hg measurement were obtained to be 102 % and 2.7 %

respectively. A method detection limit (MDL) of CV-AAS was calculated as 8 μg/L. Total iron concentration in permeate water was measured by inductively coupled plasma optical emission spectrometry (ICP-OES). The average recovery and relative standard deviation of the Fe measurement were 99% and 2.9% respectively. The MDL was calculated as 11 μg/L.

3.7 Surface characterization of solid samples and membranes

The surface of solid samples were characterized using surface analysis techniques, including scanning electron microscopy (SEM) for sample's surface topography and composition and X-ray photoelectron spectroscopy (XPS) to analyze the surface chemistry (oxidation state) of a solid. Prior to SEM analysis, the membranes were coated with palladium/gold alloy through a vacuum-sputtering technique to prevent the accumulation of electrostatic charge at the surface. Otherwise, scanning faults or other image artifacts could occur. The secondary SEM images were collected at a working distance of 10-15 mm under the acceleration voltage of 20-25 kV. Image magnification ranged from 200 to ×80,000. The oxidation states of final solid deposited on the membrane were investigated using a Kratos Axis Ultra Imaging XPS. The XPS spectra were obtained using a monochromatic Al Kα X-rays. To correct shift of XPS spectra caused by charge effects, the binding energy of the C 1s at 284.6 ± 0.1 eV was used as an internal reference to calibrate all collected XPS spectra. The high resolution narrow scans for S 2P, Hg 4f, Fe 2P, O 1s and C 1s were collected under low pass energy of 20 eV with 10 sweeps to increase the signal-to-noise. All XPS spectra were

fitted using a XPSPEAK41 fitting program to convolute each XPS spectra for identification and quantification of surface element species.

4. RESULTS AND DISCUSSION

4.1 Dead end ultrafiltration

4.1.1 Rejection of Hg-contacted pyrite using DE/UF system

The DE/UF system was used to investigate the extent of rejection of Hg-contacted pyrite by 30 kDa regenerated cellulose (RC) UF membrane as affected by various parameters such as humic acid (HA) and competing anions (Cl^-, SO_4^{2-}, and NO_3^-). The experimental sets for Hg(II) removal by pyrite supported membrane system were classified as: 1) pyrite + Hg , 2) Pyrite + Hg + anion mixtures (10 mM Cl^-, 10 mM SO_4^{2-}, 10 mM NO_3^-), 3) pyrite + Hg + 0.2 mg/L HA, 4) pyrite + Hg + 1 mg/L HA. In the course of filtration, experimental data were presented in terms of flux, pH change, and Hg(II) and Fe concentration in permeate water.

Figure 9 shows flux decline of four different cases. Each solution showed severe flux decline due to membrane fouling. Membrane fouling can occur by pore constriction, pore blocking, or formation of cake layer by deposition of particles on the surface [80]. To evaluate the fouling mechanism, the flux model proposed in the literature [11, 80] was used. This model is presented by the following Equation:

$$J = J_0(1 + kt)^{-n} \quad (9)$$

Where, J is the flux at a given time t, J_0 is the initial flux, k is the empirical rate constant and n is the theoretical power corresponding to fouling mechanism. The values of 0.5, 1,

1.5 or 2 indicates that flux decline is due to the cake formation, internal pore constriction, partial pore blocking and complete pore blocking, respectively. In this study, all four values were applied to the flux decline model and model parameters were optimized using nonlinear regression with "nlinfit" function using MATLAB. The least value of the sum of squared residuals (SSR) provides a best fit of the model to experimental data. Table 2 shows that in the case when cake formation model was used (n = 0.5), SSR were minimum. Detailed graphs are presented in appendix. Therefore, the flux decline in Figure 9 is mainly caused by the cake formation on the surface of UF membrane. The other effects are negligible.

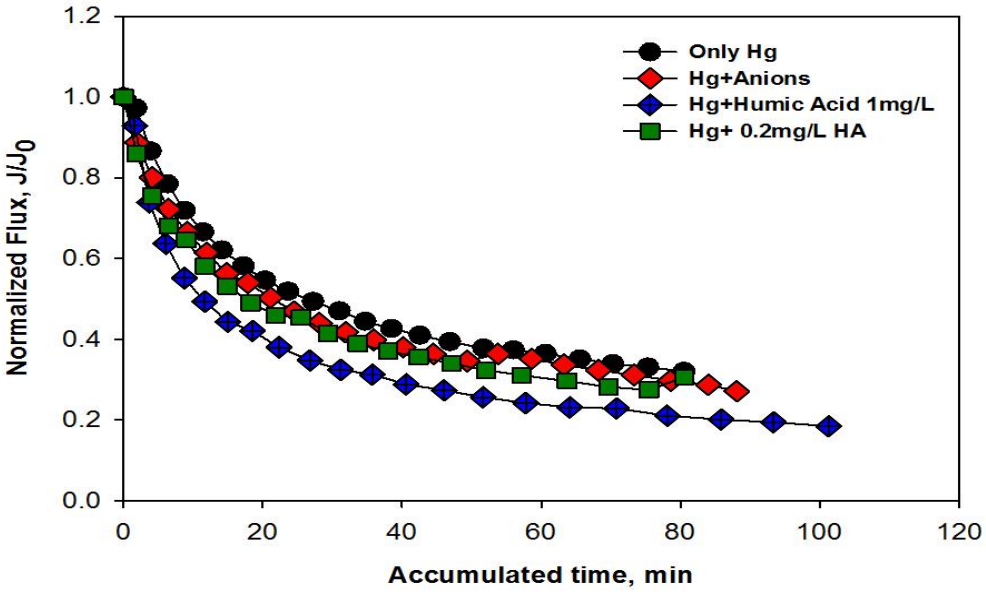

Figure 9. Flux decline of Hg(II)-contacted pyrite suspension using DE/UF system as affected by anions and HA. Conditions: 0.1 g/L pyrite, 1 mg/L Hg(II), 14.5 psi pressure, pH 8, 10 mM anions (Cl^-, SO_4^{2-}, NO_3^-), 0.2 and 1 mg/L HA.

Relatively lower permeability in the case of pyrite+Hg+HA as compared to other cases was observed. Membrane fouling would be a complicated phenomenon if organic substances are present. The co-presence of HA with Hg may result in high rate of flux decline due to the formation of irreversible gel-like compact cake layers [22, 115, 116].

Table 2. Summary of flux decline model parameters for experiments for rejection of Hg(II)-contacted pyrite under various solution compositions.

Sample	n = 0.5		n = 1		n = 1.5		n = 2	
	SSR	K	SSR	k	SSR	k	SSR	k
Only Hg	0.0054	0.1108	0.0291	0.0350	0.0573	0.0198	0.0770	0.0137
Hg + Anions	0.0024	0.1391	0.0516	0.0411	0.0967	0.0228	0.1273	0.0155
Hg + 1mg/L HA	0.0095	0.2560	0.0454	0.0692	0.0972	0.0372	0.1348	0.0250
Hg + 0.2 mg/L HA	0.0030	0.1651	0.0517	0.0484	0.0940	0.0267	0.1226	0.0182

Humic substances can form complexes with both Hg(II) [20, 24] and pyrite [25], finally creating macromolecules. Deposition of these larger macromolecule can make thick cake

layer on the surface of the membrane. HA are negatively charged because of presence of negatively charged carboxylic or phenolic group, eventually causing electrostatic repulsion between molecules of HA. However, complexation of HA with pyrite or with Hg could reduce electrostatic repulsion between HA molecules, which help to form coiled and spherical shape among them, finally producing a more compact layer on the surface of membrane [22, 38, 117]. However, there is no substantial difference in flux in case of Hg+0.2 mg/L HA comparing with solutions without HA. The flux decline depends on feed solution composition [118]. For HA, the flux decline of the case with 0.2 mg/L HA was not much different than with 1 mg/L HA. Moreover, with decreasing HA concentration, the size of complexation molecules can decrease [23, 113]. Reduced size of complexation molecules may result in thin cake layer on the surface of membrane, possibly leading to less flux decline. Similarly, the presence of anions also resulted in slightly greater flux decline than that of only Hg, because of deposition of precipitate salts on the membrane surface. The precipitated layer makes the Hg-contacted pyrite cake layer denser and thicker. The precipitated salt also can block pore entrance due to increased precipitated salt over filtration time.

Figure 10 shows several pictures of the membrane before and after filtration experiments and after drying in anaerobic chamber. After drying the membrane surface looks like yellowish color for all cases but more yellowish for both HA (Figure 10e, f). The change in color may be related to the oxidation of membrane surface. Quantitative analysis of elements by XPS (Figure 11) shows high percentage of elemental oxygen in all cases. High percentage of elemental oxygen would be resulted from exposure of

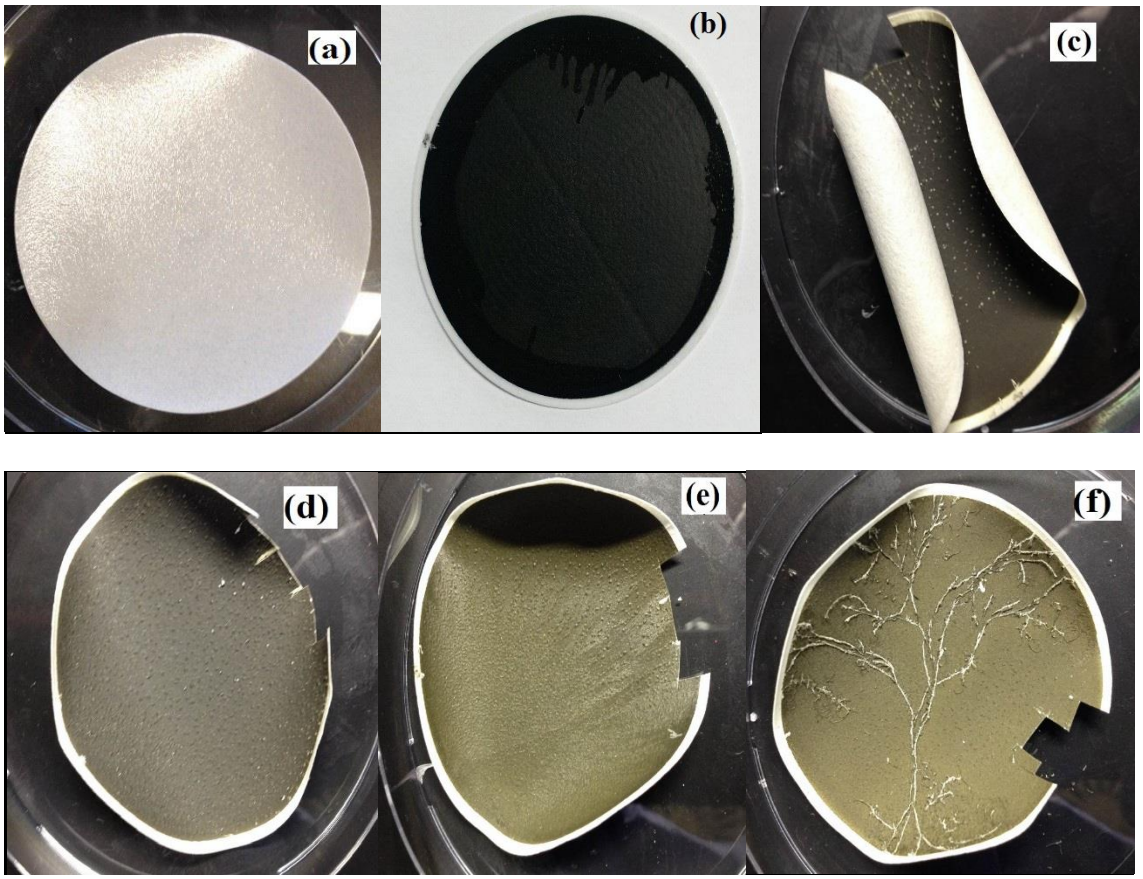

Figure 10. Images of RC membrane surfaces: (a) before filtration, (b) after filtration, and (c), (d), (e), and (f) are surface images of membrane for after drying in the anaerobic chamber in case of only Hg(II), Hg+anions, Hg+0.2 mg/L HA and Hg+1 mg/L HA respectively.

membrane to air during transportation to anaerobic chamber after experiments and during preparation of sample for SEM and XPS analysis.

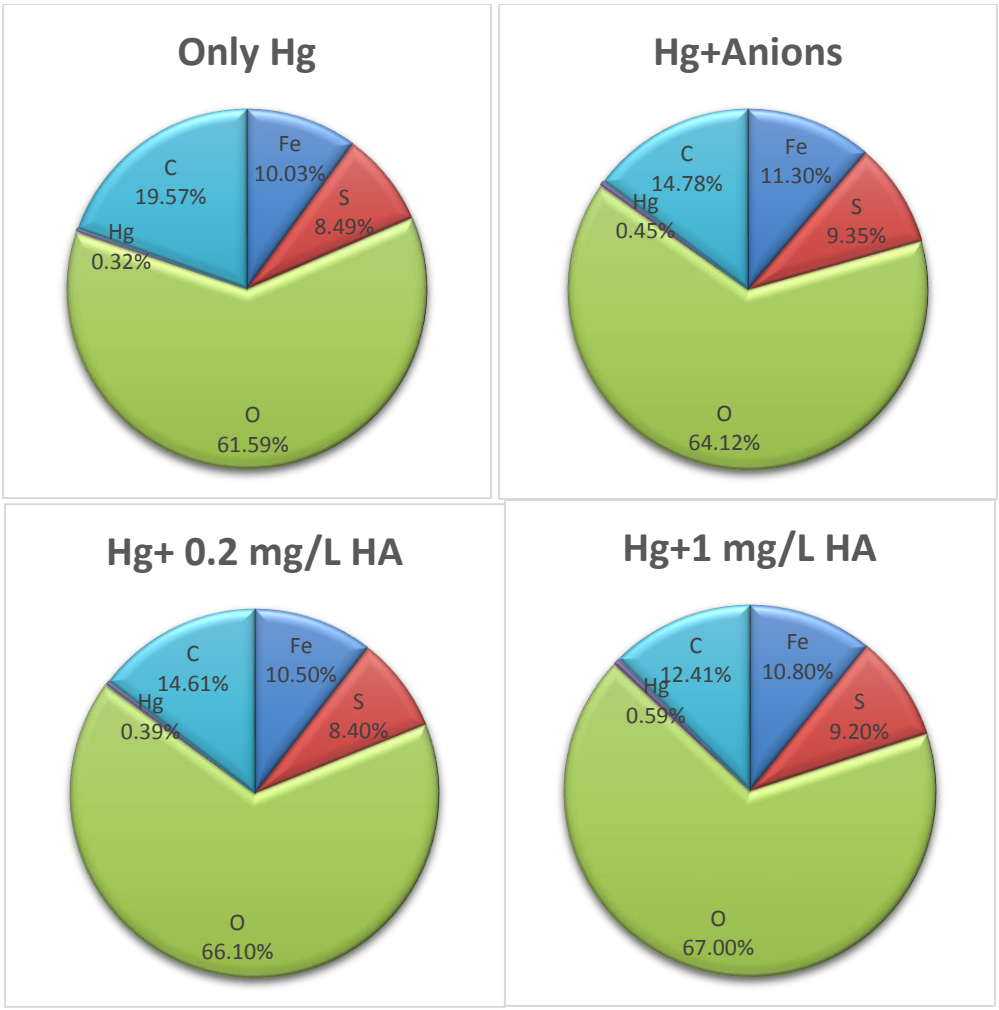

Figure 11. Quantitative analysis of elements on the membrane surface by XPS. Conditions: pH 8, anoxic conditions under 14.5 psi pressure.

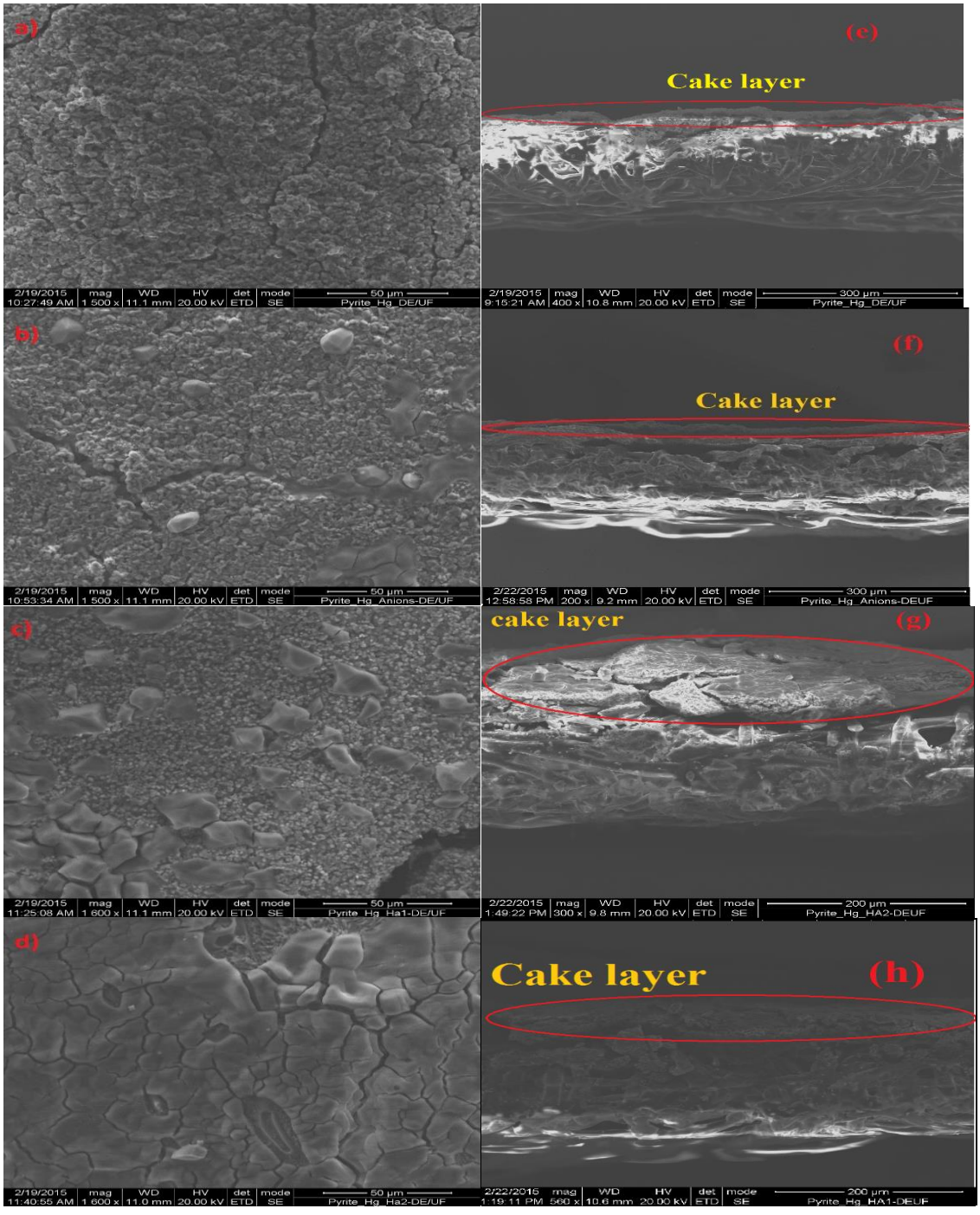

Figure 12. SEM images of RC membrane surfaces. Left side shows top view and right side shows cross sectional view of membranes for all conditions: (a, e) only Hg(II), (b, f) Hg+anions, (c, g) Hg+0.2 mg/L HA, (d, h) Hg+1 mg/L HA. Red circle denotes the cake layers. Conditions: pH 8, anoxic conditions under 14.5 psi pressure.

Figure 12 shows the top view and cross sectional view of SEM images of membrane surfaces for all conditions. The cross sectional images (Figure 12e, f, g, h) of the membrane surface depicts that Hg-contacted FeS_2 formed a thick cake layer on the membrane surface. No particle penetrated into the pore of the membrane. Top view images (Figure 12a, b, c, d) show that the cake layer covered the whole area of membrane surface. So, cake formation on the membrane surface was the dominant fouling mechanism in all cases. Top view images also show that in case of Hg and Hg+anions, fouling layers look like relatively porous whereas layers for case of Hg+0.2 mg/L HA is less porous and some gel like material over the porous material. In case of Hg+1mg/L HA, the surface was almost completely covered by gel-like layer. The deposition of the gel-like layer is attributed to highest flux decline comparing to others. The SEM images also show different morphology development on the membrane surface. There are many cube-like crystal particles which are major shape of pyrite, with their particles clusters evident in case of HA. The difference in morphology is related to the final solids resulted from the interaction of Hg(II) and pyrite in presence of different chemicals. This particle clusters may be related to the precipitation of Hg-HA on the membrane surface along with the complex of Hg-pyrite which might form cube-like structure.

At the same time, other parameters such as pH, concentrations of Hg and Fe in the same permeate water were measured and their relative experimental results are shown in Figure 13 and Figure 14. Figure 13a shows that the initial pH of 8 decreased to near pH 6 at all cases.

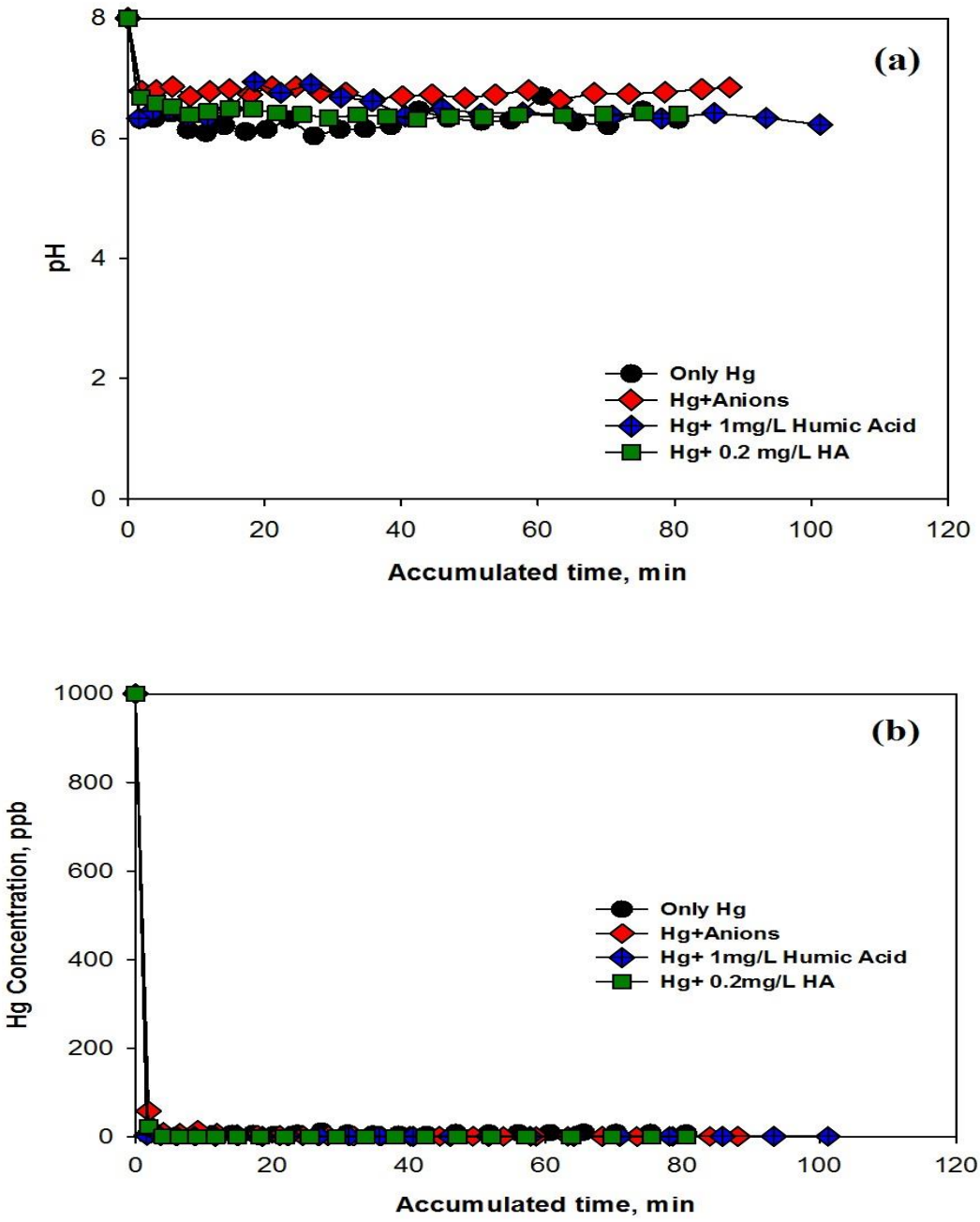

Figure 13. Time-profiled (a) pH and concentrations of (b) Hg in the permeate water obtained from DE/UF system for rejection of Hg(II)-contacted pyrite suspension as affected by anions and HA. conditions: 0.1 g/L pyrite, 1 mg/L Hg(II), 10 mM anions (Cl^-, SO_4^{2-}, NO_3^-), 0.2 and1 mg/L HA, 14.5 psi pressure, pH 8, anoxic condition.

The decrease of pH 8 to around pH 6 is likely due to sorption of Hg-hydroxo complexes onto pyrite surface by releasing proton into solution [1, 8, 23].

$$FeS_2 + Hg^{2+} + H_2O = FeS_2 \cdots\cdots Hg(OH)_n^{(2-n)+} + H^+ \quad (4.1)$$

Furthermore, pyrite is thermodynamically unstable in the aqueous media with dissolved oxygen [1, 119]. It cannot be ensured that the whole process is completely anoxic condition. During transferring the feed solutions from glove box to feed water reservoir, the feed solutions were partially exposed to air for few seconds. Pyrite oxidation is a complex phenomenon and possibilities are numerous. Both sulfur and iron (II) can be oxidized. Pyritic sulfur can be oxidized to sulfate by dissolved oxygen. But the oxidation of Fe(II) produce Fe(III) which is another oxidizing agent for pyrite, eventually leading to pyrite oxidation by both oxygen and Fe(III) and increase the acidity of the solution [1, 8, 119-122] as below reaction equations.

$$FeS_2 + 7/2\ O_2 + H_2O = Fe^{+2} + 2SO_4^{2-} + 2H^+ \quad 4.2$$

$$Fe^{+2} + 1/4\ O_2 + H^+ = Fe^{+3} + 1/2\ H_2O \quad 4.3$$

$$FeS_2 + 14\ Fe^{3+} + 8H_2O = 15Fe^{+2} + 2SO_4^{2-} + 16H^+ \quad 4.4$$

At neutral or basic pH, the oxidation kinetics was reported to be fast [27]. Slightly less pH decrease was observed in presence of anions in the solution comparing with other solutions. This may be due to the complexation between Hg(II) and anions

such as Hg-Cl_2 [123], resulting in less free Hg available for formation of Hg-OH^+ or FeS_2-Hg-OH complex.

In this study, all cases reached around 99% removal of Hg (Figure 13b), indicating that almost all mercury were adsorbed onto pyrite nanoparticles and the final solids were completely rejected by ultrafiltration membrane system. The presence of anions and HA didn't affect the removal efficiency of the system.

Figure 14 shows that Fe was not detected in the permeate water. As almost 100 % removal of mercury was achieved and there is no Fe in permeate water, the possibility of the formation of significant quantities of HgS which results from replacing Fe with Hg in the solid phase and release Fe can be eliminated. However, the possibility of formation of small amount of HgS cannot be ruled out by only the relationship between Hg removal and Fe release. None detection of Fe in permeate water can occur in two ways: a) Fe released due to structural substitution by Hg can be re-adsorbed on pyrite surface or precipitated as iron (hydr)oxide, b) No Fe release from pyrite at all. Our experimental methodology cannot distinguish between these two phenomena. Surface characterization technique such as XPS will be helpful to identify various reaction products and reaction mechanisms. Considering all of the aspects, adsorption of mercury species onto pyrite surface and the resulting surface complexation seems to be the most plausible removal mechanism of mercury as one of the various possible scenarios.

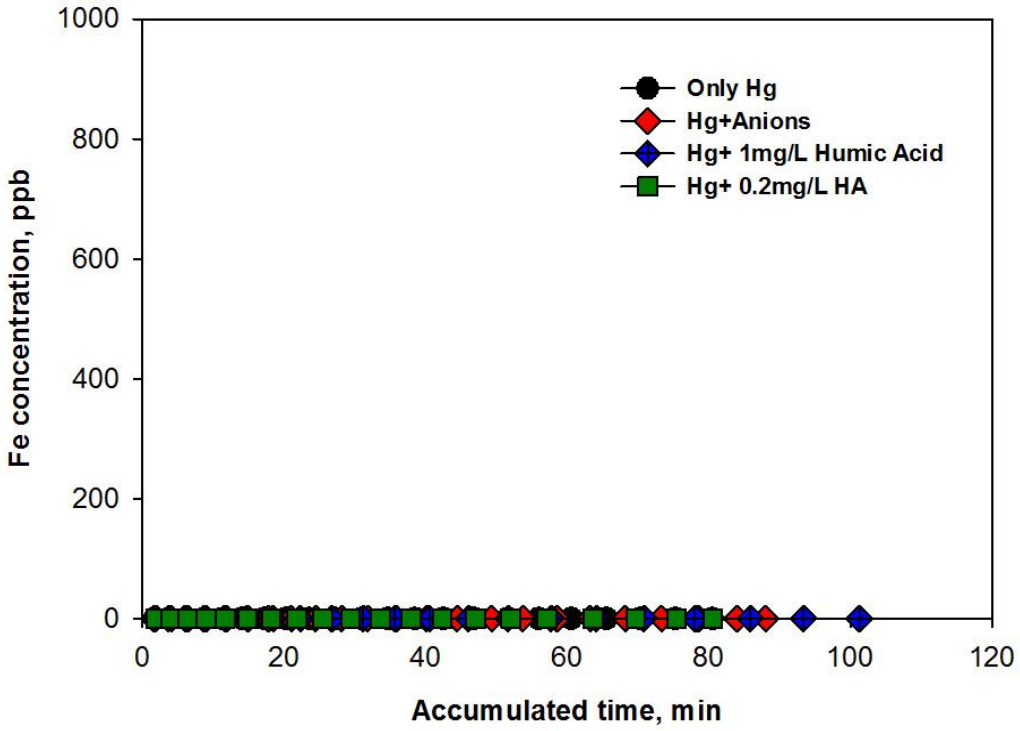

Figure 14. Time-profiled Fe concentration in the permeate water obtained from DE/UF system for rejection of Hg(II)-contacted pyrite suspension as affected by 10mM anions and HA: 0.1 g/L pyrite, 1 mg/L Hg(II),10 mM anions (Cl^-, SO_4^{2-}, NO_3^{2-}), 0.2 and 1 mg/L HA,14.5 psi pressure, pH 8, anoxic condition

4.1.2 Stability of Hg/pyrite-deposited DE/UF system

The physical and chemical stability of Hg(II)-contacted pyrite deposited on the membrane surface was evaluated using 0.1M thiosulfate concentration because thiosulfate has strong affinity [1, 17] for mercury. The chemical stability was evaluated by detecting Hg in the permeate water after flowing thiosulfate solution through the solids-loaded membrane. Figure 15 shows that there were no substantial changes in flux for all cases, indicating the transmembrane pressure (TMP) occurred by flow rate of

thiosulfate passed through all types of pyrite-deposited membrane which did not affect physically the cake layers formed on the surface of membrane.

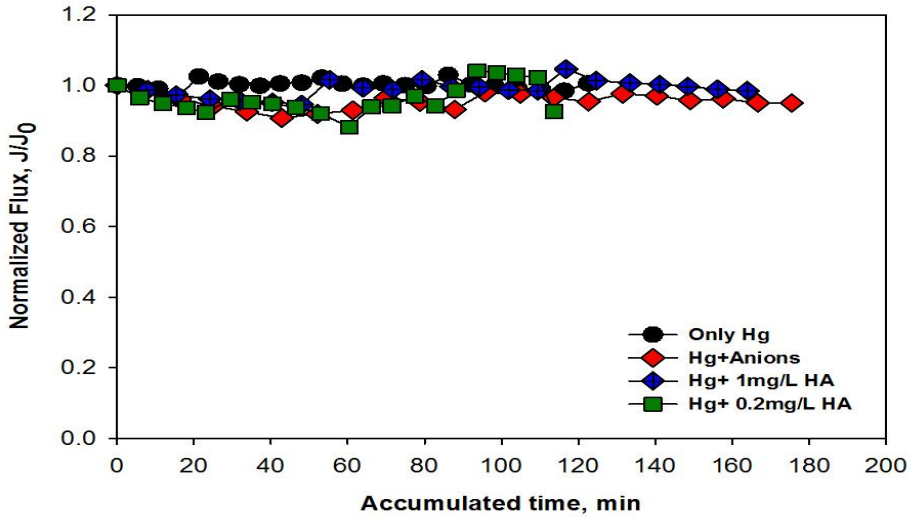

Figure 15. Flux decline of Hg(II)-, Hg(II)/anions-, Hg(II)/HA-contacted pyrite deposited on the membrane surface as fed by 0.1M thiosulfate ($S_2O_3^{2-}$) solution: 14.5 psi pressure, pH 8, anoxic condition.

To evaluate desorption of Hg and effect of thiosulfate on the behavior of the system, variation of pH and Hg concentration were monitored over time of flowing thiosulfate through solids-loaded membrane and the experimental results are shown in Figure 16. Herein, the range of pH (Figure 16a) varied between 7.5 and 6.8 for all experimental conditions, but the magnitude of change is not significant comparing with the rejection test in the second step (Figure 13). The change in pH may be due to the

interaction of thiosulfate with the solid deposited on the membrane. Thiosulfate can be oxidized to tetrathionate by residual dissolved oxygen or iron (III) mediated by pyrite [124]. Thiosulfate and tetrathionate can be decomposed to sulfate and proton via disproportionation reaction according to equation (4-5) and (4-6) [125] and pH of the solution.

$$S_2O_3^{2-} + H_2O = SO_4^{2-} + HS^- + H^+ \quad 4.5$$

$$S_4O_6^{2-} + 12H_2O = 9SO_4^{2-} + 7HS^- + 17H^+ \quad 4.6$$

Figure 16b shows that there was insignificant Hg release after contact with thiosulfate, which means that the pyrite contacted with Hg, or Hg/anions, or Hg/HA that were deposited on the membrane surface are very stable by formation of certain precipitates or surface complexes. For comparison, Behra (2001) [1] found more than 89% desorption of Hg form Hg(II)-contacted pyrite after 3 hours contact with 0.1M thiosulfate solution at pH 7.1. Hyland (1990) [17] also found around 90% desorption of Hg from the Hg(II)-contacted pyrite after contact with 0.1M thiosulfate at pH 6.7. The different level of sorption/desorption for Hg(II) may be due to different experimental conditions and characteristics of the pyrite utilized for Hg sorption. Also, anoxic conditions were not secured during the experiments conducted by Behra (2001) and Hyland (1990). Oxidation of pyrite surface results in the formation of a monolayer of iron(oxyhydroxides) [1] which is less reactive than pyrite for Hg(II). Also in those experiments relatively large amount of Hg was used in adsorption test compared to our

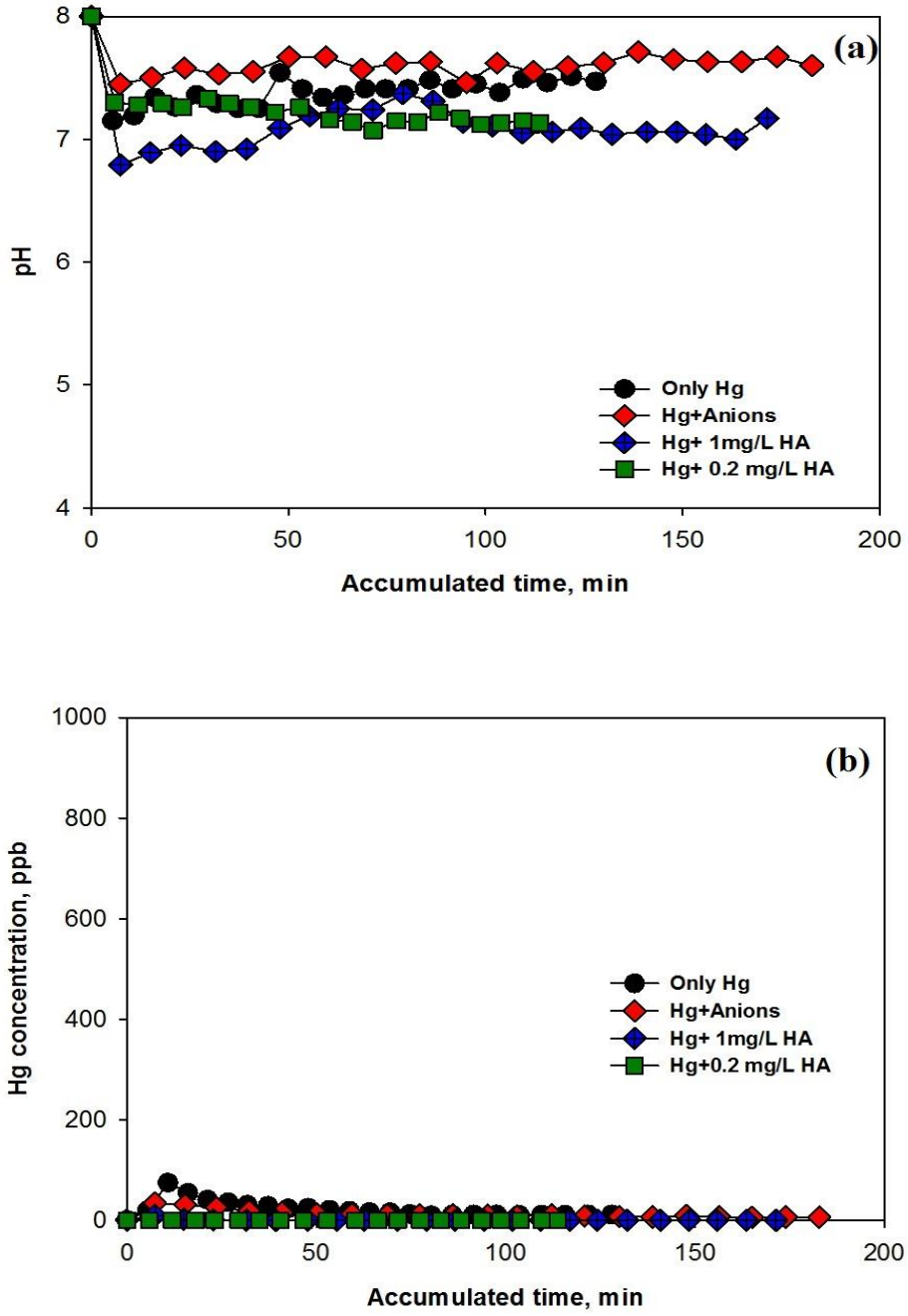

Figure 16. (a) pH and (b) Hg concentration for stability test of Hg(II), Hg(II)/anions-, Hg(II)/HA-contacted pyrite deposited on the membrane surface as fed by 0.1M thiosulfate ($S_2O_3^{2-}$) solution: 14.5 psi pressure, pH 8, anoxic condition.

experiments. Excess Hg may saturate the pyrite surface by forming a monolayer and results in a weakly bound species on the surface of monolayer.

However, in this study, detection of small amount of mercury in the permeate water were observed for cases of both only Hg(II) and Hg(II)/anions. It may be attributed to the mixed physical and chemical adsorption mechanisms. The physiosorbed Hg species are then desorbed by thiosulfate ligands. Also, in case of anions, the weakly bound Hg-Cl complex can be detached easily by strong thiosulfate ligands. It also suggest the possibility of more than one Hg species formed by interaction of Hg and different sorption sites of pyrite such as oxidized pyrite surface. Experiments conducted by Behra [1] also found low desorption of Hg at high pH using strong I^- ligands. It was suspected that pyrite surface was consisted of two surface sites; ≡S-H and ≡O-H sites, in which the Hg sorbed onto ≡O-H sites via co-oxo coordination, were desorbed by strong ligands. Hyland [17] found two types of S species in the interaction of Hg and PbS by XPS analysis in which one ($Hg_3S_2Cl_2$) was easily desorbed by thiosulfate solution at pH 6.7 while the other (HgS) was not desorbed.

4.1.3 Recycle of Hg/pyrite-deposited DE/UF system

To evaluate the remaining removal capacity of pyrites contacted with Hg, Hg/anions, or Hg/HA which were deposited on the membrane surface, additional feed solutions (i.e., Hg; Hg+anions; Hg+0.2 mg/L HA; Hg+1 mg/L HA) were prepared without pyrite and fed into DE/UF system under the same DE/UF operation conditions applied in the previous experiments. Figure 17a shows that flux was almost constant from the beginning to the end of recycle test for all types of feed solutions. In the recycle

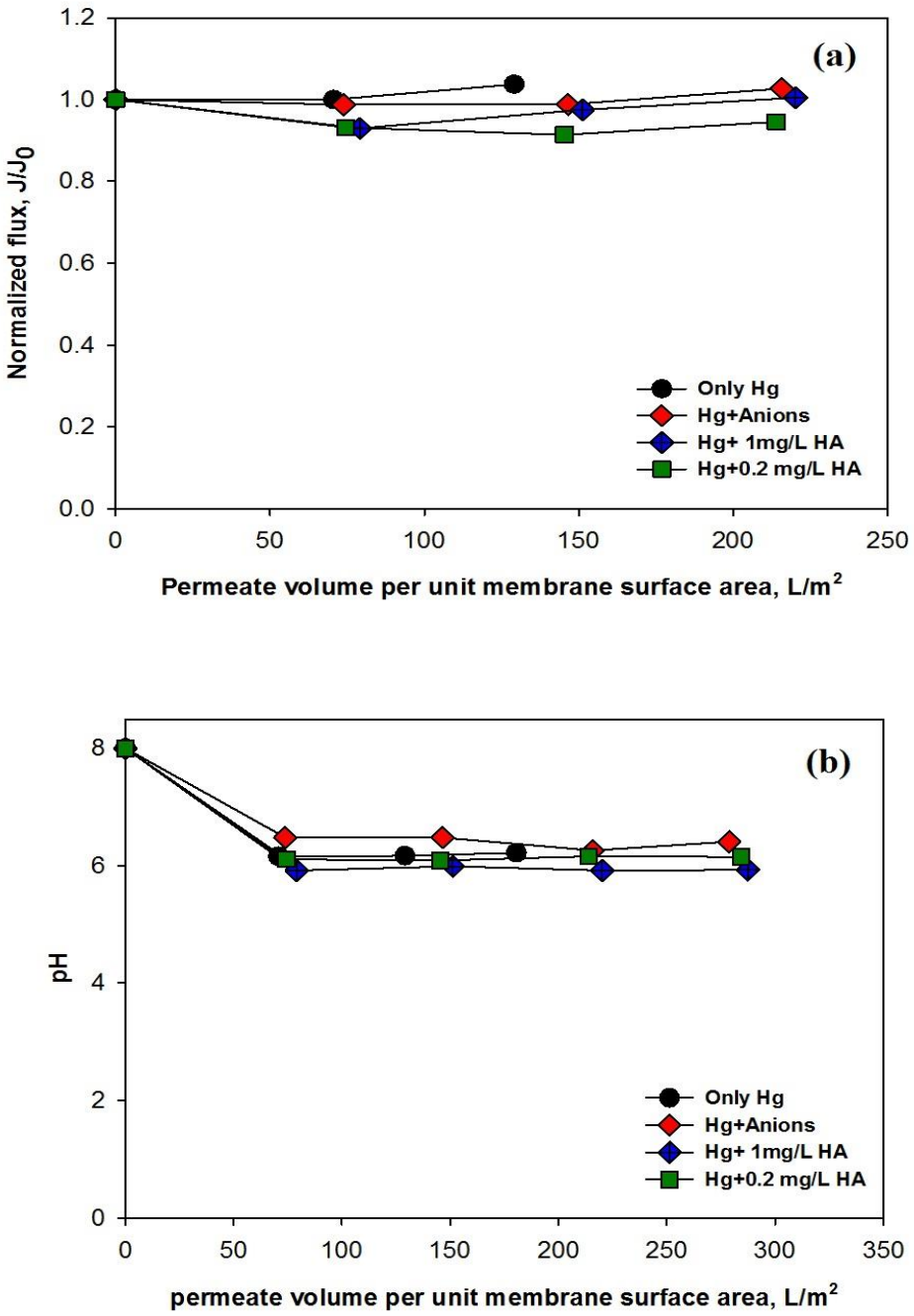

Figure 17. Results of experiment to determine additional removal capacity. (a) Normalized flux; (b) pH. Conditions: 1 mg/L Hg(II), 14.5 psi pressure, pH 8, 10 mM anions (Cl^-, SO_4^{2-}, NO_3^{2-}), 0.2 mg/L and 1 mg/L HA.

test, the added feed solution just passed through the membrane without making any physical impact on the cake layer. Figure 17b shows the change in pH with time. Similar to rejection test, pH was decreased to around 6 in all cases. Again, less decrease in pH in case of Hg+anions was observed. Similar mechanism of change of pH in rejection test is applicable here. In brief, the pH change indicates that the Hg(II) was adsorbed as hydrolyzed species(Hg-OH) on the surface of final solid deposited on the membrane. In case of Hg+anions, formation of Hg-anion complexes reduces the free Hg to make complex with OH. But the effect of anions is not much significant. And in case of HA, dissociation of HA along with ternary surface complexes of Pyrite-Hg-OH may attribute to the observed pH decrease.

However, % removal of Hg reached almost 100% and were constant until the ranges of permeate volumes (1L) that were applied in this study (Figure 18a). These results indicate that this system is efficient for continuous and complete removal of Hg from water. It also indicates further removal capability of DE/UF system for large volumes of Hg contaminated waters. Also, there was no significant release of Fe for all cases (Figure 18b).

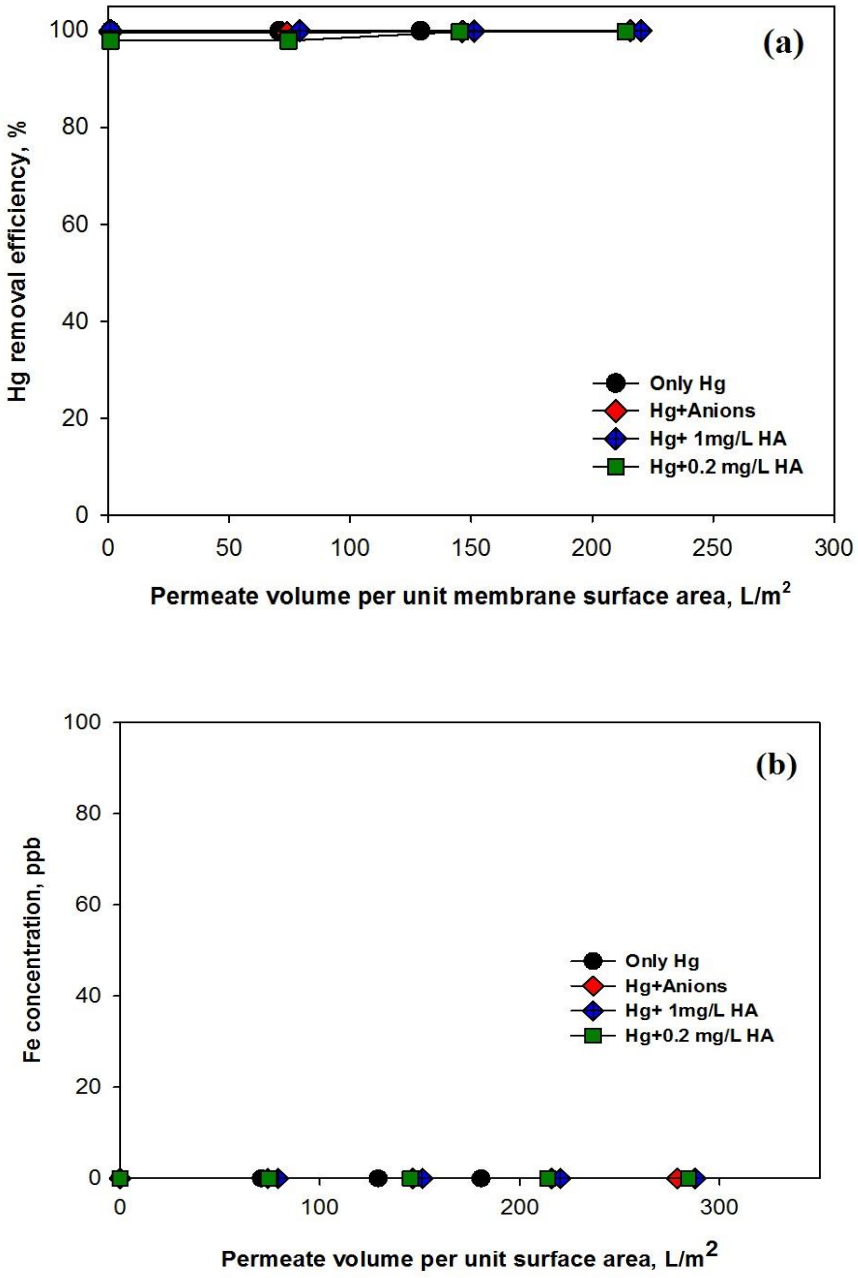

Figure 18. Results of experiment to determine additional removal capacity. (a) Hg concentration (b) Fe concentration. Conditions: 1 mg/L Hg(II), 14.5 psi pressure, pH 8, 10 mM anions (Cl^-, SO_4^{2-}, NO_3^{2-}), 0.2 mg/L and 1 mg/L HA.

4.2 Cross flow ultrafiltration

4.2.1 Rejection of Hg-contacted pyrite using CF/UF system

In order to evaluate the rejection of the final solids that were contacted with Hg(II) using cross flow ultrafiltration system, a 1000 kDa PES membrane with the mode of CF/UF under transmembrane pressure of 5 psi was used for this purpose. For a series of the filtration experiments in the Step I and II, various experimental conditions were considered: 1) Hg alone, 2) Hg + anions, 3) Hg + 1 mg/L HA, 4) Hg + 0.2 mg/L HA. The obtained experimental data are described in terms of flux, pH change and Hg(II) and Fe concentrations in permeate water.

Figure 19 shows that the flux declines in all experimental sets over filtration time, with significant decline in the solution containing Hg+1 mg/L HA. The observed flux decline could be from the formation of cake layer due to the deposition of Hg-contacted solids on the membrane surface, pore constriction and partial or complete pore blocking. The co-presence of HA with Hg may form irreversible gel like compact layer, eventually resulted in more flux decline. Similar pattern of flux decline was also observed for the experiments using DE/UF system as described in previous sections. However, the CF/UF showed higher permeability rate than that of DE/UF. This may be due to the differences in pore sizes. The membrane with larger pore size is expected to show better permeability than membrane with small pore size. The pore sizes of CF/UF membrane (0.13 μm) is larger than that of DE/UF membrane (0.004 μm). Another possible reason for improved flux is the occurrence of shear flow in CF/UF system in which feed solution is flowing tangentially with the membrane surface.

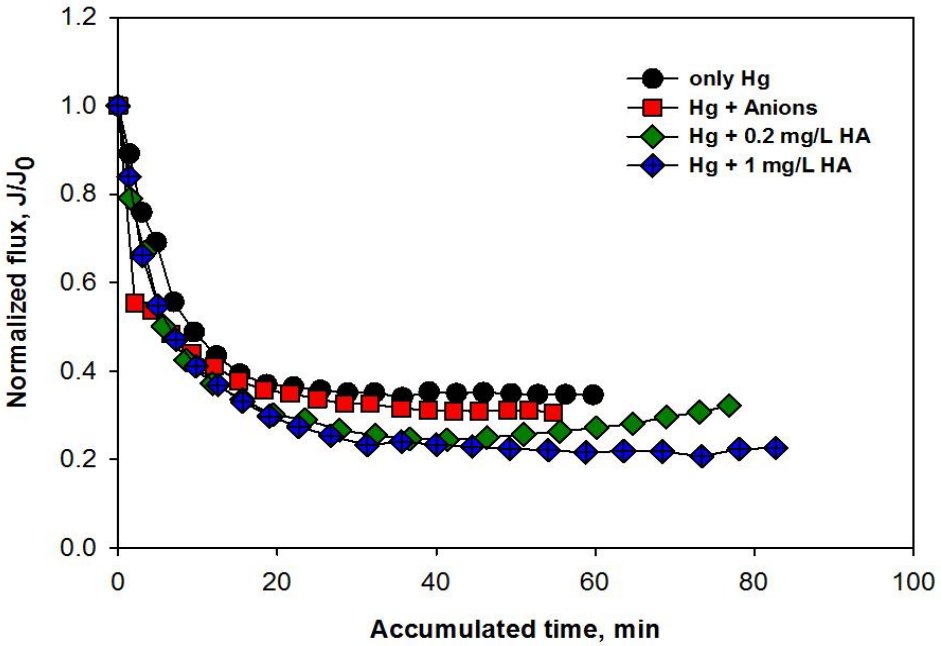

Figure 19. Flux decline of Hg(II)-contacted pyrite suspension using CF/UF system as affected by anions and HA: 0.1 g/L pyrite, 1 mg/L Hg(II), 5 psi transmembrane pressure, pH 8, 10 mM anions(Cl^-, SO_4^{2-}, NO_3^-), and 0.2 and 1 mg/L of HA.

The vibratory shear flow can prevent retention of materials on the membrane surface and increase permeate flux [11, 126].

Figure 20 shows the SEM images of PES ultrafiltration membrane obtained after filtrating each feed water containing different solution compositions. The cross-sectional and top-view SEM images of the membrane surface indicate that a thick cake layers were formed on the surface of the membrane and these layers are more substantial in the presence of HA. Also, there were no depositions of particles inside the pore.

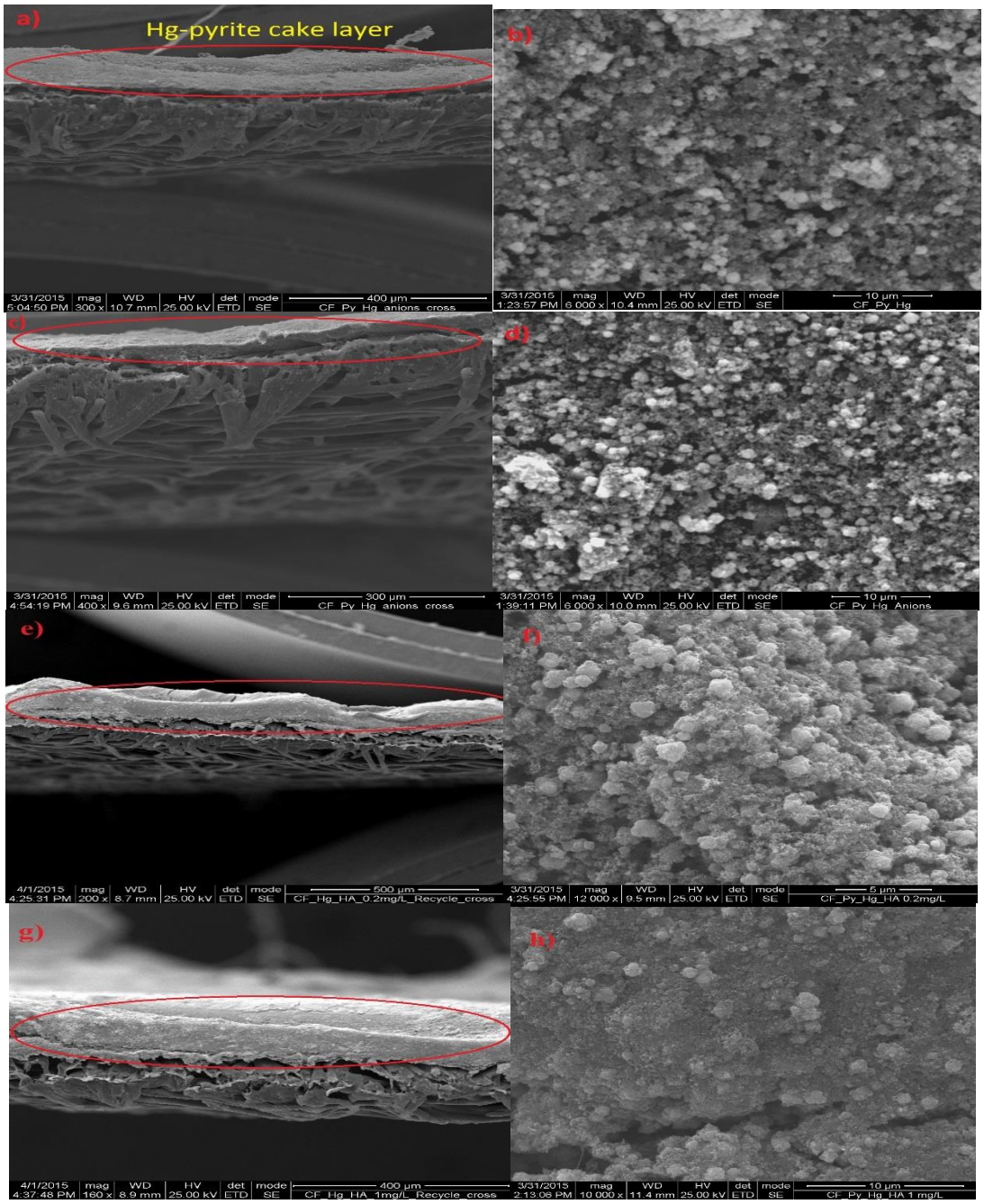

Figure 20. SEM analysis of PES CF/UF membrane after rejection test. Red circles denote cake layer. Left side shows cross sectional view and right side shows top view of membrane; (a,b) only Hg, (c,d) Hg+anions, (e,f) Hg+0.2 mg/L HA, (g,h) Hg+1 mg/L HA. Conditions: pH 8, 5 psi transmembrane pressure and anoxic condition.

Thus, these SEM results can support the hypothesis that the flux decline in the CF/UF system is attributed to fouling resulted from formation of cake layers on the membrane surface. In addition, the top-view SEM image of the solids deposited on the membrane for the case of Hg+1mg/L HA shows more dense gel-like layers than the case of Hg+0.1 mg/L HA. Thus, the higher flux decline in case of Hg+1mg/L can be caused by deposition of more dense gel-like layers on the membrane. Regardless of the type of feed water, the particles on the membrane show crystalline cubic shape of the pyrite and they are present with particle clusters.

Accordingly, the change of pH and concentrations of Hg in the same permeate water were monitored over filtration time and the experimental results are presented in Figure 21. Similar to DE/UF, considerable drop of pH was observed in all cases due to possible behavior that was described before in ‘Section 4.1.1.

Figure 21b shows Hg concentration in permeate water. Similar to DE/UF membrane system, the CF/UF membrane system completely rejected the final solids of Hg(II)-contacted pyrite, pyrite-Hg(II)-HA or pyrite-Hg(II)-anions by a fact that there is no release of Hg(II), except at initial filtration time when small amount of Hg was detected in the case of Hg without anions or HA. However, comparing with initial concentration of Hg(II), the released amount is very low.

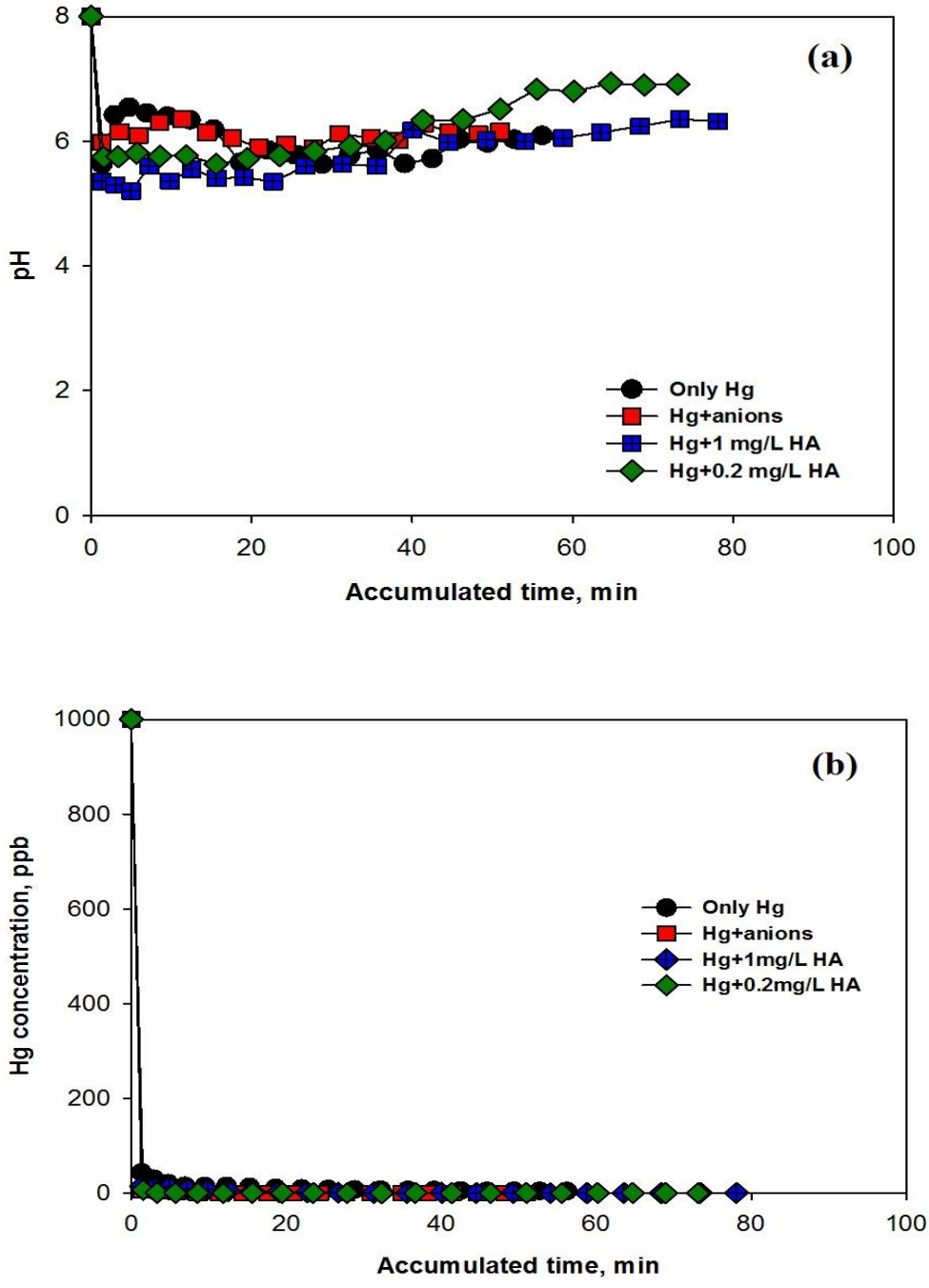

Figure 21. Measurement of (a) pH and (b) concentrations of Hg in the permeate water as affected by anions and HA: 0.1 g/L pyrite, 1 mg/L Hg(II), 5 psi transmembrane pressure, pH 8, 10 mM anions (Cl^-, SO_4^{2-}, NO_3^-), 0.2 and 1 mg/L HA.

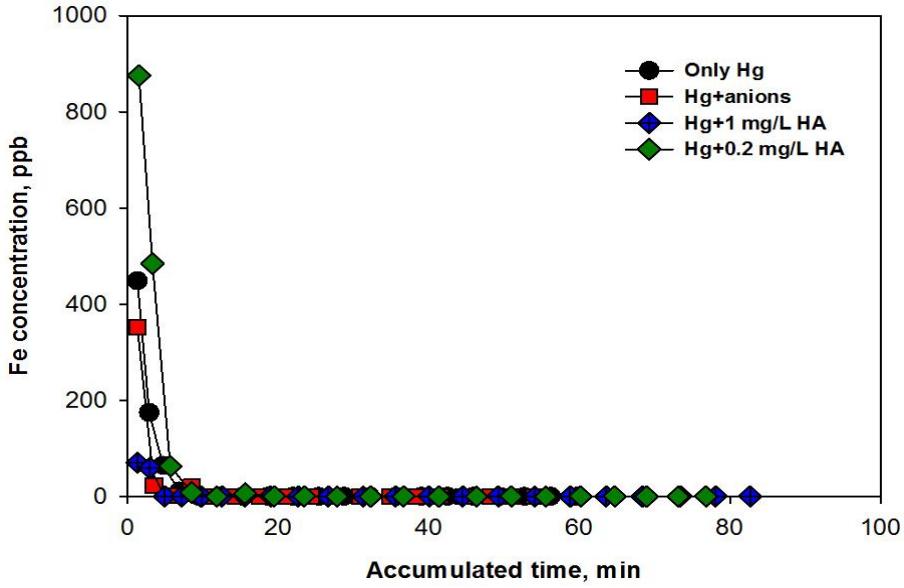

Figure 22. . Measurement of Fe concentration in the permeate water as affected by anions and HA: 0.1 g/L pyrite, 1 mg/L Hg(II), 5 psi transmembrane pressure, pH 8, 10 mM anions (Cl^-, SO_4^{2-}, NO_3^-), 0.2 and 1 mg/L HA.

Fe concentration in permeate water is shown in Figure 22. There was no release of Fe ions in the permeate water after 10 minutes of filtration, although some extent of Fe concentration was observed in all cases at the beginning of the experiment. This release might be related to leakage of small-sized pyrite particles through the membrane before cake layer formation.

4.2.2 Stability of Hg/pyrite-deposited CF/UF system

Once step II of the experiment was finished, desorption tests (step III) of Hg(II) being bonded to pyrite deposited on the membrane were subsequently performed with 0.1M thiosulfate solution. Figure 23 shows that no significant change of the flux of

thiosulfate solution through the final solids deposited on the membrane displayed after contact with 0.1M thiosulfate, meaning that cake layers formed by the pyrite solids on the membrane surface are chemically stable.

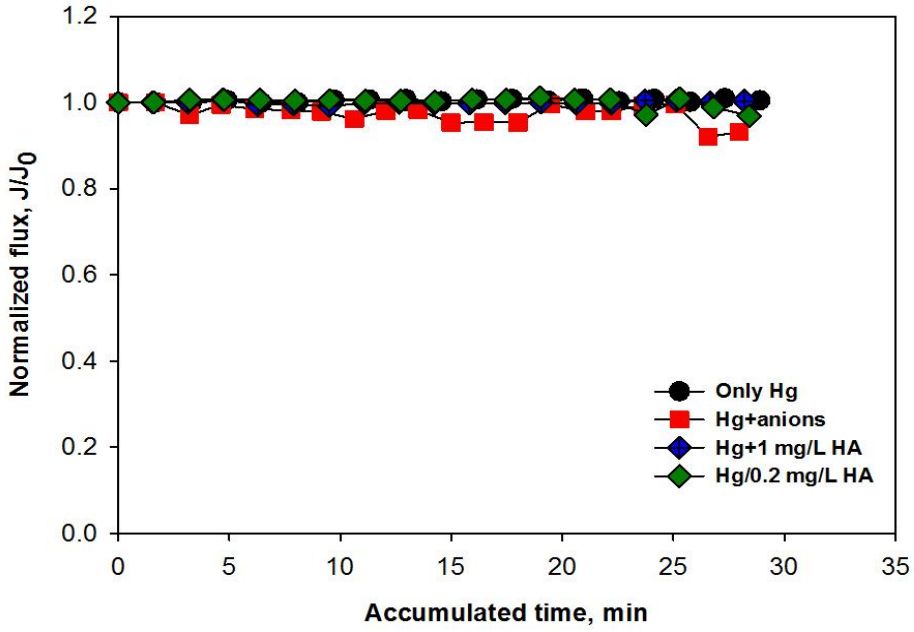

Figure 23. Time profiled flux decline for stability test of Hg(II), Hg(II)/anions-, Hg(II)/HA-contacted pyrite deposited on the membrane surface as fed by 0.1M thiosulfate ($S_2O_3^{2-}$) solution: 5 psi transmembrane pressure, pH 8, anoxic condition.

In all cases, pH initially decreased to around 7 (Figure 24a), with no significant variations of pH over filtration time, indicating that after contact with Hg-contacted pyrite, there is no further specific chemical reactions which may result in the release of proton caused by either complexation of thiosulfate with Hg-pyrite complexes or the

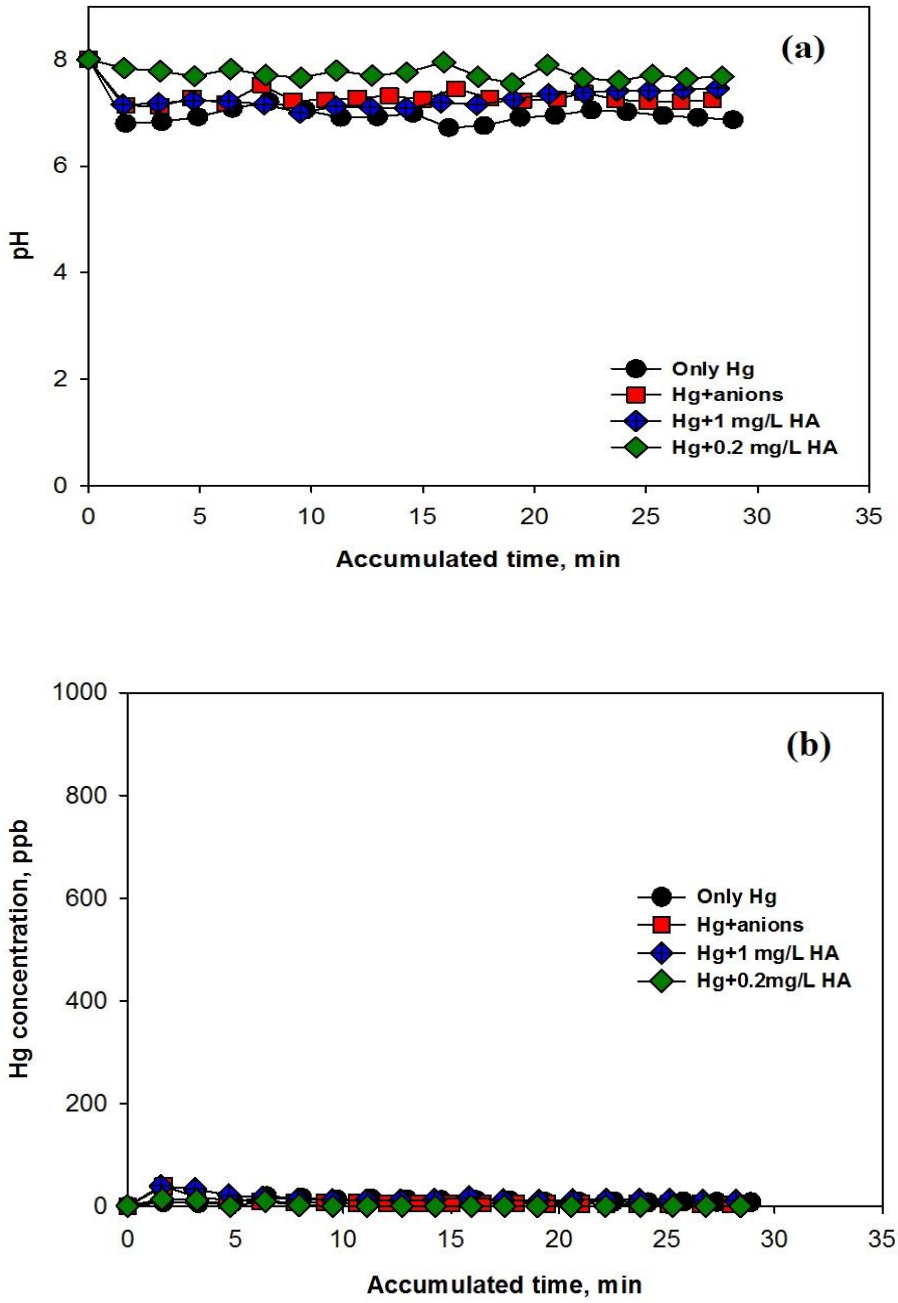

Figure 24. Time profiled a) pH and b) Hg concentration in permeate water for stability test of Hg(II), Hg(II)/anions-, Hg(II)/HA-contacted pyrite deposited on the membrane surface as fed by 0.1M thiosulfate ($S_2O_3^{2-}$) solution: 5 psi transmembrane pressure, pH 8, anoxic condition.

resulting structural change of the pyrite. Thus, the Hg(II) being bonded to final solids retained on the membrane is chemically stable. Thiosulfate can be partially oxidized to tetrathionate by dissolved residual oxygen [124].

Small amount of Hg(II) was detected in all solutions with concentration levels less than 20 μg/L after 5 minutes of filtration of thiosulphate solution (Figure 24b). The occurrence of Hg(II) in the permeate water might be caused by a little amount of the relative weak complexes of Hg(II) with pyrite that would be easily broken by shear flow occurred by cross-flow mode. That will be true for only initial contact time of thiosulphate solution during desorption test. In general, the surface of pyrite consists of two sorption sites[1] such as ≡S-H and ≡Fe-OH sites, in which Hg(II) sorbed onto ≡Fe-OH sites can be desorbed by strong ligands, whereas the Hg(II) associated with ≡S-H sites cannot be desorbed easily by thiosulphate. As the amount of Hg desorbed by thiosulfate is apparently very low after 5 minutes of initial filtration time, it can be said that the percentage of the latter species is predominant over the former species.

4.2.3 Recycle of Hg/pyrite-deposited CF/UF system

To investigate the additional sorption capacity of all types of solids-deposited UF membrane for Hg(II) (recycle test), additional volumes of Hg(II) solutions were fed into CF/UF system without or with anions and humic acid in a way that was conducted in the previous step (Step I and II) excluding Step III. Figure 25a shows that flux was almost constant from the beginning to end of recycle test for all types of feed solutions. The added feed solution just passed through the membrane while Hg(II) was being deposited onto the membrane without making any physical impact on the cake layer.

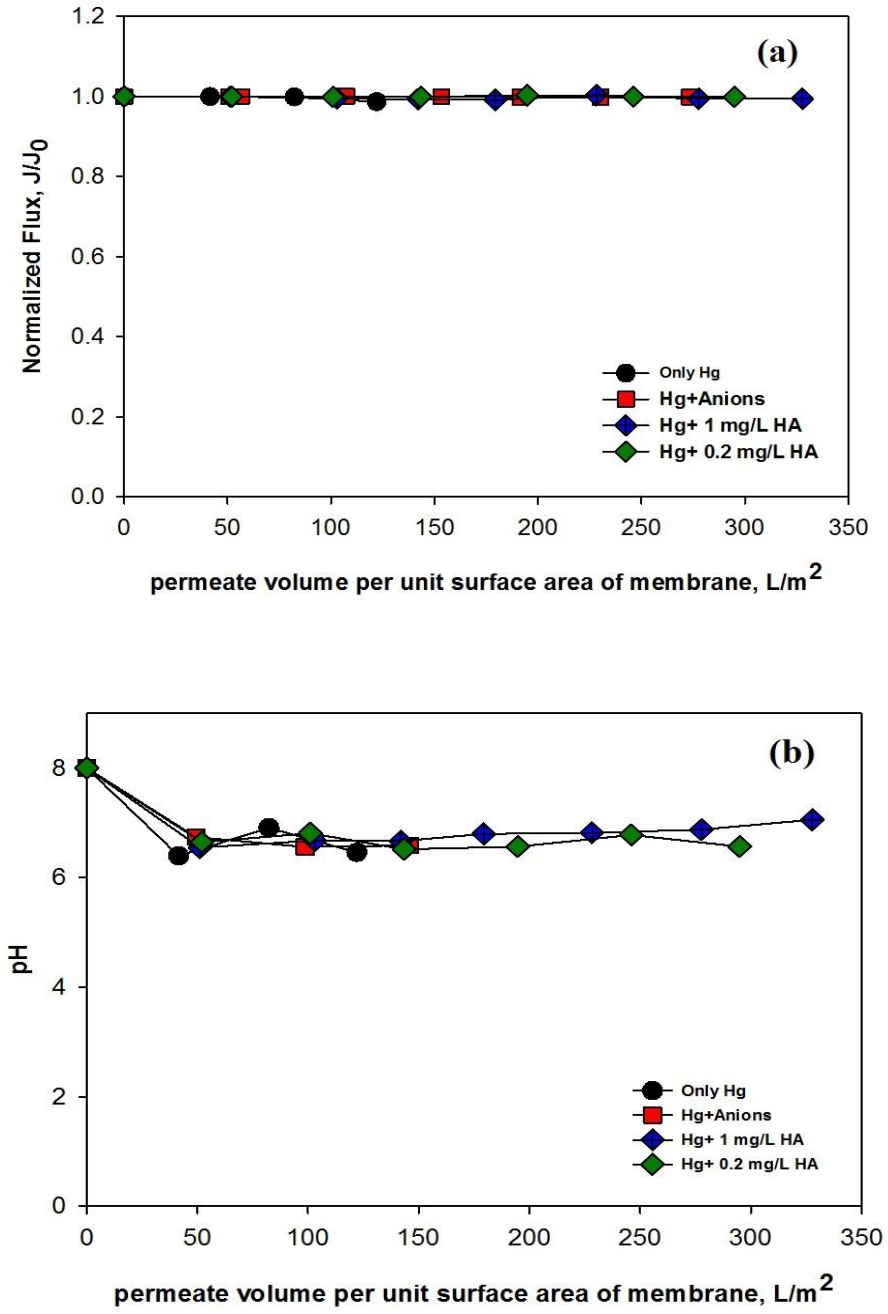

Figure 25. a) Normalized flux and b) pH in experiments for determining additional removal capacity. Conditions: 1 mg/L Hg(II), pH 8, 10 mM anions (SO_4^{2-}, NO_3^-, Cl^-), 0.2 and 1 mg/L HA, 5 psi transmembrane pressure.

These additional feed solutions are not involved in fouling that cause flux decline. In the recycle test, changes of pH (Figure 25b) in permeate water for all cases were similar to pH changes in all cases for DE/UF system and rejection test for CF/UF system, where the pH is believed to be affected by surface complexes of hydrolyzed species or formation of precipitates of Hg with pyrites in the presence or absence of anions or HA.

However, almost 100% of Hg was removed for all cases and this removal level was continued until complete consumption of all feed solutions (Figure 26a). Similar results were obtained in case of DE/UF, although the volume of feed solution in the case of CF/UF system was twice the volume used in DE/UF system. Significant amount of Fe was found in the permeate water for case of Hg + 1 mg/L HA, while other cases show no detection of Fe in the permeate water (Figure 26b). With increasing HA concentration, pyrite surface can reach to saturation by adsorption of HA. After saturation, excess HA may induce surface reaction between HA and pyrite and results in dissolution of Fe into solution. That is why solutions containing 1 mg/L HA showed higher Fe release than that of 0.2 mg/L HA. In case of anions, as anions form nonsorbing complex, the possibility of pyrite surface saturation by anions can be ruled out.

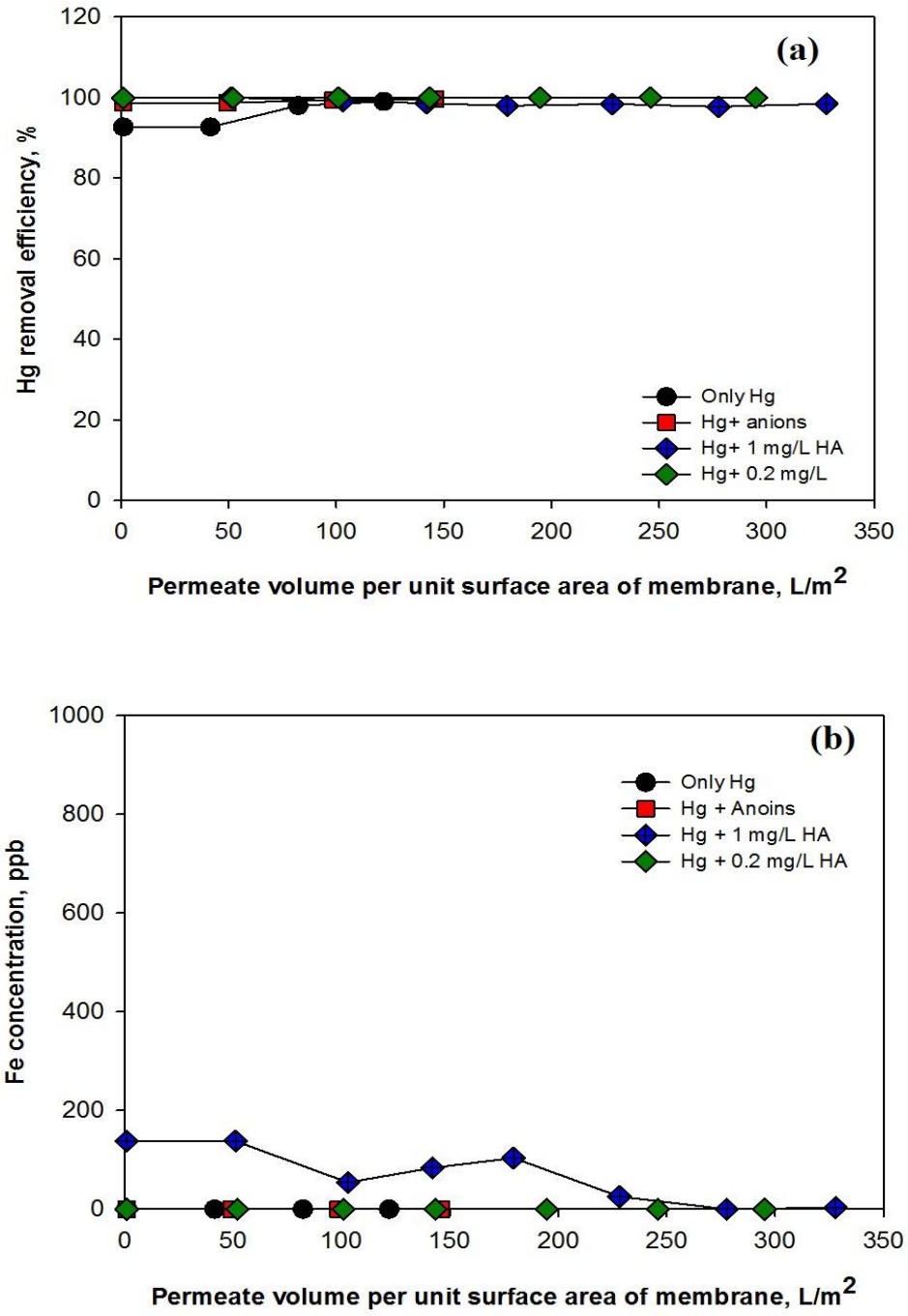

Figure 26. a) % of Hg removal and (b) Fe concentration in permeate water collected from experiments for determining additional removal capacity. Conditions: 1 mg/L Hg(II), 5 psi transmembrane pressure, pH 8, 10 mM anions (SO_4^{2-}, NO_3^-, Cl^-), 0.2 and 1 mg/L HA.

5. CONCLUSION

This study investigated the removal of mercury(II) from wastewater by pyrite (FeS_2) and the separation of its final solids using ultrafiltration membrane system. The membrane systems used in this study for separation of the final solids were dead-end (DE/UF) and cross flow (CF/UF) ultrafiltration membrane systems. The overall treatment system is called reactive adsorbent membrane (RAM) process. The first task for the RAM process was to synthesize nanoparticles of pyrite using microwave digestion method, and SEM analysis showed that synthesized nanoparticle pyrite was compromised of about 83% of the particles have average particle size of 400 nm.

In the DE/UF system, Hg(II)-contacted pyrite was completely rejected by the membrane. Presence of anions and humic acid (HA) did not affect the rejection of Hg(II)-contacted pyrite. However, flux decline in case of Hg + 1 mg/L HA + pyrite was found to be faster than that of other cases. The order of flux decline is: Hg +1mg/L HA + pyrite > Hg + 0.2mg/L HA + pyrite > Hg + anions + pyrite > Hg + pyrite. To evaluate the fouling mechanism, a flux decline model was used and the model parameters were optimized by nonlinear regression using MATLAB. Based on values of sum of squared residuals (SSR) between the results of flux decline model and experimental data, the membrane fouling was ascribed to the formation of cake layer on the membrane surface The SEM analysis supported the formation of such cake layer on the membrane surface with no internal pore blocking by particles. It was evident from the SEM images that the presence of HA exacerbated the fouling by making irreversible gel-like cake layers on

the membrane surface. Meanwhile, considerable pH decrease was observed in the permeate water for all cases. For the case of Hg+pyrite, the complexation of hydrolyzed species of mercury (Hg-OH) with pyrite would be the main reason for the pH decrease. In case of anions, relatively less pH decrease was observed because of the formation of nonsorbing Hg-anions complexes which are able to reduce the free Hg ions to be sorbed as Hg-OH complexes. In case of Hg+HA, the dissociation of HA may be responsible for pH decrease. However, there was no significant release of Fe in the permeate water for all cases. This may rule out one of our hypothesis that HgS can form by the structural substitution of Fe by Hg, but the released Fe can re-sorb onto the pyrite surface.

Desorption experiment using 0.1 M sodium thiosulfate ($Na_2S_2O_3$) solution showed that most of the mercury that had been adsorbed by pyrite still remained on the membrane surface after contacting with thiosulfate solution, indicating that Hg(II)-containing stable solid residuals were formed by pyrite. Meanwhile, there was no change in flux during the desorption test, indicating that thiosulfate passed through the cake layer on the membrane without affecting the structure of the cake layer. Slight decrease of pH in the permeate water was observed during the desorption test, possibly due to the interaction of thiosulfate with the solid deposited on the membrane surface or decomposition of thiosulfate by disproportionation reaction.

To evaluate additional mercury removal capacity of Hg-contacted pyrite deposited on the membrane, recycle test was conducted by reusing the Hg/pyrite-laden membrane for treating additional volumes of water contaminated with Hg(II). Results showed almost 100% removal of mercury until the consumption of all feed solution

volume that was applied without any physical impact on the cake layer. Other results such as pH change and Fe release showed almost similar pattern that were observed in rejection test. These results indicate that the proposed method using DE/UF successfully meet the objective of this study for continuous and efficient removal of Hg(II) from wastewater or water contaminated with mercury.

The CF/UF system showed almost similar results that were observed in the DE/UF system. However, the CF/UF system showed relatively better flux compared to the DE/UF system. This may be due to the larger pore size of the membrane used in the CF/UF system and occurrence of shear flow near the surface of CF/UF membrane which can prevent the accumulation of particles on the membrane surface. Also, release of Fe were observed at the beginning of the experiment when CF/UF was used, possibly due to the partial dissolution of pyrite by surface oxidation or formation of small amount of HgS and substitution of Fe by Hg. However, the amount of Fe released is so small that can be considered negligible. Desorption test for the CF/UF system showed similar behavior to that observed with DE/UF

For recycle test, the CF/UF system showed almost complete (100%) removal of Hg(II) from feed water that was provided by a double amount of the feed water supplied in the recycle test for the DE/UF system. Therefore, the CF/UF system is successfully proven for meeting the objectives of this study that the methodology suggested here will provide continuous and complete removal of Hg(II) from wastewater or water contaminated with mercury.

The final goal of this research was to develop a treatment technology for continuous and complete removal of mercury from wastewater. The proposed reactive adsorbent membrane (RAM) hybrid process successfully demonstrated the continuous and complete removal of mercury from water. However, the effect of other operational parameters such as pressure and temperature on the efficiency of the RAM process for mercury removal needs to be further examined. The stability of final residuals should be evaluated in oxic condition. Use of other surface analysis techniques such as Extended X-Ray absorption fine structure (EXAFS), Fourier Transform Infrared Spectroscopy (FTIR) will help us to better understand the reaction mechanism between pyrite and mercury in the presence of various solution compositions.

REFERENCES

1. Behra, P., *XPS and XAS study of the sorption of Hg(II) onto pyrite.* Langmuir, 2001. **17**(13): p. 3970-3979.
2. Urgun Demirtas, M., *Achieving very low mercury levels in refinery wastewater by membrane filtration.* Journal of Hazardous Materials, 2012. **215-216**: p. 98-107.
3. Peters, R.W., Y. Ku, and D. Bhattacharyya, *Evaluation of recent treatment techniques for removal of heavy metals from industrial wastewaters.* AlChE Symposium Series, 1985. **81**: p. 243.
4. Ritter, J. and J. Bibler, *Removal of mercury from waste-water - Large-scale performance of an ion-exchange process.* Water Science and Technology, 1992. **25(3)**: p. 165-172.
5. Wagner Dobler, I., *Removal of mercury from chemical wastewater by microoganisms in technical scale.* Environmental Science & Technology, 2000. **34**(21): p. 4628-4634.
6. Fu, F. and Q. Wang, *Removal of heavy metal ions from wastewaters: A review.* Journal of Environmental Management, 2011. **92**(3): p. 407-418.
7. EPA/625/R-97/004, *Aqueous mercury treatment, Capsule report*. Office of Research and Development,U.S. EPA, July 1997.
8. Bower, J., et al., *Immobilization of mercury by pyrite (FeS_2).* Environmental Pollution, 2008. **156**(2): p. 504-514.

9. Jean, G., *Heavy metal adsorption by sulphide mineral surfaces.* Geochimica et Cosmochimica Acta, 1986. **50**(7): p. 1455-1463.

10. Ehrhardt, J., *XPS study of the sorption of Hg(II) onto pyrite FeS 2.* Surface and Interface Analysis, 2000. **30**(1): p. 269-272.

11. Han, D.S., et al., *Reactive iron sulfide (FeS)-supported ultrafiltration for removal of mercury (Hg(II)) from water.* Water Research, 2014. **53**(0): p. 310-321.

12. Brown, J.R., *Mercury removal from water by iron sulfide minerals, an electron spectroscopy for chemical analysis (ESCA) study.* Environmental Science & Technology, 1979. **13**(9): p. 1142-1144.

13. Svensson, M., B. Allard, and A. Düker, *Formation of HgS—mixing HgO or elemental Hg with S, FeS or FeS2.* Science of The Total Environment, 2006. **368**(1): p. 418-423.

14. Ravichandran, M., et al., *Inhibition of precipitation and aggregation of metacinnabar (mercuric sulfide) by dissolved organic matter isolated from the Florida Everglades.* Environmental Science & Technology, 1999. **33**(9): p. 1418-1423.

15. Perdicakis, M., N. Grosselin, and J. Bessière, *Interaction of pyrite pulps with Ag+ and Hg2+ ions. Electrochemical characterization of micrometric grains.* Analytica Chimica Acta, 1999. **385**(1–3): p. 467-485.

16. Biester, H., *Solubility and changes of mercury binding forms in contaminated soils after immobilization treatment.* Environmental Science & Technology, 1998. **32**(18): p. 2755-2762.

17. Hyland, M.M., *XPS and AES studies of Hg(II) sorption and desorption reactions on sulphide minerals.* Geochimica et Cosmochimica Acta, 1990. **54**(7): p. 1957-1967.

18. Gavilan, K.C., et al., *Mercury sorption on a thiocarbamoyl derivative of chitosan.* Journal of Hazardous Materials, 2009. **165**(1–3): p. 415-426.

19. Barrow, N.J., *The effects of pH and chloride concentration on mercury sorption. II. By a soil.* The Journal of Soil Science, 1992. **43**(2): p. 305-312.

20. Melamed, R., F.E. Trigueiro, and R.C.V. Boas, *The effect of humic acid on mercury solubility and complexation.* Applied Organometallic Chemistry, 2000. **14**(9): p. 473-476.

21. Gu, B., *Mercury reduction and complexation by natural organic matter.* Proceedings of the National Academy of Sciences of the United States of America, 2011. **108**(4).

22. Hong, S. and M. Elimelech, *Chemical and physical aspects of natural organic matter (NOM) fouling of nanofiltration membranes.* Journal of Membrane Science, 1997. **132**(2): p. 159-181.

23. Liang, P., et al., *Effects of salinity and humic acid on the sorption of Hg on Fe and Mn hydroxides.* Journal of Hazardous Materials, 2013. **244–245**(0): p. 322-328.

24. Haitzer, M., *Binding of mercury(II) to aquatic humic substances: Influence of pH and source of humic substances.* Environmental Science & Technology, 2003. **37**(11): p. 2436-2441.

25. Acai, P., *Pyrite passivation by humic acid investigated by inverse liquid chromatography.* Colloids and Surfaces. A, Physicochemical and Engineering Aspects, 2009. **337**(1-3): p. 39-46.

26. Skyllberg, U., *Competition between disordered iron sulfide and natural organic matter associated thiols for mercury(II)-An EXAFS study.* Environmental Science & Technology, 2010. **44**(4): p. 1254-1259.

27. Bonnissel Gissinger, P., *Surface oxidation of pyrite as a function of pH.* Environmental Science & Technology, 1998. **32**(19): p. 2839-2845.

28. Barron-Zambrano, J., et al., *Mercury removal from aqueous solutions by complexation—ultrafiltration.* Desalination, 2002. **144**(1–3): p. 201-206.

29. Bessbousse, H., *Increase in permeate flux by porosity enhancement of a sorptive UF membrane designed for the removal of mercury(II).* Journal of Membrane Science, 2010. **364**(1-2): p. 167-176.

30. Uludag, Y., H.Ö. Özbelge, and L. Yilmaz, *Removal of mercury from aqueous solutions via polymer-enhanced ultrafiltration.* Journal of Membrane Science, 1997. **129**(1): p. 93-99.

31. Maximous, N.N., G.F. Nakhla, and W.K. Wan, *Removal of heavy metals from wastewater by adsorption and membrane processes: A comparative study.* World Academy of Science, Engineering and Technology,, 2010. **Vol.64**: p. 594-599

32. Jung, J., et al., *Feasibility of micellar-enhanced ultrafiltration (MEUF) or the heavy metal removal in soil washing effluent.* Desalination, 2008. **222**(1–3): p. 202-211.

33. Cho, J., G. Amy, and J. Pellegrino, *Membrane filtration of natural organic matter: factors and mechanisms affecting rejection and flux decline with charged ultrafiltration (UF) membrane.* Journal of Membrane Science, 2000. **164**(1–2): p. 89-110.

34. Cho, J., G. Amy, and J. Pellegrino, *Membrane filtration of natural organic matter: comparison of flux decline, NOM rejection, and foulants during filtration with three UF membranes.* Desalination, 2000. **127**(3): p. 283-298.

35. Tarabara, V., *Constant transmembrane pressure vs. constant permeate flux: Effect of particle size on crossflow membrane filtration.* Environmental Engineering Science, 2002. **19**(6): p. 343-355.

36. Jawor, A. and E. Hoek, *Removing cadmium ions from water via nanoparticle-enhanced ultrafiltration.* Environmental Science & Technology, 2010. **44**(7): p. 2570-2576.

37. Weng, Y.-H., et al., *Effect of hydrophobicity of humic substances on electro-ultrafiltration.* Desalination, 2012. **284**(0): p. 128-134.

38. Zularisam, A.W., et al., *Role of natural organic matter (NOM), colloidal particles, and solution chemistry on ultrafiltration performance.* Separation and Purification Technology, 2011. **78**(2): p. 189-200.

39. UNEP, *Global mercury assessment 2013: sources, emissions, releases and environmental transport*. 2013, UNEP Chemical Branch: Geneva, Switzerland.

40. SATOH, H., *Occupational and environmental toxicology of mercury and its compounds.* Industrial Health 2000, 2000: p. 153–164.

41. TA, G. and B. JD, *Principles of clinical toxicology. 2nd ed*. 1990, New york: Raven press.

42. Clarkson, T.W., L. Magos, and G.J. Mayers, *The toxicology of mercury — current Exposures and clinical manifestations.* The New England journal of Medicine, 2003. **349**(18): p. 1731-1737.

43. USEPA, *Treatment technologies for mercury in soil, waste, and water*. 2007, United States Environmental Protection Agency (USEPA).

44. Selin, N., *Global biogeochemical cycling of mercury: A Review.* Annual Review of Environment and Resources, 2009. **34**(1): p. 43-63.

45. Ullrich, S., *Mercury in the aquatic environment: A review of factors affecting methylation.* Critical Reviews in Environmental Science and Technology, 2001. **31**(3): p. 241-293.

46. Mason, R., *The role of microorganisms in elemental mercury formation in natural waters.* Water, Air and Soil Pollution, 1995. **80**(1): p. 775-787.

47. Alberts, J., *Elemental mercury evolution mediated by humic acid.* Science, 1974. **184**(4139): p. 895-897.

48. Xiao, Z., *Influence of humic substances on photolysis of divalent mercury in aqueous solution.* Water, Air and Soil Pollution, 1995. **80**(1): p. 789-798.

49. Amyot, M., G.A. Gill, and F.M.M. Morel, *Production and loss of dissolved gaseous mercury in coastal seawater.* Environmental Science & Technology, 1997. **31**(12): p. 3606-3611.

50. Yamamoto, M., *Stimulation of elemental mercury oxidation in the presence of chloride ion in aquatic environments.* Chemosphere, 1996. **32**(6): p. 1217-1224.

51. Gavis, J. and J.F. Ferguson, *The cycling of mercury through the environment.* Water Research, 1972. **6**(9): p. 989-1008.

52. Morel, F.M.M. and M. Kraepiel, *The chemical cycle and bioaccumulation of mercury.* Annual Review of Ecology and Systematics, 1998. **29**(1): p. 543-566.

53. Leermakers, M., *Mercury speciation in the Scheldt Estuary.* Water, Air and Soil Pollution, 1995. **80**(1-4): p. 641-652.

54. Stumm, W. and J.J. Morgan, *Aquatic chemistry : chemical equilibria and rates in natural waters*. Environmental Science and Technology. 1995: New York : Wiley, c1995, 3rd ed.

55. Ravichandran, M., et al., *Enhanced dissolution of cinnabar (mercuric sulfide) by dissolved organic matter isolated from the Florida everglades.* Environmental Science & Technology, 1998. **32**(21): p. 3305-3311.

56. Gardner, L.R., *Organic versus inorganic trace metal complexes in sulfidic marine waters—some speculative calculations based on available stability constants.* Geochimica et Cosmochimica Acta, 1974. **38**(8): p. 1297-1302.

57. Noel, W. and P.T. Vinsen, *Pyrite synthesis, characterization and uses*. 2013, New York: Nova.

58. Boszke, L., *Some aspects of speciation of mercury in a water environment.* Polish Journal of Environmental Studies, 2002. **11**(4): p. 285-298.

59. Pak, K., *Mercury methylation and demethylation in anoxic lake sediments and by strictly anaerobic bacteria.* Applied and Environmental Microbiology, 1998. **64**(3): p. 1013-1017.

60. Wang, Q., *Experimental investigation of pyrite formation under conditions approximating those found in anoxic marine sediments*. 1995, Texas A&M University: Ann Arbor. p. 105.

61. Bulut, G., et al., *Arsenic removal from aqueous solution using pyrite.* Journal of Cleaner Production, 2014. **84**(0): p. 526-532.

62. Song, J.K. and B. Batchelor, *Arsenic removal and stabilization by synthesized pyrite. [electronic resource]*. 2010: College Station, Tex. : Texas A&M University, 2010.

63. Wei, D. and K. Osseo-Asare, *Particulate pyrite formation by the Fe3+HS− reaction in aqueous solutions: effects of solution composition.* Colloids and Surfaces A: Physicochemical and Engineering Aspects, 1996. **118**(1–2): p. 51-61.

64. Wei, D., *Aqueous synthesis of finely divided pyrite particles.* Colloids and Surfaces. A, Physicochemical and Engineering Aspects, 1997. **121**(1): p. 27-36.

65. Rickard, D., *Chemistry of iron sulfides.* Chem Inform, 2007. **38**(19): p. 514-562.

66. Kim, E. and B. Kim, *Synthesis and characterization of pyrite (FeS2) using microwave irradiation.* Materials Research Bulletin, 2009. **44**(7): p. 1553-1558.

67. Huang, C.P., *The removal of mercury (II) from dilute aqueous solution by activated carbon.* Water Research, 1984. **18**(1): p. 37-46.

68. Wajima, T., *Adsorption behaviors of mercury from aqueous solution using sulfur-impregnated adsorbent developed from coal.* Fuel Processing Technology, 2011. **92**(7): p. 1322-1327.

69. Sen, A., *Adsorption of mercury(II) by coal fly ash.* Water Research, 1987. **21**(8): p. 885-888.

70. Deshicar, A.M., S.S. Bokade, and S.S. Dara, *Modified hardwickia binata bark for adsorption of mercury (II) from water.* Water Research, 1990. **24**(8): p. 1011-1016.

71. Macch, G., *Uptake of mercury by exhausted coffee grounds.* Environmental Technology Letters, 1986. **7**(1-12): p. 431-444.

72. Knocke, W.R., *Mercury(II) sorption by waste rubber.* Water Research, 1981. **15**(2): p. 275-282.

73. Cox, M., *Removal of mercury(II) from aqueous solution on a carbonaceous sorbent prepared from flax shive.* Journal of Chemical Technology and Biotechnology, 2000. **75**(6): p. 427-435.

74. El Shafey, E.I., *Removal of Zn(II) and Hg(II) from aqueous solution on a carbonaceous sorbent chemically prepared from rice husk.* Journal of Hazardous Materials, 2010. **175**(1): p. 319-327.

75. Zabihi, M., *Removal of mercury from water by carbonaceous sorbents derived from walnut shell.* Journal of Hazardous Materials, 2009. **167**(1): p. 230-236.

76. Farooq, U., et al., *Biosorption of heavy metal ions using wheat based biosorbents – A review of the recent literature.* Bioresource Technology 101 (2010), 2010: p. 5043–5053.

77. Bhatnagar, A., et al., *Coconut-based biosorbents for water treatment - A review of the recent literature.* Advances in Colloid and Interface Science, 2010: p. 160, (1-2), 1-15.

78. Tawabini, B., et al., *Removal of mercury from water by multi-walled carbon nanotubes.* Water Science and Technology, 2010. **61**(3): p. 591-8.

79. Lee, E.K., V. Chen, and A.G. Fane, *Natural organic matter (NOM) fouling in low pressure membrane filtration — effect of membranes and operation modes.* Desalination, 2008. **218**(1–3): p. 257-270.

80. Jawor, A., *Removing cadmium ions from water via nanoparticle-enhanced ultrafiltration.* Environmental science & technology, 2010. **44**(7): p. 2570-6.

81. Wikipedia. *Membrane technology*. 2015 [cited 2015 4/30/2015]; Available from: http://en.wikipedia.org/wiki/Membrane_technology.

82. Negri, M.C., P. Gillenwater, and M. Urgan Demirtas, *Emerging technologies and approaches to minimize discharges into Lake Michigan. Phase 2, Module 3 Report*. 2011, Energy System Division, Argonne National Laboratory.

83. Guo, W., H.-H. Ngo, and J. Li, *A mini-review on membrane fouling.* Bioresource Technology, 2012. **122**(0): p. 27-34.

84. Nnanna, G., et al., *Emerging technologies and approaches to minimize heavy metal discharges into lake michigan*. 2010, Purdue University Calumet Water Institute, Hammond.

85. Looney, B., *Removal of mercury from low-concentration aqueous streams using chemical reduction and air stripping.* Journal of Environmental Engineering, 2003. **129**(9): p. 819-825.

86. Kang, S.-Y., et al., *Competitive adsorption characteristics of Co2+, Ni2+, and Cr3+ by IRN-77 cation exchange resin in synthesized wastewater.* Chemosphere, 2004. **56**(2): p. 141-147.

87. Zhao, X., *Selective extraction of trace mercury and cadmium from drinking water sources.* Water Environment Research, 2005. **77**(3): p. 212-218.

88. Green-Ruiz, C., *Mercury(II) removal from aqueous solutions by nonviable Bacillus sp. from a tropical estuary.* Bioresource Technology, 2006. **97**(15): p. 1907-1911.

89. Oehmen, A., et al., *Mercury removal from water streams through the ion exchange membrane bioreactor concept.* Journal of Hazardous Materials, 2014. **264**(0): p. 65-70.

90. Vinod, V.T.P., et al., *Bioremediation of mercury (II) from aqueous solution by gum karaya (Sterculia urens): A natural hydrocolloid.* Desalination, 2011. **272**(1–3): p. 270-277.

91. Hassen, A., et al., *Effects of heavy metals on pseudomonas aeruginosa and bacillus thuringiensis.* Bioresource Technology, 1998. **65**(1–2): p. 73-82.

92. Southworth, G., *Mercury abatement report on the U.S. Department of Energy's Oak Ridge Y-12 plant for the fiscal year 1996.* 1996, U.S. Department of Energy's Oak Ridge: Oak Ridge, Tennessee.

93. Looney, B.B., et al., *Ultralow level mercury treatment using chemical reduction and air stripping: Scoping report*. 2000, Westinghouse Savannah River Company: Aiken. p. 28.

94. Yantasee, W., et al., *Removal of heavy metals from aqueous systems with thiol functionalized superparamagnetic nanoparticles.* Environmental Science & Technology, 2007. **41**(14): p. 5114-5119.

95. Lisha, K.P., *Towards a practical solution for removing inorganic mercury from drinking water using gold nanoparticles.* Gold Bulletin, 2009. **42**(2): p. 144-152.

96. Lo, *Gold nanoparticle-aluminum oxide adsorbent for efficient removal of mercury species from natural waters.* Environmental Science & Technology, 2012. **46**(5): p. 2724-30.

97. Parham, H., B. Zargar, and R. Shiralipour, *Fast and efficient removal of mercury from water samples using magnetic iron oxide nanoparticles modified with 2-mercaptobenzothiazole.* Journal of Hazardous Materials, 2012. **205–206**(0): p. 94-100.

98. Shih, Y.-C., et al., *Combined tween 20-stabilized gold nanoparticles and reduced graphite oxide–Fe3O4 nanoparticle composites for rapid and efficient removal of mercury species from a complex matrix.* ACS Applied Materials & Interfaces, 2014. **6**(20): p. 17437-17445.

99. Sheela, T., et al., *Kinetics and thermodynamics studies on the adsorption of Zn(II), Cd(II) and Hg(II) from aqueous solution using zinc oxide nanoparticles.* Powder Technology, 2012. **217**(0): p. 163-170.

100. Liu, Y., *Nanocomposites of graphene oxide, Ag nanoparticles, and magnetic ferrite nanoparticles for elemental mercury (Hg 0) removal.* RSC Advances, 2015. **5**(20): p. 15634-15640.

101. Desai, I. and B. Boulanger, *Mercury removal from aqueous systems using commercial and laboratory prepared metal oxide nanoparticles. [electronic resource]*. 2010: College Station, Tex. : Texas A&M University, 2010.

102. Hadavifar, M., et al., *Adsorption of mercury ions from synthetic and real wastewater aqueous solution by functionalized multi-walled carbon nanotube with both amino and thiolated groups.* Chemical Engineering Journal, 2014. **237**(0): p. 217-228.

103. Journet, C., *Carbon nanotube synthesis: from large-scale production to atom-by-atom growth.* Nanotechnology, 2012. **23**(14): p. 142001.

104. Prasek, J., et al., *Methods for carbon nanotubes synthesis-review.* Journal of Materials Chemistry, 2011. **21**(40): p. 15872-15884.

105. Bandaru, N.M., et al., *Enhanced adsorption of mercury ions on thiol derivatized single wall carbon nanotubes.* Journal of Hazardous Materials, 2013. **261**(0): p. 534-541.

106. Luo, G., et al., *Carbon nanotube-silver composite for mercury capture and analysis.* Energy & Fuels, 2010. **24**(1): p. 419-426.

107. Shawky, H., *Chitosan/carbon nanotube composite beads: Preparation, characterization, and cost evaluation for mercury removal from wastewater of some industrial cities in Egypt.* Journal of Applied Polymer Science, 2012. **125**(1): p. E93-E101.

108. Gethard, K., O. Sae-Khow, and S. Mitra, *Water desalination using carbon-nanotube-enhanced membrane distillation.* ACS Applied Materials & Interfaces, 2011. **3**(2): p. 110-114.

109. Zhang, Y., et al., *Characterization of mercury concentrations in snow and potential sources, Shanghai, China.* Science of The Total Environment, 2013. **449**(0): p. 434-442.

110. Barringer, J.L., et al., *Mercury concentrations in water from an unconfined aquifer system, New Jersey coastal plain.* Science of The Total Environment, 2005. **346**(1–3): p. 169-183.

111. Bower, J., *Immobilization of mercury by pyrite (FeS2).* Environmental Pollution, 2008. **156**(2): p. 504-514.

112. Brown Jr, G., *Sorption of trace elements on mineral surfaces: Modern perspectives from spectroscopic studies, and comments on sorption in the marine environment.* International Geology Review, 2001. **43**(11): p. 963-1073.

113. Gu, B.H., et al., *Mercury reduction and complexation by natural organic matter in anoxic environments.* Proceedings of the National Academy of Sciences of the United States of America, 2011. **108**(4): p. 1479-1483.

114. Leito, I., et al., *Estimation of uncertainty in routine pH measurement.* Accreditation and Quality Assurance, 2002. **7**(6): p. 242-249.

115. Schäfer, A.I., *Fouling effects on rejection in the membrane filtration of natural waters.* Desalination, 2000. **131**(1): p. 215-224.

116. Howe, K., *Fouling of microfiltration and ultrafiltration membranes by natural waters.* Environmental Science & Technology, 2002. **36**(16): p. 3571-3576.

117. Saravia, F., C. Saravia, and F. Zwiener, *Interactions between membrane surface, dissolved organic substances and ions in submerged membrane filtration.* Desalination, 2006. **192**(1): p. 280-287.

118. Zhu, X., *Colloidal fouling of reverse osmosis membranes: Measurements and fouling mechanisms.* Environmental Science & Technology, 1997. **31**(12): p. 3654-3662.

119. Descostes, M., *Use of XPS in the determination of chemical environment and oxidation state of iron and sulfur samples: constitution of a data basis in binding energies for Fe and S reference compounds and applications to the evidence of surface species of an oxidized pyrite in a carbonate medium.* Applied Surface Science, 2000. **165**(4): p. 288-302.

120. Karthe, S., R. Szargan, and E. Suoninen, *Oxidation of pyrite surfaces: a photoelectron spectroscopic study.* Applied Surface Science, 1993. **72**(2): p. 157-170.

121. Lowson, R.T., *Aqueous oxidation of pyrite by molecular oxygen.* Chemical Reviews, 1982. **82**(5): p. 461-497.

122. Rimstidt, J.D. and D.J. Vaughan, *Pyrite oxidation: a state-of-the-art assessment of the reaction mechanism.* Geochimica et Cosmochimica Acta, 2003. **67**(5): p. 873-880.

123. Barrow, N.J., *The effects of pH and chloride concentration on mercury sorption. I. By goethite.* The Journal of Soil Science, 1992. **43**(2): p. 295-304.

124. Xu, Y. and M.A.A. Schoonen, *The stability of thiosulfate in the presence of pyrite in low-temperature aqueous solutions.* Geochimica et Cosmochimica Acta, 1995. **59**(22): p. 4605-4622.

125. Bak, F., *A novel type of energy metabolism involving fermentation of inorganic sulphur compounds.* Nature, 1987. **326**(6116): p. 891-892.

126. Petala, M.D. and A.I. Zouboulis, *Vibratory shear enhanced processing membrane filtration applied for the removal of natural organic matter from surface waters.* Journal of Membrane Science, 2006. **269**(1–2): p. 1-14.

APPENDIX

Code for calculating flux decline parameters on MATLAB®

```
%   nlinfit_flux

global n;
global j_i;

n = input('Enter n value: ');
j_i = input('Enter j_i value: ');

[t,J]=initvar('fluxdecline.txt');
[beta,r,z]=nlinfit(t,J,@flux,0.1);
betaci=nlparci(beta,r,z);

t_min=min(t);
t_max=max(t);
xplot=[t_min:(t_max-t_min)/2000:t_max];
Jmod=j_i*(1+beta(1)*xplot).^(-n);
normal_J_m=Jmod/j_i;
normal_J=J/j_i;
figure,plot(t,normal_J,'o');hold on;plot(xplot,normal_J_m);

%Calculate the sum of square error
SSE=0;
xplot=xplot'
normal_J_m=normal_J_m'
for i = 1:size(t,2)
   for j = 1:size(xplot,1)-1
      if xplot(j,1)<=t(i) && xplot(j+1,1)>t(i)
         x1=xplot(j,1);
         x2=xplot(j+1,1);
         y1=normal_J_m(j,1);
         y2=normal_J_m(j+1,1);
         break;
      end
   end
   y_model=linear_interpolation(x1,y1,x2,y2,t(i));
   SSE=SSE+(y_model-normal_J(i))^2;
end
GOF=sqrt(SSE/(size(t,2)-2))/mean(normal_J_m)
```

Flux decline Model prediction for Ultrafiltration

Only Hg + pyrite:

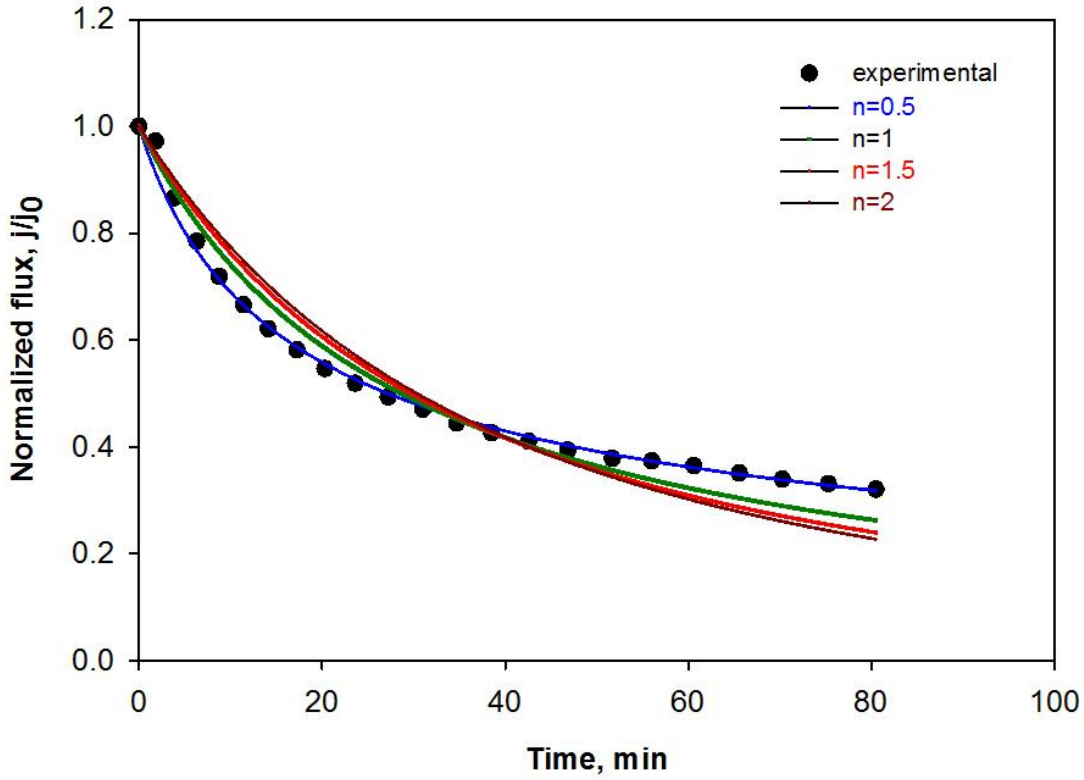

Figure A1. Normalized flux and model predictions for ultrafiltration of Hg-contacted FeS2. Conditions: 30 kDa RC membrane, 1 mg/L Hg(II), 0.1 g/L FeS2, pH 8, 15 psi pressure, 30 min pre contact time of Hg(II) with FeS2 prior to feeding into the DE/UF membrane.

Hg + Anions + pyrite:

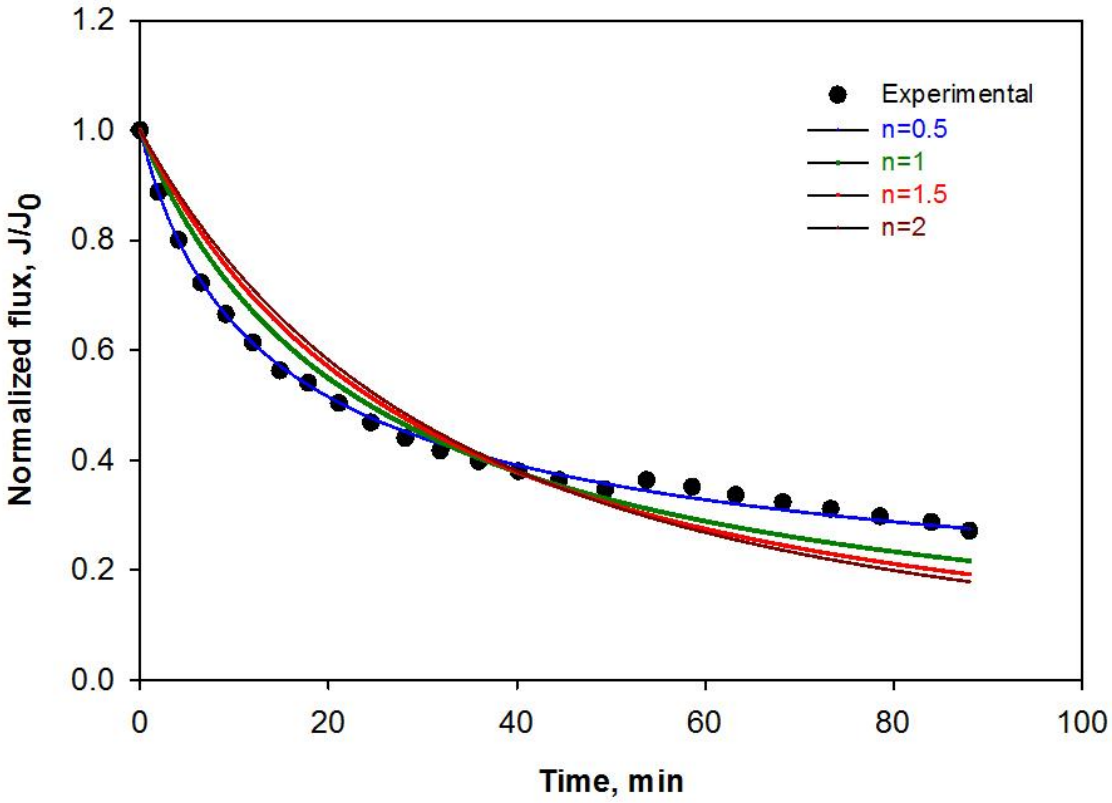

Figure A2. Normalized flux and model predictions for ultrafiltration of Hg-contacted FeS_2. Conditions: 30 kDa RC membrane, 1 mg/L Hg(II), 10 mM of anions(Cl^-, NO_3^-, SO_4^{2-}), 0.1 g/L FeS_2, pH 8, 15 psi pressure, 30 min pre contact time of Hg(II) with FeS_2 prior to feeding into the DE/UF membrane.

Hg + 0.2 mg/L HA + pyrite:

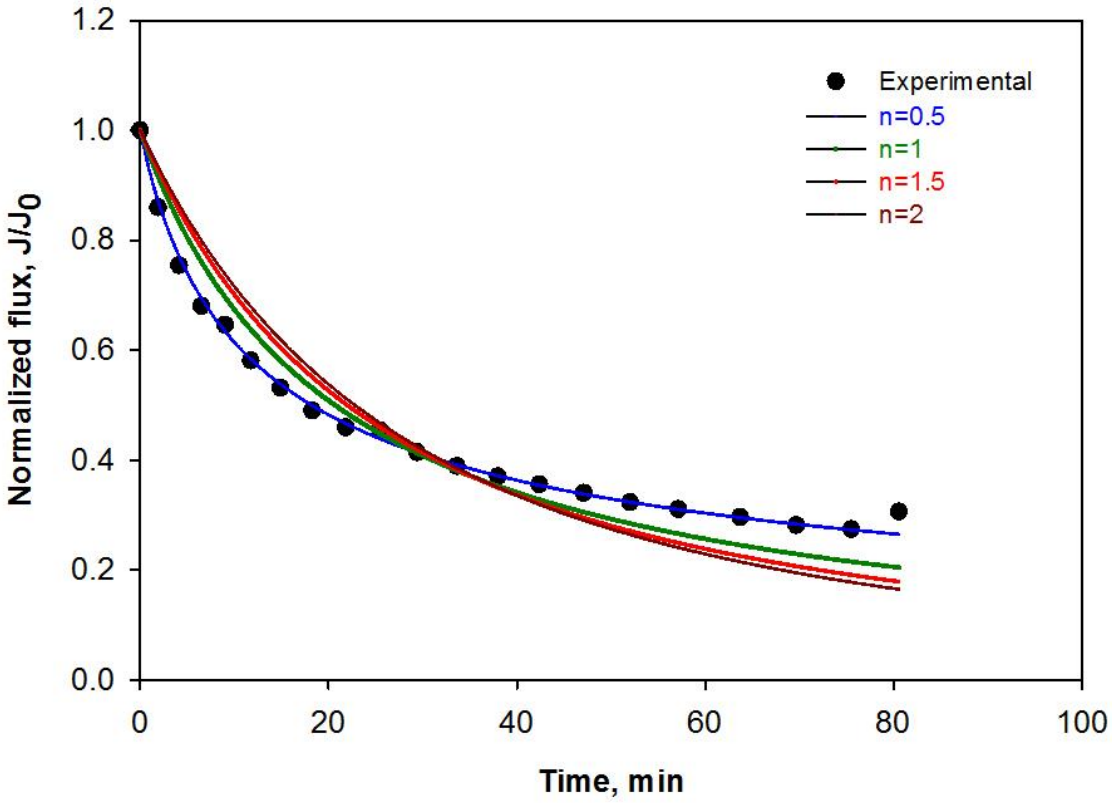

Figure A3. Normalized flux and model predictions for ultrafiltration of Hg-contacted FeS_2. Conditions: 30 kDa RC membrane, 1 mg/L Hg(II), 0.2 mg/L HA, 0.1 g/L FeS_2, pH 8, 15 psi pressure, 30 min pre contact time of Hg(II) with FeS_2 prior to feeding into the DE/UF membrane.

Hg + 1 mg/L HA + pyrite:

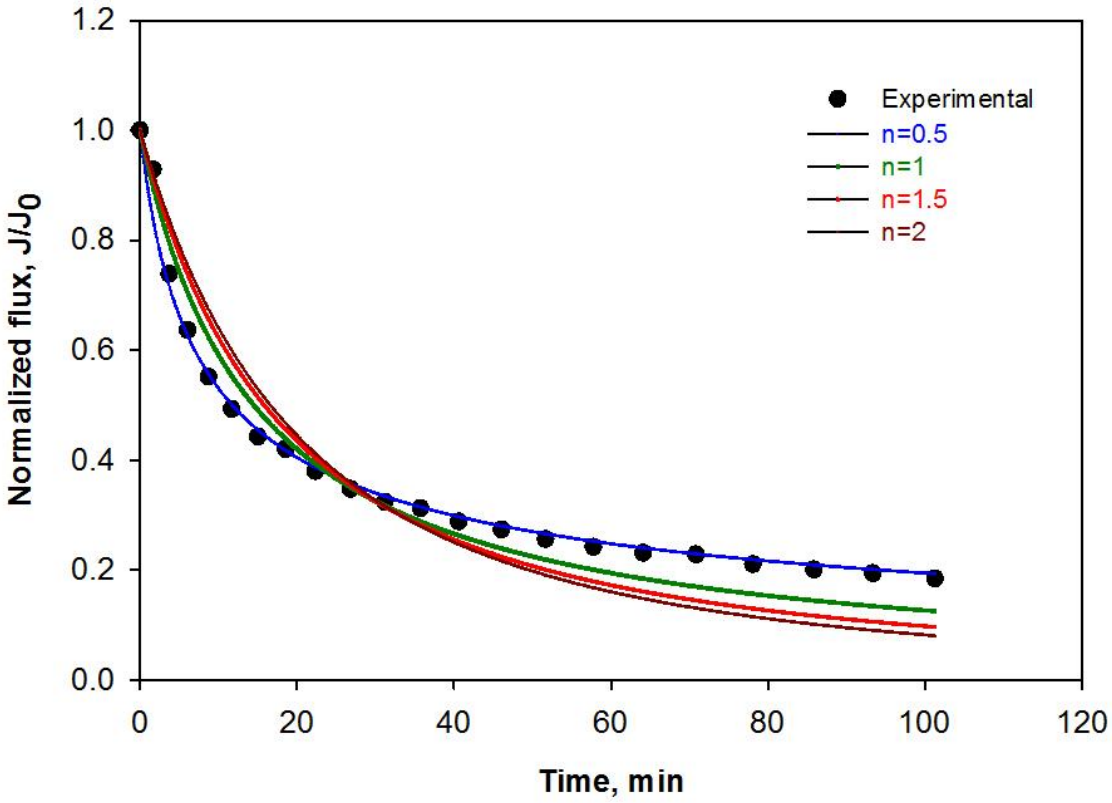

Figure A4. Normalized flux and model predictions for ultrafiltration of Hg-contacted FeS_2. Conditions: 30 kDa RC membrane, 1 mg/L Hg(II), 1 mg/L HA, 0.1 g/L FeS_2, pH 8, 15 psi pressure, 30 min pre contact time of Hg(II) with FeS_2 prior to feeding into the DE/UF membrane.

XPS analysis

Quantification report:

Dead End Ultrafiltration:

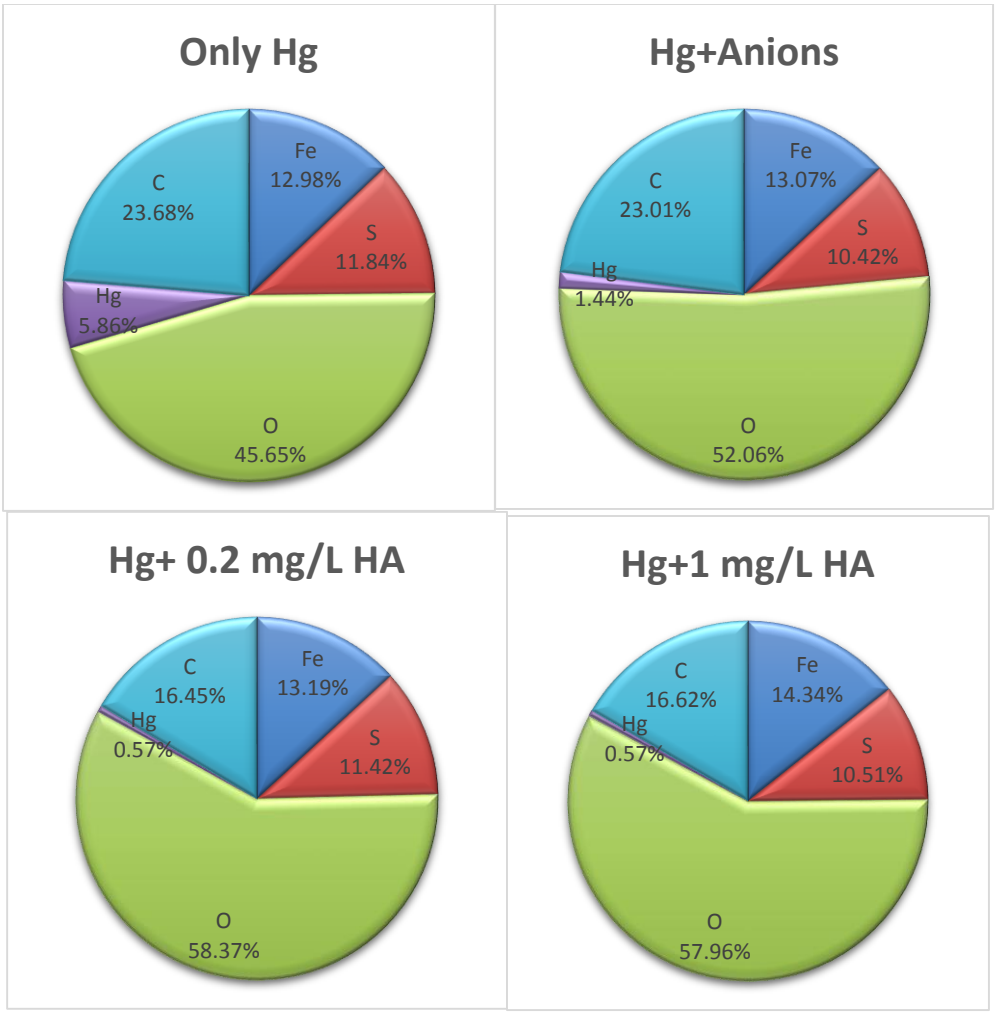

Figure A5. Quantitative analysis of elements on the membrane surface for recycle test of DE/UF. Conditions: 30 kDa RC membrane with Hg-contacted pyrite layer. pH 8, 15 psi pressure.

Cross Flow Ultrafiltration:

Rejection test:

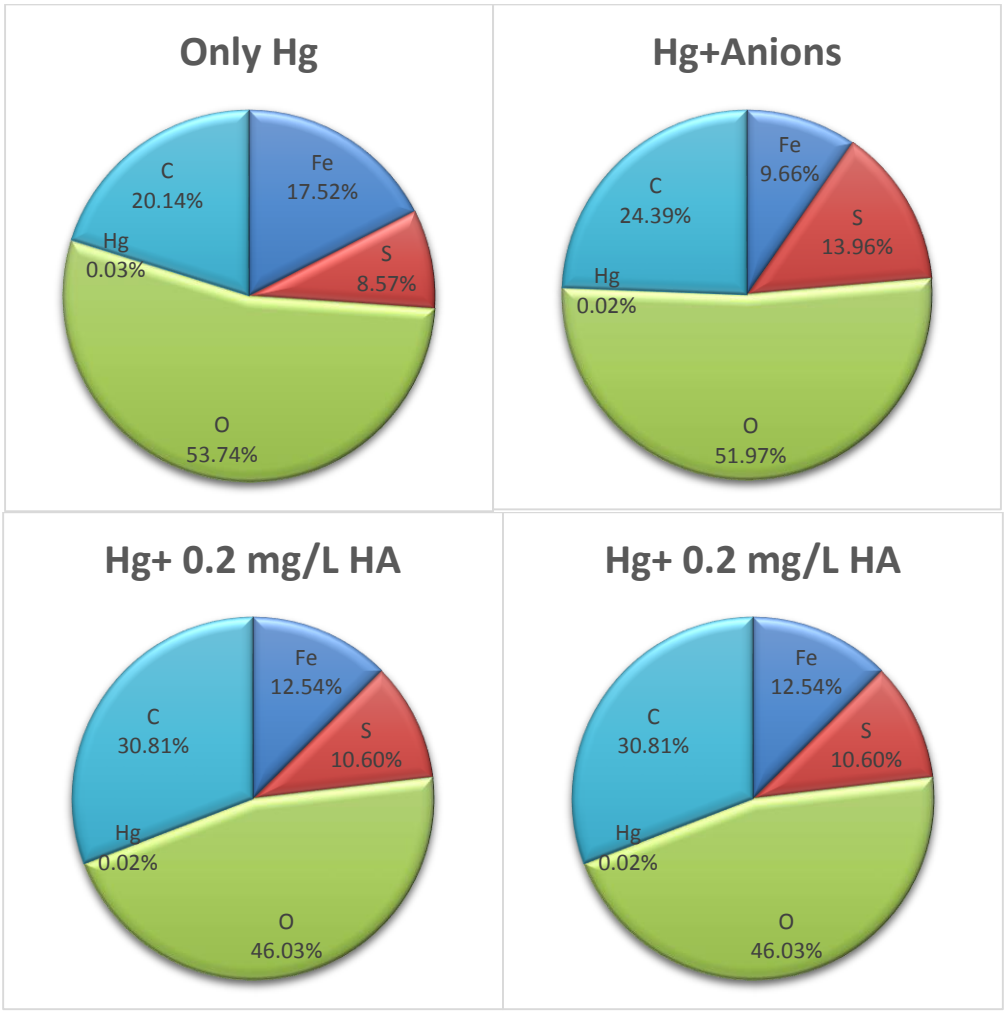

Figure A6. Quantitative analysis of elements on the membrane surface for rejection test of CF/UF system. Conditions: 0.1 g/L pyrite, 1 mg/L Hg(II),10 mM anions (Cl^-, SO_4^{2-}, NO_3^{2-}), 0.2 and 1 mg/L HA, 5 psi transmembrane pressure, pH 8, anoxic condition.

Recycle test:

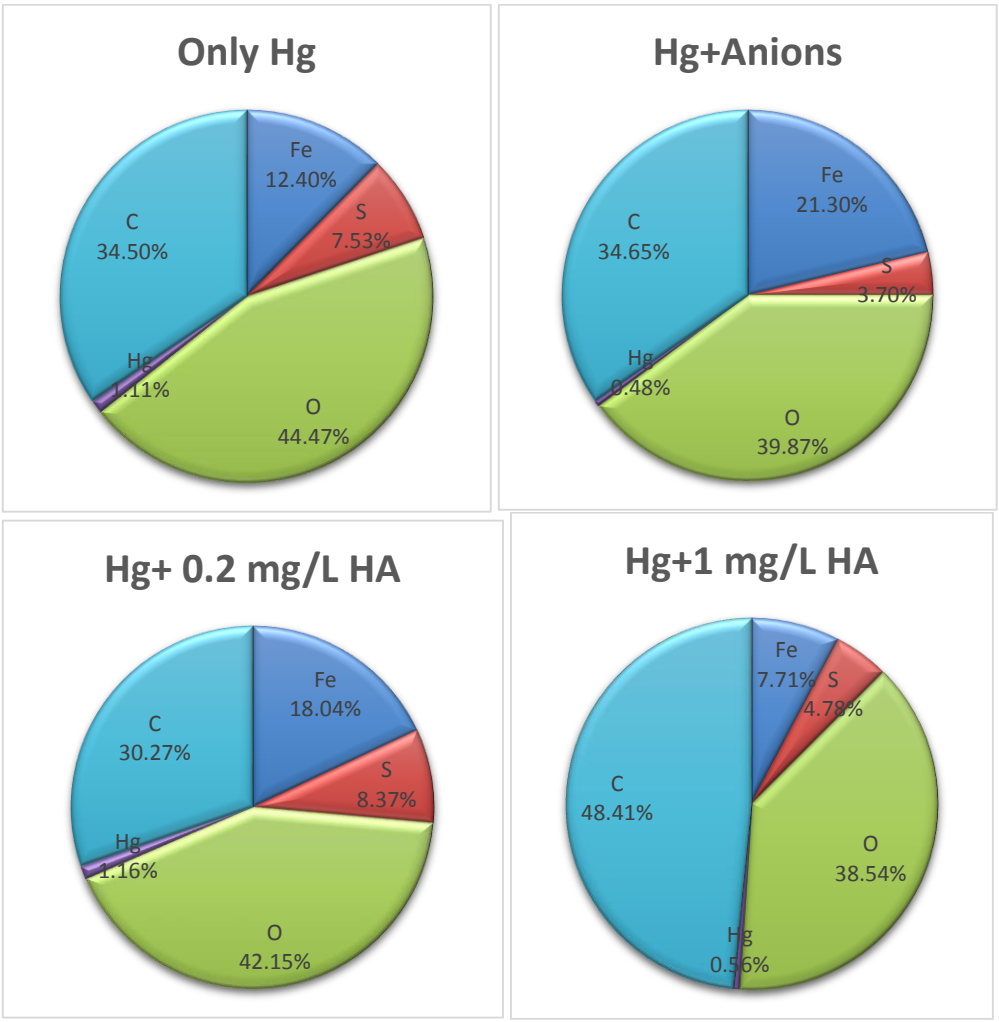

Figure A7. Quantitative analysis of elements on the membrane surface for recycle test of CF/UF system. Conditions: 1000 kDa RC membrane with Hg-contacted pyrite layer, pH 8, 15 psi pressure.

XPS spectrum:

Dead end ultrafiltration:

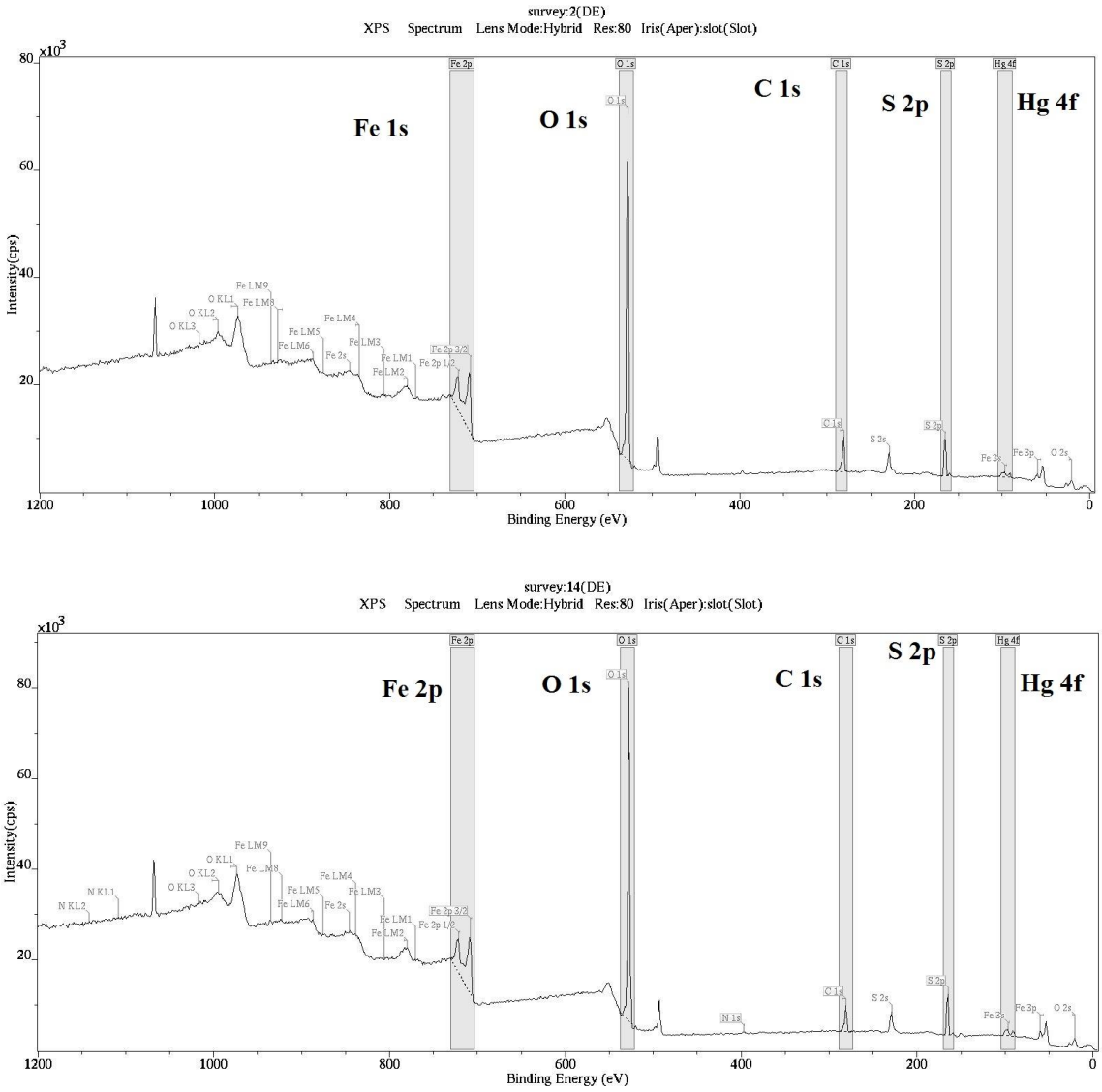

Figure A8: XPS spectrum of rejection test for DE/UF system: only Hg (top) and Hg + Anions (bottom)

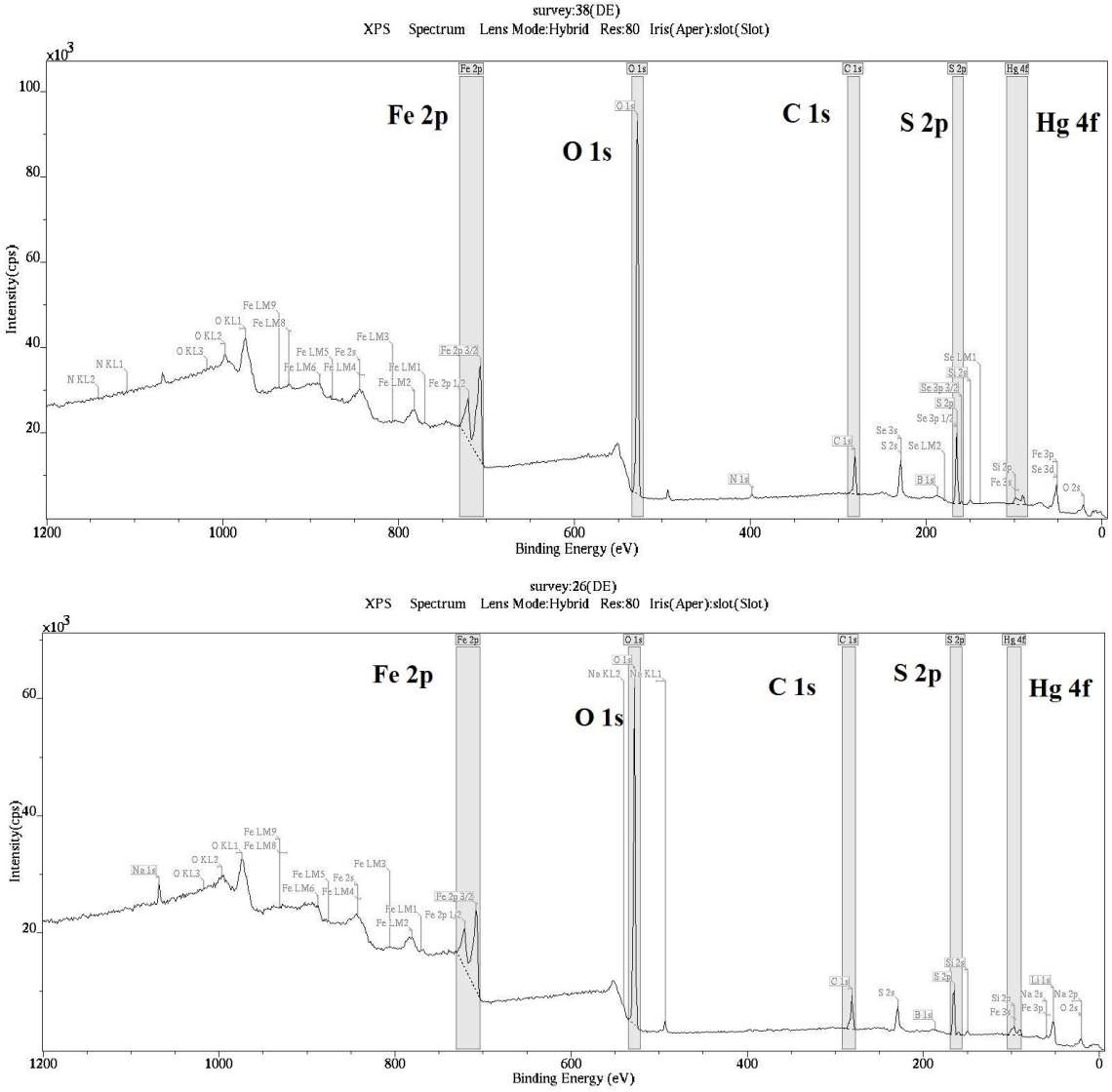

Figure A9. XPS spectrum of rejection test for DE/UF system: Hg + 0.2 mg/L HA (top) and Hg + 1 mg/L HA (bottom).

Cross flow ultrafiltration:

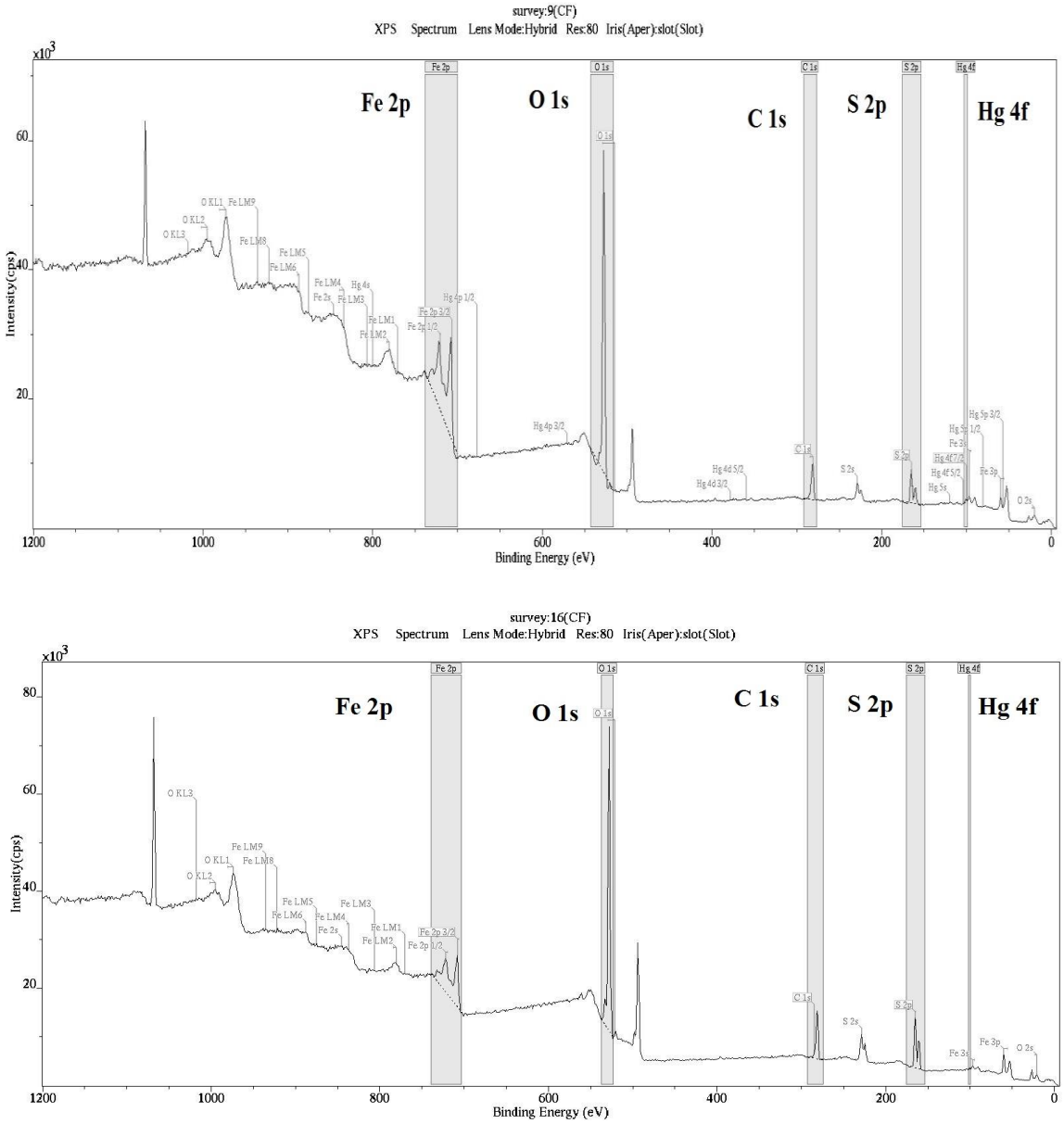

Figure A10. XPS spectrum of rejection test for CF/UF system: only Hg(top) and Hg + Anions (bottom).

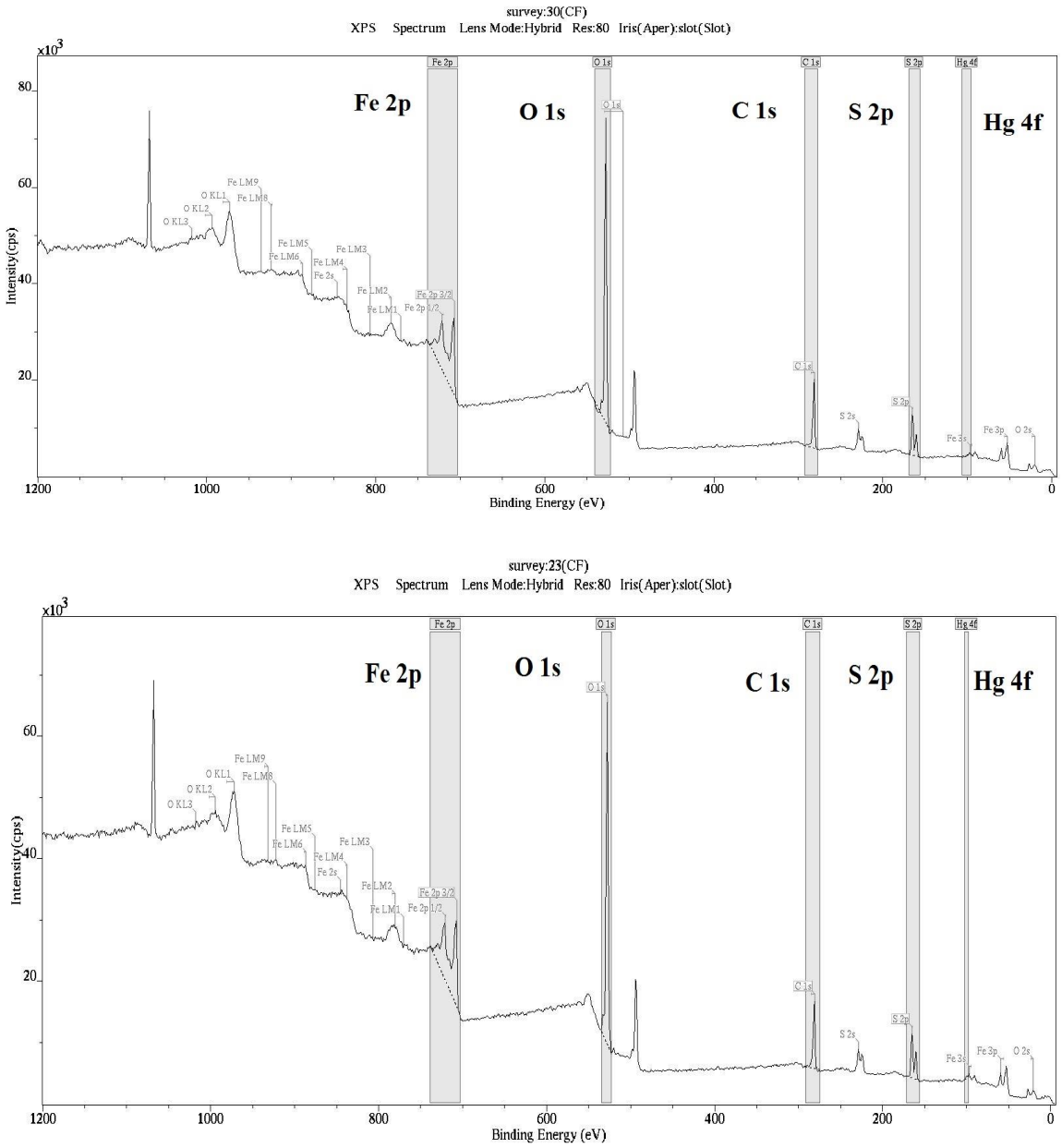

Figure A11. XPS spectrum of rejection test for DE/UF system: Hg + 0.2 mg/L HA (top) and Hg + 1 mg/L HA (bottom).